

A STUDY OF UNUSUAL DIAMONDS  
FROM THE GEORGE CREEK K1 KIMBERLITE DYKE, COLORADO

VOLUME I  
TEXT AND REFERENCES

by  
INGRID LEE CHINN

THESIS SUBMITTED IN FULFILMENT  
OF THE REQUIREMENTS FOR THE DEGREE OF  
DOCTOR OF PHILOSOPHY

UNIVERSITY OF CAPE TOWN

MAY, 1995

The University of Cape Town has been given the right to reproduce this thesis in whole or in part. Copyright is held by the author.

The copyright of this thesis vests in the author. No quotation from it or information derived from it is to be published without full acknowledgement of the source. The thesis is to be used for private study or non-commercial research purposes only.

Published by the University of Cape Town (UCT) in terms of the non-exclusive license granted to UCT by the author.

## DECLARATION

I hereby declare that the work presented in this thesis is my own, except where otherwise stated in the text.

Signed by candidate

INGRID LEE CHINN

.May, 1995

## ABSTRACT

Cathodoluminescence photomicrographs of diamonds from the George Creek K1 (section 28) kimberlite dyke in Colorado reveal complex intergrowth relationships between CO<sub>2</sub>-free and CO<sub>2</sub>-bearing diamond growth generations. The distribution of the CO<sub>2</sub>-bearing diamond in some specimens suggests that this generation is younger than the CO<sub>2</sub>-free diamond growth generation, although the age relationships are mostly ambiguous. CO<sub>2</sub>-bearing diamond appears to have crystallized from fluids which invaded fractures and etched embayments in the CO<sub>2</sub>-free diamond growth generation, which shows evidence of plastic deformation.

The CO<sub>2</sub>-free diamond growth generation commonly exhibits features caused by extreme plastic deformation during mantle residence time. Abundant yellow-green plastic slip planes transect zones of customary blue cathodoluminescence in many diamonds, and raised lamination lines have been recognized on resorption surfaces.

The complexity and intensity of surface etch features in most George Creek diamonds, including the CO<sub>2</sub>-bearing growth generation, suggests that the diamonds were subjected to multiple episodes of etching and resorption. Extensive development of hexagonal and trigonal etch pits resulted from the action of oxidizing CO<sub>2</sub>-H<sub>2</sub>O fluids, and some late-stage etching is believed to have occurred in the hypabyssal dyke system prior to kimberlite eruption.

The presence of high pressure sub-microscopic CO<sub>2</sub> inclusions in the CO<sub>2</sub>-bearing diamond growth generation was detected using Fourier Transform Infra-red (IR) spectroscopy. The wide range in pressure estimates from the position of the CO<sub>2</sub> absorption peaks suggests that annealing and partial decrepitation of the inclusions occurred during prolonged mantle residence time. The volume increase caused by graphite precipitation on the inclusion walls may be responsible for geologically unreasonable pressure estimates in excess of 200 kb at room temperature, whereas pressure estimates near atmospheric pressure may reflect partial decrepitation of CO<sub>2</sub> inclusions.

The CO<sub>2</sub>-bearing diamond generation lacks spectral evidence of substitutional nitrogen defects. In contrast, most diamonds of the CO<sub>2</sub>-free growth generation are characterized by low contents of highly-aggregated nitrogen defects, and variable platelet development. Infra-red spectra indicate that the nitrogen content varies from below the detection limit to ~2115 at. ppm in the CO<sub>2</sub>-free diamonds studied. Significant variation in nitrogen content and aggregation state was detected within single diamonds. Quantitative analyses of the nitrogen aggregation states are consistent with the equilibration of the George Creek diamonds at temperatures of ~1220 °C for an assumed mantle residence time of 1.25 Ga.

From the 100 diamonds cracked for inclusion recovery, no peridotitic inclusions were recovered, and careful visual inspection failed to identify any peridotitic inclusions in the uncracked diamonds. Websteritic orthopyroxene-clinopyroxene ( $\pm$  phlogopite) inclusions were recovered from two diamonds. A single green garnet inclusion was also assigned to the websteritic paragenesis. The following eclogitic mineral inclusions were recovered: 30 diamonds contained clinopyroxenes, 28 contained garnets, 6 contained rutiles, 9 contained ilmenites, and single diamonds contained sulphide, moissanite and silicon oxide inclusions.

The presence of two compositionally distinct groups of eclogitic clinopyroxene and garnet inclusions attests to the heterogeneity of the diamondiferous mantle sampled by the George Creek K1 kimberlite. Group GC1 inclusions are more magnesian in composition than Group GC2 inclusions, and generally contain detectable Cr. Group GC2 inclusions are characterized by higher K, Na, Al, Fe and Ti contents than Group GC1 inclusions.

The compositional distinctions between Group GC1 and Group GC2 inclusions may reflect heterogeneity of oceanic protoliths interpreted to have been recycled into the mantle by subduction. Subduction of differentiated mafic intrusions rich in Ti and Fe may have enriched the diamond growth region in Ti and Fe which promoted the crystallization of rutile and ilmenite. The dominance of eclogitic mineral inclusions, and the preliminary results of the carbon isotopic composition of George Creek diamonds are consistent with diamond growth following subduction of oceanic material (including carbon depleted in the heavy  $^{13}\text{C}$  isotope) into the Colorado-Wyoming lithospheric mantle.

Marked enrichment of K in George Creek clinopyroxene inclusions draws attention to the importance of this mineral as a reservoir for K under conditions of high pressure in the lithospheric mantle. Elevated levels of Na and Ti in eclogitic garnet inclusions are also thought to reflect high pressure crystallization, and the bulk composition of the diamond growth region.

Pressure estimates of diamond formation were made from the Al content of websteritic orthopyroxene inclusions assumed to have crystallized in equilibrium with the websteritic garnet inclusion. The pressure estimates fall within the diamond stability field at the assumed diamond formation temperature of 1138 °C. No inclusions indicative of extremely high pressure crystallization (e.g. majoritic garnet) were recovered.

The coexistence of discrete garnet-clinopyroxene inclusion pairs in several diamonds permitted the estimation of mantle temperatures of 1071 - 1178 °C (mean = 1138 °C), interpreted to correspond to eclogitic diamond formation. Lower temperatures of 912 - 977 °C were calculated for touching bi- or poly-mineralic inclusions which were able to re-equilibrate in response to changes in temperature and pressure. The latter temperature estimates are believed to have been representative of mantle temperatures immediately prior to kimberlite eruption in the Devonian.

# CONTENTS (VOLUME I)

	page
<u>1. INTRODUCTION</u> .....	1
<u>2. GEOLOGICAL SETTING OF THE GEORGE CREEK KIMBERLITE DYKES</u> .....	5
2.1. GEOLOGICAL EVOLUTION OF THE COLORADO-WYOMING KIMBERLITE PROVINCE.....	5
2.1.1. <i>The composition of the Colorado-Wyoming lithospheric mantle</i> .....	6
2.2. DISCOVERY OF THE COLORADO-WYOMING KIMBERLITE PROVINCE.....	8
2.3. THE GEORGE CREEK KIMBERLITE DYKES.....	9
2.3.1. <i>The diamond-bearing potential of the George Creek kimberlites</i> .....	10
<u>3. PHYSICAL CHARACTERISTICS OF GEORGE CREEK DIAMONDS</u> .....	12
3.1. INTRODUCTION.....	12
3.2. METHODS.....	12
3.3. RESULTS.....	13
3.3.1. <i>Size</i> .....	13
3.3.2. <i>Primary morphology</i> .....	13
3.3.3. <i>Crystal state</i> .....	15
3.3.4. <i>Colour</i> .....	15
3.3.5. <i>Resorption</i> .....	17
3.3.6. <i>Surface features</i> .....	19
3.3.6a. <i>Growth features</i> .....	19
3.3.6b. <i>Deformation features</i> .....	20
3.3.6c. <i>Etch features</i> .....	21
3.3.7. <i>Mineral inclusion content</i> .....	23
<u>4. INFRA-RED ABSORPTION PROPERTIES OF GEORGE CREEK DIAMONDS</u> .....	25
4.1. INTRODUCTION.....	25
4.1.1. <i>Infra-red classification of diamonds</i> .....	25
4.2. METHODS.....	28
4.3. RESULTS.....	30
4.3.1. <i>Nitrogen content</i> .....	30
4.3.2. <i>Nitrogen aggregation state</i> .....	30
4.3.3. <i>Platelet development</i> .....	34
4.3.4. <i>Hydrogen content</i> .....	35
4.3.5. <i>Possible spectral evidence of deformation</i> .....	35
4.3.6. <i>CO<sub>2</sub>-bearing diamonds</i> .....	36
4.3.6a. <i>Variability of the CO<sub>2</sub> absorption peaks</i> .....	37
4.3.6b. <i>Investigation of interference from background atmospheric CO<sub>2</sub> and possible orientation effects</i> .....	38
4.3.6c. <i>Pressure estimates from CO<sub>2</sub> absorption peaks</i> .....	39

## CONTENTS (VOLUME I) CONTINUED...

	page
<b>5. CATHODOLUMINESCENCE PROPERTIES OF GEORGE CREEK DIAMONDS</b>	<b>42</b>
5.1. INTRODUCTION	42
5.2. METHODS	43
5.3. RESULTS	43
5.3.1. Plate GC005	43
5.3.2. Plate GC006	44
5.3.3. Plate GC028	44
5.3.4. Plate GC037	45
5.3.5. Plate GC042	45
5.3.6. Plate GC036	46
5.3.7. Plate GC101	47
5.3.8. Plate GC008	48
5.3.9. Plate GC030	49
5.3.10. Plate GC150	49
5.3.11. Plate GC151	49
5.3.12. Plate GC171	50
5.3.13. Unpolished diamonds	50
5.3.14. Cathodoluminescence spectra	51
<b>6. GEOLOGICAL IMPLICATIONS OF CO<sub>2</sub>-BEARING DIAMONDS</b>	<b>53</b>
6.1. INTRODUCTION	53
6.2. THE STABILITY OF CO <sub>2</sub> IN MANTLE ASSEMBLAGES	54
6.3. IMPLICATIONS FOR DIAMOND GENESIS	57
<b>7. MINERAL INCLUSIONS</b>	<b>59</b>
7.1. INTRODUCTION	59
7.1.1. Peridotitic paragenesis	59
7.1.2. Eclogitic paragenesis	60
7.1.3. Mineral inclusions from cubic diamonds and fibrous diamond coat	60
7.1.4. Radiometric dating of diamond inclusions	61
7.2. METHODS	61
7.3. MINERALOGY	63
7.3.1. Black rosettes	64
7.3.2. Clinopyroxene	64
7.3.3. Orthopyroxene	66
7.3.4. Garnet	67
7.3.5. Phlogopite	68
7.3.6. Ilmenite	69
7.3.7. Rutile	70
7.3.8. Coesite	71

## CONTENTS (VOLUME I) CONTINUED...

	page
7.3.9. <i>Moissanite</i> .....	72
7.3.10. <i>Epigenetic inclusions</i> .....	72
7.4. THERMOBAROMETRY.....	72
7.5. IMPLICATIONS OF GEORGE CREEK INCLUSION MINERALOGY.....	75
7.5.1. <i>Evidence of subduction</i> .....	75
7.5.2. <i>Evidence of mantle metasomatism</i> .....	76
7.5.3. <i>Significance of K-rich inclusions</i> .....	77
7.5.4. <i>Compositional heterogeneity of the Colorado-Wyoming mantle</i> .....	77
<u>8. A MODEL FOR THE GENESIS AND MANTLE RESIDENCE OF GEORGE CREEK DIAMONDS</u> .....	 79
<u>ACKNOWLEDGEMENTS</u> .....	83
<u>REFERENCES</u> .....	84

# 1. INTRODUCTION

Mineral inclusions encapsulated in diamonds retain their primary crystallization composition unless secondary alteration is facilitated by the presence of fractures (Harris, 1968). The study of diamond inclusions therefore reveals valuable information regarding the nature of different diamond crystallization environments through space and time. In addition to the implications for mantle evolution, an understanding of how, where and why diamonds form is critical to the success of diamond exploration programmes.

Radiometric dating of diamond inclusions has provided unequivocal evidence that most diamonds of the peridotitic and eclogitic parageneses are xenocrysts of considerably greater age than the kimberlite or lamproite which served as a transporting medium to the surface of the earth (e.g. Kramers, 1979; Richardson *et al.*, 1984). The ancient ages determined for diamonds of the peridotitic paragenesis require the existence of thick and relatively cool continental lithosphere in the Archaean for the regional geotherm to have intersected the diamond stability field. Information pertinent to the early history of the earth may thus be obtained from the study of diamond inclusions.

Diamonds form most commonly in deep regions of the sub-continental lithospheric mantle characterized by peridotitic or eclogitic mineralogy (Meyer, 1985). Peridotitic inclusions may be divided into harzburgitic and lherzolitic sub-parageneses on the absence and presence of clinopyroxene respectively (e.g. Harris, 1992). Inclusions with compositions appropriate to wehrlitic, websteritic and calc-silicate sub-parageneses have also been recovered (Gurney *et al.*, 1984a; Sobolev *et al.*, 1984), indicating that diamond genesis may occur in mantle regions of significantly disparate mineralogy and bulk composition.

The volatile-enriched nature of fluid inclusions contained within fibrous cubic and coated diamonds implies that these diamonds grew in the presence of evolved fluids rich in K, and high but variable proportions of CO<sub>2</sub> and H<sub>2</sub>O (Navon *et al.*, 1988; Schrauder and Navon, 1994). Fluid compositions appear to vary continuously between a carbonatitic end-member rich in carbonate, Ca, Fe, Mg and P, and a hydrous end-member rich in Si and Al (Schrauder and Navon, 1994).

Chemical and thermal effects caused by the subduction of slabs of oceanic lithosphere into the mantle have been invoked to explain diamond genesis (e.g. Frank, 1967; Kesson and Ringwood, 1989b). Serpentinization of oceanic basalt and peridotite during subduction results in the removal of calcium from pyroxenes and its deposition in associated rodingites (Coleman,

1977; pp: 107). The extreme calcium depletion found in harzburgitic diamond inclusions and xenoliths has been attributed to their formation from subducted bodies of meta-serpentinite (Schulze, 1986). Water released by dehydration of subducted serpentinite bodies may initiate melting in mantle domains of eclogitic composition, and diamonds of the eclogitic paragenesis may crystallize at depths of ~150 - 400 km from such melts (Kesson and Ringwood, 1989b). The interaction of slab-derived melts with peridotite of the overlying mantle wedge provides a further mechanism for the formation of peridotitic diamonds (Kesson and Ringwood, 1989b).

Diamonds of the eclogitic paragenesis exhibit a wide range in carbon isotopic composition from -35 to +3 ‰  $\delta^{13}\text{C}$  (Kirkley *et al.*, 1991). In comparison, the isotopic composition of biogenic carbon contained within Precambrian sediments varies from -51 to -10 ‰ (Kirkley *et al.*, 1991). A more restricted range of  $\delta^{13}\text{C}$  values between -5 to +5 ‰ is characteristic of Archaean and Precambrian marine carbonate rocks (Veizer and Hoefs, 1976). The depletion of many diamonds of the eclogitic paragenesis in the heavier  $^{13}\text{C}$  isotope may reflect subduction of organic carbon into regions of the mantle where eclogitic diamond crystallization could occur (Sobolev and Sobolev, 1980; Kirkley *et al.*, 1991).

In an attempt to understand the heterogeneity of the Colorado-Wyoming mantle, and the complexities of diamond genesis and mantle residence time, 888 diamonds from the George Creek K1 (section GC 28) kimberlite dyke have been described in terms of their physical characteristics, inclusion composition, cathodoluminescence and IR absorption properties. Episodes of deformation, etching and resorption have modified the primary growth features of diamonds during residence in the mantle. The relationships between physical characteristics of the diamonds studied have been investigated in order to establish the relative timing of episodes of diamond growth, deformation, etching and resorption.

Cathodoluminescence photomicrographs have revealed complementary information regarding the complex intergrowth of at least two diamond generations. Anomalous luminescence colours caused by the presence of sub-microscopic  $\text{CO}_2$  inclusions characterize a diamond growth generation believed to be younger than the diamond generation(s) with normal cathodoluminescence. Evidence of extreme plastic deformation and radiation damage from  $\alpha$ -particle decay has also been recognized from cathodoluminescence photomicrographs.

The complex intergrowth relationships between different diamond growth generations in many of the George Creek diamonds necessitate considerable spatial resolution in the determination of carbon isotope compositions. For this reason the present method used at the University of Cape Town for carbon isotope determination (i.e. analysis of small fragments from diamonds

cracked open in a steel diamond cracker) is not suitable for these specimens. An investigation of the relationships between carbon isotope compositions and cathodoluminescence properties of polished diamond plates is currently being undertaken using the ion-probe at the University of Edinburgh.

A preliminary study of potential differences between the stable isotope composition of CO<sub>2</sub>-bearing and CO<sub>2</sub>-free growth generations has been completed by J. M. Gibson of the Department of Earth Science at the Open University. Results are presented in Table 1.1 and Fig. 1.1. CO<sub>2</sub>-bearing and CO<sub>2</sub>-free growth generations both show a depletion in the <sup>13</sup>C isotope, which has also been recognized in diamonds from the adjacent Sloan kimberlite. As discussed previously, this may reflect a contribution of organic carbon recycled to the diamond growth region by subduction. Analyses of CO<sub>2</sub>-bearing and CO<sub>2</sub>-free growth generations in the same diamond were obtained for only two specimens, both of which show a variation of ~2 ‰ δ<sup>13</sup>C, with the CO<sub>2</sub>-bearing fractions having the “lighter” carbon isotopic composition, but “heavier” nitrogen isotopic composition. However, it would be premature to discuss the stable isotopic composition of George Creek diamonds until a meaningful data set is obtained.

Infra-red absorption characteristics of George Creek diamonds have been analyzed in detail, in particular to explain the presence of the CO<sub>2</sub>-bearing diamond growth generation. The factors controlling the stabilization of free CO<sub>2</sub> fluid in the mantle are discussed with respect to mantle composition, temperature, pressure and oxygen fugacity. Consideration of these and other factors, such as the composition and evolution of the Colorado-Wyoming mantle, is necessary to explain the unique abundance of CO<sub>2</sub>-bearing diamonds from the George Creek locality.

The compositions of mineral inclusions have been investigated by electron microprobe, allowing for an interpretation of the mineralogy and metasomatic history of the diamond growth environment(s). Estimates of diamond formation temperatures have been made on the basis of major element partitioning between coexisting mineral inclusion pairs. An independent method, based on quantitative IR analysis of the aggregation state of substitutional nitrogen defects contained within diamonds, has also been used to estimate time-averaged mantle residence temperatures. Discrepancies between temperature estimates from the two methods are most likely to reflect uncertainties inherent in the calculations used, but possible implications for the thermal evolution of the diamondiferous mantle are discussed.

Relationships between the different diamond growth generations, inclusion compositions, and physical characteristics of George Creek diamonds have been interpreted within the framework of existing knowledge of the evolution of the Colorado-Wyoming mantle. Previous studies of

mantle-derived xenoliths (e.g. McCallum *et al.*, 1975, Ater *et al.*, 1984; Eggler *et al.*, 1987a, b) and diamond inclusions (e.g. Meyer and McCallum, 1986; Otter, 1990) from the State Line District have revealed the compositional heterogeneity and complex thermochemical evolution of the lithospheric mantle in this region. A model consistent with the tectonomagmatic development of the Colorado-Wyoming mantle is proposed to explain the different episodes of diamond genesis and the processes of deformation and resorption which have affected the diamonds sampled by the George Creek dyke system. In a broader context, the implications of processes involved in the genesis and mantle residence history of George Creek diamonds are interpreted with respect to diamond formation worldwide.

## **2. GEOLOGICAL SETTING OF THE GEORGE CREEK KIMBERLITE DYKES**

In contrast to most economically viable diamondiferous kimberlites from southern Africa and other parts of the world (Clifford, 1966), the kimberlites found in the Colorado-Wyoming Kimberlite Province are located “off craton” in a mobile belt of Proterozoic age (Karlstrom and Houston, 1984). The geological setting of the State Line district is described in terms of a collisional model (Eggler *et al.*, 1988) which involves northward thrusting of allochthonous Proterozoic rocks over cratonic rocks of the Archaean Wyoming Province. The country rocks exposed in the Colorado-Wyoming Kimberlite Province are thus unrelated to lithologies preserved at depth in the lower crust and upper mantle.

Magmatism arising from the collision of the Wyoming Province with an island arc terrane lying to the south ceased at 1.81 Ga, and accretion of the terrane was completed by 1.63 Ga (Hoffman, 1988). A similar tectonic setting in a Proterozoic mobile belt also characterizes the Argyle lamproite in Australia (Hancock and Rutland, 1984), and may be responsible for certain similarities (such as the abundance of eclogitic inclusions and highly-aggregated nature of substitutional nitrogen defects) in diamonds from George Creek and Argyle.

Unlike the majority of kimberlite occurrences in the State Line district, the George Creek kimberlites constitute a dyke system. Only minor amounts of tuffisitic kimberlite are present representing diatreme facies material (M. E. McCallum, pers. comm., 1995). This is similar to the adjacent Chicken Park diatreme-dyke system, except that the George Creek dykes are more limited in areal extent (M. E. McCallum, pers. comm., 1995).

### **2.1. GEOLOGICAL EVOLUTION OF THE COLORADO-WYOMING KIMBERLITE PROVINCE**

The study of inclusion-bearing diamonds and upper mantle xenoliths sampled by kimberlite eruptions in the Colorado-Wyoming Kimberlite Province provides insight into the magmatic, metasomatic, and tectonic events associated with the development and subsequent destruction of continental mantle lithosphere. Knowledge of these processes is essential if the conditions necessary for diamond genesis in the mantle are to be understood.

Figure 2.1. illustrates that radiometric ages determined for rocks decrease southwards from the Wyoming Province, indicative of continued accretion of younger material onto the craton

during continent - island arc collision (Van Schmus and Bickford, 1981). Model Nd ages of > 2.5 Ga within the Wyoming Province attest to the existence of a stable craton in the Archaean (Bennett and De Paolo, 1987). The Proterozoic Cheyenne Belt shear zone marks the suture between 2.5 - 2.0 Ga miogeosynclinal rocks of the Wyoming Province and 1.8 - 1.6 Ga eugeosynclinal rocks of a southern terrane which was juxtaposed at 1.85 - 1.63 Ga (Bennett and De Paolo, 1987; Hoffman, 1988; Karlstrom and Houston, 1984). Metamorphic and structural data suggest that bimodal calc-alkaline island arc lithologies, now preserved as highly deformed amphibolite facies gneisses and schists (Divis, 1976), were thrust northwards over the older greenschist facies rocks of the Wyoming Province (Eggler *et al.*, 1988).

The products of three broad phases of Proterozoic magmatism may be recognized; the earliest event at 1.78 Ga produced syntectonic quartz diorites above the southwardly-dipping subduction zone (Karlstrom and Houston, 1984). Three sizeable mafic intrusions, viz. the 1.78 Ga Elkhorn Mountain Gabbro (Snyder, 1980), undated Lake Owen and Mullen Creek mafic complexes, are located south of the Cheyenne Belt. Platinoids are associated with the latter two intrusions (M. E. McCallum, pers. comm., 1995) which are characterized by igneous layering (Karlstrom and Houston, 1984). Smaller bodies of metagabbro, olivine metagabbro, metadiorite and metapyroxenite are also present south of the Cheyenne Belt (Houston *et al.*, 1989). These mafic bodies may represent lower crustal intrusions in the island arc terrane, or remnants of oceanic material comprising tectonically emplaced ophiolite sequences (Karlstrom and Houston, 1984).

Deformation, metamorphism and significant crustal contamination accompanied plutonism during the second phase of felsic magmatism spanning 1.70 - 1.65 Ga (Karlstrom and Houston, 1984). A third phase of post-tectonic intrusive activity contributed to the further growth of continental crust and produced the 1.44 Ga Laramie anorthosite complex (Subbayarudu, 1975) and the 1.4 Ga Sherman Granite (Hills *et al.*, 1968; Peterman *et al.*, 1968; Subbayarudu, 1975). Rotation of thrusts to a vertical orientation occurred in response to crustal shortening, with the uplift and erosion of 10 - 15 km of stratigraphy at 1.5 - 1.3 Ga (Karlstrom and Houston, 1984).

### *2.1.1. The composition of the Colorado-Wyoming lithospheric mantle*

The wide variety of xenoliths sampled by kimberlites of the Colorado-Wyoming province alludes to the highly heterogeneous nature of the lithospheric mantle at the time of kimberlite eruption. Xenoliths recovered include lower crustal granulites, carbonatites, eclogites, depleted and enriched spinel-, spinel-garnet- and garnet peridotites, enriched ilmenite-garnet

peridotites, garnet pyroxenites, spinel-garnet and garnet websterites, and megacrysts (McCallum *et al.*, 1975; Kirkley, 1980; Eggler *et al.*, 1987a, b). The depleted (in basaltic components) xenolith suite is dominated by harzburgite, considered to be residual from extensive basic and ultrabasic Archaean magmatism analogous to that proposed to have occurred in the Kaapvaal Craton (O'Hara *et al.*, 1975; Boyd and Gurney, 1986).

The majority of enriched peridotite xenoliths are of lherzolitic composition and they are interpreted to be the products of metasomatic reaction between depleted peridotite and dykes, veins and layers of enriched garnet websterite and garnet pyroxenite (Eggler *et al.*, 1987a). Minerals in ilmenite peridotites are enriched in Fe and Ti, indicating an additional metasomatic event. Clinopyroxenes from deep infertile garnet peridotites exhibit strong LREE enrichment indicative of "cryptic" metasomatism in the Archaean, whereas clinopyroxenes from the more heterogeneous shallow lithosphere of Proterozoic age lack this LREE enrichment (Welt and Eggler, 1988).

Eclogite xenoliths are most abundant in the Sloan, Schaffer and Ferris kimberlites of the State Line district. Ater (1982) and Ater *et al.* (1984) distinguish between metaluminous (kyanite-free) and peraluminous (kyanite-bearing) eclogites. The former, which correspond to the Type II eclogite category, (MacGregor and Carter, 1970) are granoblastic in texture and may be further divided into Fe-rich and Mg-rich groups. Accessory phases associated with the metaluminous eclogites include rutile, sanidine, graphite, quartz and sphene, whereas corundum, rutile and sanidine are found in peraluminous eclogites (Ater *et al.*, 1984). Rare chromiferous eclogites containing emerald-green omphacite and purple garnet are generally found as single layers within peraluminous eclogites. Ater *et al.* (1984) interpret the eclogites studied as remnants of subducted oceanic crust which had undergone partial melting and subsolidus recrystallization.

A diamond-graphite eclogite xenolith (McCandless and Collins, 1989) and a diamond eclogite xenolith from the Sloan 2 kimberlite has been described in detail (Schulze, 1992). Both of these eclogites are distinct in composition from those described by Ater (1982) and Ater *et al.*, (1984), and contain elevated concentrations of K in clinopyroxene and Na in garnet. Thermobarometric calculations using an assumed pressure of 50 kb and the method of Ellis and Green (1979) indicate higher temperatures of equilibration (1084 - 1114 °C) for diamondiferous eclogites and eclogitic diamond inclusion minerals (Schulze, 1992; Otter and Gurney, 1989) than for non-diamondiferous eclogites (856 - 1056 °C). This would suggest a compositionally distinct (possibly deeper) source region for the diamondiferous eclogites compared to the non-diamondiferous eclogites (Schulze, 1992).

Figure 2.2 depicts the model proposed by Egger *et al.*, (1988) for the Colorado-Wyoming mantle lithosphere which was sampled by kimberlite eruption. Notable features include the heterogeneity of the shallow (< 100 km) lithosphere and the intersection of the down-dip extrapolation of the Cheyenne Belt with the greatest recorded depth of enriched garnet pyroxenite and websterite in State Line kimberlite (Egger *et al.*, 1988). This structure reflects the tectonic juxtaposition of Proterozoic and Archaean terranes which had experienced different enrichment and depletion events. The timing of these events can be constrained to at least 100 Ma before kimberlite eruption, to allow for cooling to the cool "fossil" geotherms recorded by xenoliths (Egger *et al.*, 1987a).

Entrained crustal xenoliths (Chronic *et al.*, 1969) and radiometric dating techniques (Naeser and McCallum, 1977; Smith, 1979) suggest a late Devonian age of 340 - 360 Ma for the Colorado-Wyoming kimberlites. Preliminary Rb-Sr ages of ~600 Ma, obtained from weathered samples of the George Creek kimberlite, suggest that the George Creek dykes may be significantly older than the other State Line kimberlites (C. B. Smith, pers comm.; in Carlson and Marsh, 1989). The presence of diamonds and rare diamondiferous xenoliths in State Line kimberlites implies the existence of a thick, cool, lithospheric mantle keel (conducive to diamond formation and preservation) until at least the Devonian. Although this keel has remained intact in the northern Wyoming Province, seismic and heat flow data indicate that substantial lithospheric thinning has affected the Colorado-Wyoming Kimberlite Province, possibly in response to subduction of the Farallon Plate commencing in the late Jurassic (Egger *et al.*, 1988).

## **2.2. DISCOVERY OF THE COLORADO-WYOMING KIMBERLITE PROVINCE**

The Colorado-Wyoming Kimberlite Province consists of several districts (see Fig. 2.3). More than 40 occurrences of hypabyssal and diatreme facies kimberlite have been recorded in the State Line District which is situated on the eastern flank of the northern Front Range (McCallum *et al.*, 1975; Smith *et al.*, 1979). This district is located approximately 60 km southeast of the Cheyenne Belt which forms the boundary between rocks of the Archaean Wyoming Province and Proterozoic rocks of an accreted island arc terrane (Karlstrom and Houston, 1984). The Iron Mountain district is also located "off craton" in the southern Laramie Range of Wyoming and encompasses more than 57 kimberlite diatremes, dykes and sills (Smith, 1977). Isolated kimberlite occurrences (see Fig. 2.3) include Estes Park dyke, Green Mountain diatreme, and the Sheep Rock (or Radichal) plug (Egger *et al.*, 1987a).

Kimberlite was first recognized in the State Line district in 1964 by M. E. McCallum at the Sloan diatreme (McCallum, 1991). The first authenticated diamond was recovered in 1975 from a serpentinized spinel-garnet lherzolite xenolith from the Schaffer 3 diatreme (Eggler and McCallum, 1975; McCallum and Eggler, 1976). Evaluation of the economic potential of the Colorado-Wyoming Kimberlite Province was initiated in the 1970's. Over 10 000 metric tons of kimberlite were processed, resulting in the recovery of more than 1 700 carats (McCallum, 1991). Diamond grade and quality was generally low, discouraging exploitation. The George Creek grade of 31 - 46 carats per hundred tons represents the highest recorded for the State Line district (D. B. Wyatt, written communication reported in McCallum, 1991).

### **2.3. THE GEORGE CREEK KIMBERLITE DYKES**

Three en-echelon dykes were discovered at lat. 40°53' N, long.105°42' W, in Larimer County, Colorado as a result of heavy mineral sampling, trenching and geophysical surveys (Carlson and Marsh, 1989). The following description of the George Creek kimberlite dykes is based on the findings of Carlson and Marsh (1989).

The dykes dip steeply to the northwest and their emplacement may have been controlled by east-west and northeast-southwest trending shear zones. The George Creek dykes are comprised of hypabyssal macrocystic phlogopite kimberlite which has been severely altered. The conversion of some primary ilmenites to pseudobrookites implies that the kimberlite dykes were subjected to oxidizing conditions (M. E. McCallum, pers. comm., 1992).

Diamonds investigated in this study were recovered from the K1 (or section GC 28) dyke, which is  $\pm$  1 km in length. The average width of the dyke is 0.7 m, but this varies along strike from several cm to 4 m. Contacts between the kimberlite and the surrounding amphibolite facies gneisses are sharp, with minor development of serpentine and carbonate veinlets which extend into the country rocks. The K1 kimberlite is highly carbonatized and ranges in colour from green-grey in the northeast to reddish brown-grey in the southwest. The northeastern exposures have a macrocrystic texture with abundant serpentinized olivine macrocrysts, phlogopite and minor garnet set in a fine-grained micaceous matrix. The southwestern exposures are characterized by a large proportion of crustal material in an extensively carbonatized, micaceous groundmass containing anhedral serpentinized olivine macrocrysts, scarce kelyphitized garnets and altered ilmenites. In contrast, crustal material is less prevalent in the northwest, and trace amounts of eclogites, ilmenite megacrysts and rare serpentinized peridotites are found.

The K3 dyke is highly silicified, as to a lesser degree, is the K2 (GC 29) dyke which exhibits a flow texture defined by aligned crustal xenoliths and altered mafic minerals. Both these dykes lack evidence of the extensive carbonatization which has affected the K1 kimberlite. The K3 dyke is narrow (< 1 m in width) and is approximately 400 m in length. The K2 dyke has a length of about 750 m and ranges in width from less than 1 cm to greater than 3 m. Detailed petrological descriptions of the George Creek kimberlite dykes are presented in Carlson and Marsh (1989).

### *2.3.1. The diamond-bearing potential of the George Creek kimberlites*

McCallum and Waldman (1991) discuss the diamond potential of several State Line kimberlites, as indicated by the composition of heavy mineral concentrates. Eclogitic and peridotitic garnets recovered from George Creek imply moderately high grades of both eclogitic and peridotitic paragenesis diamonds. In a plot of Cr<sub>2</sub>O<sub>3</sub> content versus CaO content (see Fig. 2.4a), several peridotitic garnets lie in the sub-calcic G10 field to the left of the 85 % line defined by Gurney and Switzer (1973), and Gurney (1984). The exceedingly sub-calcic nature of two concentrate garnets is regarded as being strongly indicative of the presence of diamonds of the harzburgitic paragenesis (McCallum and Waldman, 1991). As seen in Fig. 2.4b, six garnets fall in the worldwide eclogitic diamond inclusion field with elevated Na<sub>2</sub>O and TiO<sub>2</sub> contents, consistent with the presence of diamonds of the eclogitic paragenesis. The composition of concentrate chromites suggests low diamond potential, with most chromites containing less than 61 wt. % Cr<sub>2</sub>O<sub>3</sub>, and none falling within the diamond inclusion field (see Fig. 2.4d).

The composition of ilmenite megacrysts is thought to reflect the redox conditions prevailing in the mantle prior to kimberlite eruption, and may serve as an indicator of diamond preservation (Gurney and Moore, 1990). Figure 2.4c illustrates the presence of ilmenites rich in both Cr and Mg, indicating a low oxygen fugacity consistent with good diamond preservation. However, a population of ilmenites rich in Cr, but poor in Mg suggests that the mantle redox state was variable to more oxidising conditions which would have promoted etching and resorption of diamonds.

Ilmenite inclusions recovered from eclogitic garnet inclusions in George Creek diamonds are poor in Mg and Cr (see section 7.3.6) and are hence unrelated to the peridotitic Cr-rich ilmenites recovered from the heavy mineral concentrate. Ilmenite crystallization thus occurred in compositionally disparate regions of the lithospheric mantle under variable redox conditions. The variation in composition of macrocrystic ilmenites may therefore reflect a spatial (rather than a temporal variation) in oxygen fugacity, in the regions of the mantle sampled by the

George Creek kimberlite dykes. Crystallization of macrocrystic ilmenites rich in both Cr and Mg may have occurred in peridotitic mantle domains of a more reduced nature than those regions of the mantle in which Cr-rich, Mg-poor ilmenites formed. Evidence for such heterogeneity in the Colorado-Wyoming mantle is provided by the variable composition of enriched and depleted xenoliths recovered from kimberlites.

### **3. PHYSICAL CHARACTERISTICS OF** **GEORGE CREEK DIAMONDS**

#### **3.1. INTRODUCTION**

Detailed studies of diamonds from many individual localities have shown the existence of multiple sub-populations with different growth and mantle residence histories. Diamond sub-populations are present in different proportions in discrete kimberlite phases, diatremes or dykes of a particular locality, and these sub-populations differ amongst the various cratons (Gurney, 1989). The relationships between physical characteristics, inclusion paragenesis and composition, stable isotope composition, impurity content and nitrogen aggregation state facilitate recognition of diamond sub-populations.

Studies such as those of Robinson (1979), Robinson *et al.* (1989) and Otter (1990) have emphasized the distinction between physical characteristics of primary origin and those which develop subsequent to diamond growth. The relative timing of diamond growth, resorption and deformation episodes, reflected by the physical characteristics of diamond sub-populations, needs to be established with respect to mantle composition and evolution for diamond genesis and mantle residence to be understood.

#### **3.2. METHODS**

Bulk testing of 2 613 tons of megacrystic kimberlite breccia from the George Creek K1 (section GC 28) kimberlite by Lac Minerals yielded a total of 1 203.34 carats consisting of 80 282 diamonds. A parcel comprising 99.79 carats was provided for this study by M. E. McCallum. The parcel is not a truly representative fraction of the total recovery because of preferential incorporation of large stones with visible mineral inclusions.

Detailed descriptions of the physical characteristics of 888 diamonds from George Creek are presented in Appendix 1. The description scheme is based on that used by Otter (1990) to describe diamonds from the Sloan kimberlite in the State Line district, and was devised by M. L. Otter and M. E. McCallum, incorporating aspects of description schemes used by Harris *et al.* (1975) and Robinson (1979).

Diamonds were divided into size categories using Pierres diamond sieves. Table 3.1 lists the aperture diameter of the different Pierres sieves used to maintain a consistent difference of

0.2 mm between sieve apertures. All diamonds greater than Pierres sieve class 6 (i.e. +20 to +6) were described, but in the -6+5, -5+3 and -3+1 classes 100 representative diamonds were described, and 145 diamonds from the smallest (-1) class were studied. The diamonds studied in the -1 size class do not constitute a representative fraction of this class as diamonds with unusual colour, morphology, surface features and inclusions were selected for further investigation because this size proved most suitable for IR spectroscopy.

Diamonds were examined under a binocular microscope with a fibre-optic reflected light source and magnification of up to 240 ×. Several diamonds with unusual or typical morphology and surface features were selected for further investigation using the Cambridge S200 Scanning Electron Microscope (SEM) in the University of Cape Town's Electron Microscope Unit. An accelerating voltage of 10 kV and 20 μm aperture was used. Samples were cleaned in 30 % hydrofluoric acid, dichloromethane and then distilled water before they were mounted on aluminium stubs with colloidal silver dag. The stubs were then coated with a layer of Au/Pd ~20 nm thick to ensure electrical conductivity. The IR absorption properties and cathodoluminescence of selected specimens were also investigated and are discussed in Chapters 4 and 5 respectively.

### **3.3. RESULTS**

#### *3.3.1. Size*

The size distribution of the study sample (including those specimens not described) is depicted in Fig. 3.1. Apart from the abundance of large diamonds which was explained previously, George Creek diamonds approximate a lognormal size distribution, with an increase in number of specimens with decreasing size. To investigate the relationships between size and other properties such as colour, morphology, resorption and inclusion content, diamonds were assigned to three size categories, viz. large (+20 to +10 sieve classes), medium (-10 to +5 sieve classes and small (-5 to -1 sieve classes). The number of specimens comprising the large, medium and small size categories is 118, 425, and 345 respectively.

#### *3.3.2. Primary morphology*

Six morphological categories reflecting primary growth forms were used to describe the diamonds studied. These categories are loosely based on those of Sunagawa (1984a) and include octahedra, cubo-octahedra, cubes, macles, aggregates of small numbers of coalesced crystals, and diamonds of uncertain morphology. Diamonds comprising interpenetrant twins

were classified as aggregates. No polycrystalline aggregates of framesite, stewartite, ballas, carbonado or bort were recorded. A single diamond with modified cubic morphology was recognized and is depicted in Fig. 3.2f. Representative diamonds of the morphologies recorded for George Creek are illustrated in Figs. 3.2a - 3.2g.

Diamond dodecahedra with flat striated faces have been synthesized (Yamaoka *et al.*, 1977), indicating that under certain conditions this morphology may be a primary diamond growth form. However, dodecahedra have been shown to be the dissolution form of natural octahedral diamonds (Seal, 1963; Moore and Lang, 1974). Consequently, the primary growth form of diamonds exhibiting all stages of resorption between planar octahedra and rounded dodecahedra, was classified as octahedral. Because of its secondary nature with respect to diamond growth, the degree of resorption is described separately in section 3.3.5.

The morphology of crystals is controlled by the level of supersaturation between the liquid and solid phases during crystallization (Sunagawa, 1984b). Conditions of low carbon supersaturation promote the crystallization of single crystals, aggregates of few constituent crystals and twinned diamond crystals. In contrast, polycrystalline aggregates, fibrous cubes and fibrous diamond coats form by faster growth on multiple nucleation sites at higher degrees of supersaturation (Sunagawa, 1984a).

Synthesis of diamonds from graphite powder using non-metal catalysts at 1800 - 2200 °C and 7.7 kb has indicated the dependence of morphology on the type of catalyst used. Octahedral and cubic faces are promoted by catalytic use of MgSO<sub>4</sub> and Na<sub>2</sub>SO<sub>4</sub>, but less regular rounded morphologies result from the use of Mg(OH)<sub>2</sub> (Akaishi, 1993). Temperature and pressure of crystallization also influences the morphology of diamonds. Diamonds synthesized by Bovenkerk (1961) and Bezrukov *et al.*, (1970) were characterized by cubic morphology at lower temperatures or higher pressures than those required to produce octahedral morphology. This relationship may also control the morphology of natural diamonds, but does not permit simple interpretation as the growth rate of particular faces is affected by innumerable poorly understood physical and chemical factors (Sunagawa, 1984a, b).

Figure 3.3 illustrates the relationship between size and morphology for the three diamond size categories. The percentage of macles and aggregates decreases with decreasing size, whereas the percentage of octahedra increases. The percentage of aggregates containing macle components was calculated for the three size categories and followed the same trend of decreasing percentage of macles with decreasing size (see Fig. 3.4). The recognition of macles

(contact twins) was aided by the presence of macle lines with a distinctive herringbone pattern illustrated in Fig. 3.2e.

### 3.3.3. *Crystal state*

The crystal state of diamonds was described in terms of the percentage of the original volume lost by cleavage or fracture. In addition to unbroken whole crystals, chipped crystals (< 10 % volume loss), broken crystals (10 - 50 % volume loss) and fragments (> 50 % volume loss) were recognized. Whole and chipped crystals comprise 20, 17 and 31 % of the large, medium and small size classes respectively. Broken diamonds and fragments constitute the remaining 80, 83 and 69 % of these classes.

The presence of cavities with well-faceted cubo-octahedral morphology on breakage surfaces of approximately a quarter of the large and medium size diamonds and on 14 % of the small size diamonds was recorded. A cleavage surface displaying an inclusion cavity enclosed within a truncated trigonal etch pit is illustrated in Fig. 3.2p. The relative lack of inclusion cavities in diamonds of the small size category is consistent with the greater percentage of whole and chipped diamonds in this size category. The smaller diamonds have fewer large inclusions which could have caused breakage. This supports the hypothesis of Sutton (1928) that much diamond breakage occurs during depressurization as a result of stress caused by differential expansion between diamonds and encapsulated mineral inclusions.

Unetched, unresorbed cleavage and fracture surfaces result from brittle deformation which post-dates the major etching and resorption events. Some of this late-stage breakage may have occurred during diamond recovery. In contrast, 28, 22 and 27 % of the large, medium and small diamonds respectively exhibit resorbed breakage surfaces indicative of relatively early breakage which preceded resorption. Many breakage surfaces also reflect the development of etch pits which resulted from oxidation subsequent to crystal breakage.

### 3.3.4. *Colour*

Diamonds were assigned to nine categories on the basis of primary body colour, viz. colourless, off-white, grey, yellow, brown-yellow, yellow-brown, brown, red-brown and yellow-and-brown. A variable component of colourless diamond was found to be present in all the coloured diamonds that were subsequently cracked open for inclusion recovery, even very dark specimens which previously appeared to lack any colourless component. Colour

transitions in multiply-coloured diamonds spanned a continuum from sharp (fracture-related ?) to gradational boundaries (see Figs. 3.9a and 3.9b).

The proportion of colourless, grey and off-white diamonds decreases with decreasing size, whereas the proportion of all shades of brown and yellow increases with decreasing size (see Fig. 3.6). This trend is similar to the usual worldwide trend except for the increasing proportion of yellow diamonds with decreasing size (Harris, 1992). Infra-red spectroscopy demonstrated that all CO<sub>2</sub>-bearing diamonds from George Creek have some degree of yellow, brown or red-brown discolouration, and the presence of this sub-population strongly affects the colour distribution. Two CO<sub>2</sub>-bearing diamonds are illustrated in Figs. 3.9a and 3.9b.

However, diamonds of yellow, brown, or red-brown colour from the Congo do not contain CO<sub>2</sub>-absorption peaks in their IR spectra (H. J. Milledge, pers. comm., 1993). The single CO<sub>2</sub>-bearing diamond of unknown origin described by Schrauder and Navon (1993) displays yellow and colourless zonation. Thus the presence of high-pressure CO<sub>2</sub> in diamond appears to result in variable brown or yellow discolouration, but these colours do not necessarily imply the presence of CO<sub>2</sub>.

The causes of diamond body colour are complex, and are related to the interplay of many chemical and physical processes. The presence of trigonal N<sub>3</sub> defect centres, comprising three substitutional nearest-neighbour nitrogen atoms (Davies *et al.*, 1978; Bursill and Glaisher, 1985) imparts a yellow colour to diamonds (Loubser and Wright, 1973). This defect does not appear to be the cause of the yellow and brown-yellow colour of CO<sub>2</sub>-bearing diamonds from George Creek, as burning of these diamonds yielded negligible nitrogen (J. M. Gibson, pers. comm., 1994).

Brown (and scarce red and pink) diamonds from most localities worldwide commonly exhibit lamination lines caused by plastic slip (Harris, 1992) and hence these colours are believed to be largely due to deformation. The brown colour is attributed to the presence of graphitic or amorphous carbon along (111) lattice planes (Urusovskaya and Orlov, 1964).

Most grey diamonds from George Creek contain abundant small black rosette inclusions, which appear to be responsible for this discolouration. Infra-red studies of grey diamonds which possess absorption in the visible spectrum, in particular at 525, 545, 555 and 563 nm, suggest that the grey colour may be accompanied by the presence of substitutional hydrogen (Fritsch and Scarratt, 1989).

Green and rare brown surface discolouration was recognized in 3 % of the diamonds which were described. This discolouration is caused by  $\alpha$ -particle damage (Vance *et al.*, 1973) from the radioactive decay of uranium atoms. Temperatures in excess of 600 °C are required to change the colour of the radiation damage from green to brown (Vance *et al.*, 1973), implying that radiation damage occurs subsequent to kimberlite eruption, or all radiation damage would be brown in colour. Contact with uranium-bearing minerals such as perovskite produces discrete haloes on diamonds, whereas overall green staining results from the presence of uranium dissolved in circulating groundwater (Gurney, pers. comm., 1994). Unless radiation damage occurred as haloes, recognition of the primary body colour necessitated breaking diamonds to reveal the internal colour.

### 3.3.5. Resorption

Exposure of smooth-faced octahedral diamonds to oxidizing agents at elevated temperatures results in progressive dissolution at four-fold axes, until rounded dodecahedral (tetrahexahedroidal) morphology is attained (Robinson, 1979). The complete conversion of a regular octahedral diamond to dodecahedral morphology removes a minimum of 45 % of the original mass and volume of the diamond (Robinson, 1979).

Experimental graphitization of diamond octahedra at temperatures in excess of 1850 °C results in their conversion to dodecahedral morphology (Davies and Evans, 1972). Any process which forms trigonal etch pits on octahedral faces would also result in progressive conversion to dodecahedral morphology (Frank and Puttick, 1958). This is confirmed by the results of Kanda *et al.* (1977), who produced trigonal etch pits and curved resorption surfaces by reacting diamond octahedra with water vapour at temperatures of 1100 - 1500 °C and pressure of 50 kb. Thus the development of dodecahedral morphology and etch pits may result from the same process of oxidation. In this study discrete pits generated by oxidation are referred to as etch features, whereas relatively uniform rounded surfaces generated by oxidation are referred to as resorption features. The remarkable etch features of George Creek diamonds are discussed in section 3.3.6c.

Diamonds were assigned to six resorption categories, based on the scheme of D. N. Robinson as used by Otter (1990). Following McCallum *et al.* (1994), an additional sixth category comprising unresorbed, smooth-faced octahedra was incorporated into the classification scheme which is depicted in Fig. 3.8. The visual classification of diamond resorption is semi-quantitative, as resorption category 1 includes diamonds with 1 - 55 % preservation of primary morphology, and any irregularity of crystal shape complicates classification (Otter, 1990). If

the resorption category was not easily determined by visual inspection, diamond resorption was classified as uncertain.

Approximately a quarter of the George Creek diamonds studied exhibit differential resorption (or pseudohemimorphism, Robinson, 1979). This has been ascribed to partial protection of the diamond from oxidizing agents (e.g. the kimberlite magma and/or C-O-H fluids) within a xenolith (Robinson, 1979; Robinson *et al.*, 1989). For differentially resorbed specimens, the numerical average of the recorded resorption categories was computed. In each of the three size categories the numerical values representing the resorption categories of all diamonds were averaged, excluding those of uncertain resorption. These average resorption values facilitate semi-quantitative comparison of the relationship between size and resorption, as a value of 6 represents the total absence of resorption features and a value of 1 indicates tetrahedral morphology.

Large, medium and small size categories have average resorption values of 4.3, 4.1 and 3.6 respectively, implying a general increase in resorption with decreasing size, as has been observed for diamonds from other localities (Whitlock, 1973; Harris *et al.*, 1979; Otter, 1990). A larger proportion (44 %) of the small diamonds exhibit differential resorption compared to the medium and large diamonds (31 % of both size categories excluding those of uncertain resorption). The estimates of differential resorption may underestimate the actual percentages as it is likely that many diamonds classified as having uncertain resorption are differentially resorbed.

The relationship between diamond size and resorption is not simple. Small diamonds are more susceptible to resorption due to their high ratio of surface area to volume, but assuming that the resorption occurs dominantly in the kimberlite magma, the depth of diamond release from the enclosing xenolith has an additional influence on the degree of resorption (Robinson *et al.*, 1989). Haggerty (1986) proposes that most diamond resorption takes place during mantle residence, rather than during transport in the kimberlite magma. However, the deformation events which produce lamination lines (revealed on resorption surfaces) must occur prior to resorption events. Alternatively, Robinson *et al.* (1989) suggest that plastic deformation occurs during conduit development, and that most resorption occurs during entrainment of diamonds in the kimberlite magma.

No uniformly unresorbed diamonds of category 6 were found in sieve classes larger than +8. Diamonds (including differentially resorbed specimens) exhibiting preservation appropriate to classification as resorption category 6, comprise 22 small and 12 medium diamonds. Half of

these diamonds are of octahedral morphology, and the remaining half are aggregates. Unresorbed diamonds are predominantly colourless (59 %) and none shows deformation features, which may be manifested as linear arrays of trigonal etch pits on octahedral surfaces (Harris, 1992). These unresorbed specimens may represent a distinct sub-population, distinguished by distinctive colour proportions, morphology, apparent lack of deformation and lack of resorption.

Small peridotitic diamonds from Argyle and Sloan are predominantly unresorbed, in contrast to the larger eclogitic diamonds (Jaques *et al.*, 1989; Otter, 1990). The growth of these sub-populations (or their liberation from protecting xenoliths) must have postdated the major resorption event(s). Alternatively, unresorbed sub-populations may have resided in mantle domains which were not affected by extensive deformation or oxidation. During transport to the surface unresorbed diamonds must have been protected from resorption by some mechanism. A possible explanation is that these diamonds were enclosed in xenoliths which disaggregated at a late stage in the kimberlite eruption when most of the oxidizing volatiles had been degassed.

Unfortunately, the scarcity of inclusions large enough for microprobe analysis in the unresorbed diamonds from George Creek prevented the identification of the paragenesis of these diamonds. However, the presence of a few small inclusions of similar colour to eclogitic clinopyroxenes recovered from larger diamonds suggests that these unresorbed diamonds may be of the eclogitic paragenesis. Visual inspection based on inclusion colour failed to identify any peridotitic garnets or clinopyroxenes.

### 3.3.6. *Surface features*

Surface features are described with reference to the terminology of Robinson (1979), Otter (1990) and McCallum (pers. comm., 1992), used to describe diamonds from other North American localities. It is useful to distinguish between surface features caused by primary growth processes, deformation events, and oxidizing agents, in order to establish the sequence of events which affected the various diamond sub-populations during mantle residence.

#### 3.3.6a. Growth features

Primary growth features may be modified or destroyed by subsequent events of deformation, resorption, etching or renewed diamond growth. Hence, few surface features attributable to primary growth processes are recorded (Robinson, 1979), and include smooth faces, serrate

laminae, triangular plates and possibly knob-like asperities. The preponderance of these features (including knob-like asperities) in diamonds enclosed in xenoliths is compatible with their origin during diamond growth (Robinson, 1979; Shee *et al.*, 1982; Otter, 1990). Growth features are termed xenolithic features by Otter (1990), but the former term is preferred in this study as none of the diamonds studied was recovered from a xenolith.

Growth features are absent in the large and medium size categories, whereas 4 % of the small diamonds are characterized by one or more growth features. The abundance of growth features may be over estimated due to the preferential inclusion of unresorbed diamonds in the -1 sieve class. The most common growth features encountered are smooth faces, triangular plates and serrate laminae; only one diamond exhibits knob-like asperities (see Figs. 3.2a, 3.2i and 3.2j).

### 3.3.6b. Deformation features

As described previously, plastic deformation of diamond results in the development of slip planes which are highlighted as lamination lines on resorbed tetrahedral faces. Temperatures in excess of 1000 °C are required for diamond to deform plastically at pressures under 30 kb, although plastic behaviour may occur at lower temperatures under higher pressures (De Vries, 1975). Deformation thus occurs during mantle residence, and the deviatoric stress required implies that the diamonds were present in a subsolidus environment or liquid-crystal mush of less than 23 % liquid (Gurney, 1989).

Parallel wide (>100  $\mu\text{m}$  separation between individual lamination lines) and fine lamination lines dominate the deformation features recognized in George Creek diamonds. A single colourless diamond with intersecting lamination lines (Scotch Plaid texture) is illustrated in Fig. 3.2l. Extremely prominent wide lamination lines occur on the resorbed breakage surface of the large off-white diamond depicted in Fig. 3.2k.

A decrease in the percentage of diamonds with deformation features is recorded with decreasing size (see Fig. 3.5). This reflects a marked decrease in deformation features, as the higher degree of resorption of smaller diamonds should promote recognition of deformation features. Figure 3.7 illustrates the relationship between colour and the presence of deformation features. Colourless specimens constitute the majority (75 %) of plastically deformed diamonds.

Harris *et al.* (1983) report a positive correlation between plastic deformation and brown colour for diamonds from seven South African kimberlites. This relationship and the total proportion

of deformed diamonds is independent of diamond size. Robinson *et al.* (1989) suggest that heating of plastically deformed diamonds is necessary for graphitization and concomitant development of brown (and red and pink) colour. If heating is required during plastic deformation for the development of brown colour, the lack of brown colour in the majority of plastically deformed George Creek diamonds would imply the lack of a heating event during deformation. However, the association between plastic deformation and brown discolouration is still not fully understood, and other physical and chemical factors contribute to diamond colouration.

Type II diamonds (nitrogen-free) have a higher initial density of dislocations, lack platelets which appear to impede the movement of dislocations, and thus are susceptible to plastic deformation (Evans, 1976). The CO<sub>2</sub>-bearing parts of George Creek diamonds lack IR absorption peaks characteristic of substitutional nitrogen and platelets, and thus should show the highest incidence of lamination lines. Yet lamination lines are found most commonly on colourless diamonds lacking CO<sub>2</sub>. This suggests that the major deformation event(s) occurred prior to crystallization of the CO<sub>2</sub>-bearing sub-population or that most of the CO<sub>2</sub>-bearing diamonds resided in a region in the mantle which escaped major deformation. The former proposal is favoured because certain cathodoluminescence features of the CO<sub>2</sub>-free zones of many CO<sub>2</sub>-bearing diamonds indicate that they have been plastically deformed, as discussed in chapter 5.

### 3.3.6c. Etch features

Etch features produced on diamonds vary in morphology according to the temperature and pressure prevailing during oxidation, the nature of the oxidizing agent and the crystallographic orientation of the etched surface. Cubic faces and breakage surfaces parallel to cubic planes are characterized by tetragonal etch pits, as depicted in Figs. 3.2ad and 3.2ae. Trigonal and hexagonal etch pits develop on octahedral faces or breakage surfaces parallel to octahedral faces. By convention cubic and trigonal etch pits are said to have positive orientation if the margins of the pits are parallel to the edges of the face on which they occur, whereas the inverse orientation is referred to as negative orientation (Frank *et al.*, 1958).

Robinson (1979) reviews published diamond etching experiments, and presents results from high pressure experiments. Reaction of diamonds with molten kimberlite at low pressure produces negatively oriented etch pits at 1450 °C (Frank and Puttick, 1958), whereas Harris and Vance (1974) report the formation of negative etch pits at all temperatures > 1300 °C. The later authors note that at 1050 °C positive trigonal pits result from kimberlite which liberates

mostly water vapour, and that negative features are formed if mainly CO<sub>2</sub> is released. Diamonds exposed to molten kimberlite with added CO<sub>2</sub> at temperatures of 1150 - 1450 °C and a pressure of 30 kb develop negative etch pits exclusively (Robinson, 1979). Low pressure etching of diamonds by wet O<sub>2</sub> at T > 1000 °C, or by water vapour or wet CO<sub>2</sub> at T > 950 °C also produces negatively oriented pits (Evans and Sauter, 1961; Phaal, 1965). Hexagonal pits form at 900 - 1000 °C, possibly due to the combined action of O<sub>2</sub> and wet CO<sub>2</sub> which yield positive and negative trigonal etch pits respectively at this temperature (Phaal, 1965).

Reaction of diamonds with dry CO<sub>2</sub> results in the development of etch pits of irregular morphology (Phaal, 1965) as depicted in Fig. 3.2af. The action of dry CO<sub>2</sub> is also responsible for low-relief, lustrous “chemically polished” surfaces seen rarely on natural diamonds (Phaal, 1965). This surface texture is relatively common in diamonds from the Ellendale lamproites in Australia (Hall and Smith, 1984) and is also displayed by two George Creek diamonds, one of which contains a small proportion of CO<sub>2</sub>-bearing diamond. The rest of the CO<sub>2</sub>-bearing diamonds from George Creek lack “chemically polished” surfaces. The CO<sub>2</sub> fluid responsible for the development of “chemical polish” was present in the diamondiferous mantle under conditions which were unfavourable to diamond growth and conducive to resorption. The lack of a CO<sub>2</sub>-bearing growth generation in “chemically polished” diamonds from Ellendale provides further evidence that “chemically polished” surfaces develop during relatively late-stage diamond resorption.

George Creek diamonds are characterized by the intense development of hexagonal, trigonal and minor tetragonal and irregular etch pits (see Figs.3.2y to 3.2al). No positively oriented etch pits were observed. The texture comprising abundant hexagonal and trigonal etch pits > 50 μm in diameter is referred to as coarse etch sculpture (CES); similarly etch sculpture (ES) comprises etch pits < 50 μm in size (M. E. McCallum, pers. comm., 1992). Diamonds of all colours and morphologies exhibit etch pits, and only 10 % are unetched or only lightly etched.

The extreme development of etch textures may imply prolonged exposure of most George Creek diamonds to oxidizing C-O-H fluids in a hypabyssal environment. The occurrence of multiple etching episodes caused by different oxidizing agents is suggested by the variable nature of the etch pits: some diamonds exhibit only negative trigonal, tetragonal or hexagonal pits, others trigonal and hexagonal (± tetragonal ± irregular) pits. The size, depth, regularity and abundance of the etch pits also varies, even on different surfaces of individual diamonds.

Heavily etched, pitted hemispherical cavities (Robinson, 1979) are a prominent surface feature, especially in the larger diamonds (see Fig. 3.2al). This surface feature was recognized in 64 %

of the large diamonds, 37 % of the medium diamonds and 10 % of the small diamonds. The origin of these cavities is uncertain, but may be due to etching of inclusion cavities, as the decreasing percentage of diamonds with pitted hemispherical cavities is similar to the trend of decreasing percentage of diamonds with large inclusions and inclusion cavities on breakage surfaces, recorded with decreasing diamond size.

Deep ruts, depicted in Figs. 3.2d, 3.2t and 3.2ag - 3.2ak, characterize 34 % of the large diamonds, 22 % of the medium diamonds and 14 % of the small diamonds. The decrease in prevalence of ruts with decreasing diamond size reflects the lower proportion of aggregates amongst smaller diamonds, as ruts may develop between individual crystals of aggregates (see Figs. 3.3d, 3.2t, 3.2aj and 3.2ak). Ruts may also form along planar zones of weakness or radiate from inclusion cavities. In the George Creek diamonds ruts were invariably associated with severe etching. Orlov (1977) attributes the development of sinuous ruts (or etch channels) to the localized migration of oxidizing fluids which penetrate cracks in xenoliths.

Surface features associated with resorption surfaces are dominated by elongate hillocks and micro-hillocks, illustrated in Figs. 3.2w and 3.2x. Imbricate wedges (see Fig. 3.2n) are less common, but are also restricted to resorption surfaces. The trend of imbricate wedge and hillock elongation is parallel to the strike of octahedral growth layers. The morphology of elongate hillocks is determined by differential resistance of individual growth layers to resorption (Robinson, 1979). Hexagonal etch pits are developed on elongate hillocks of 23 % of the George Creek diamonds because well-developed hillocks are approximately equivalent to octahedral surfaces.

Corrosion sculpture (see Fig. 3.2m) is limited to resorbed tetrahexahedroidal faces (Robinson, 1979) and hence develops subsequent to the major resorption episode(s). Rapid, brief etching by a gaseous oxidizing agent is believed to be responsible for the development of corrosion sculpture (Gorina, 1971). Corrosion sculpture appears to be limited to diamonds recovered from the deeper levels of the Kimberley mines (Wager, 1914). Consistent with their recovery from a hypabyssal kimberlite dyke, 15 % of the George Creek diamonds studied exhibit some degree of corrosion sculpture, but this surface texture is never particularly well developed.

### *3.3.7. Mineral inclusion content*

Visual assessment of mineral inclusion content revealed the presence of one or more black rosettes in 73 % of the diamonds. Black rosettes and rutile inclusions proved to be the only minerals unequivocally associated with the CO<sub>2</sub>-bearing diamond generation, apart from a

single pure silicon oxide inclusion. The percentage of diamonds with visible orange inclusions (garnet and less common rutile) is estimated at 9 %. Green or colourless (i.e. clinopyroxene) inclusions are found in 23 % of the diamonds. However, these estimates are subject to the limitations in identifying inclusions caused by the severe etching of the diamonds and the preferential incorporation of inclusion-bearing minerals in the study sample. The compositions of minerals extracted and analyzed by electron microprobe are discussed in Chapter 7.

## **4. INFRA-RED ABSORPTION PROPERTIES OF** **GEORGE CREEK DIAMONDS**

### **4.1. INTRODUCTION**

Infra-red (IR) spectroscopy has considerably advanced the understanding of the defect content of diamonds and the thermal maturation processes which alter these defects during residence in the lithospheric mantle. Experimental investigations of kinetic processes involved in nitrogen aggregation have been hampered by the difficulties inherent to the high pressures and temperatures required. Calculations of either diamond mantle residence time or average equilibration temperature may be made if one of these variables is known, using activation energies derived experimentally for the nitrogen aggregation processes. However, the results obtained are subject to large uncertainties, particularly as deformation of diamonds may enhance the rate of nitrogen aggregation (Evans, 1992). Thermal modelling of diamond mantle residence time from spectrally determined nitrogen aggregation states will provide a valuable technique to supplement thermobarometric information derived from mineral inclusions, once a better understanding of the factors affecting nitrogen aggregation is achieved.

The presence of water and carbonate ions in coated diamonds has been detected using IR spectroscopy (Chrenko *et al.*, 1967; Navon *et al.*, 1988). Subsequently, Schrauder and Navon (1993) attributed IR absorption peaks at 2376 and 650  $\text{cm}^{-1}$  in an uncoated diamond to the  $\nu_3$  and  $\nu_2$  vibrations of solid  $\text{CO}_2$  respectively. The excellent agreement of the absorption peaks with spectra from solid  $\text{CO}_2$  was cited as evidence that the  $\text{CO}_2$  now possesses some degree of crystalline structure (Schrauder and Navon, 1993). The pressure-dependence of the position of the 2376  $\text{cm}^{-1}$  peak was used to infer that the  $\text{CO}_2$  is now present in sub-microscopic inclusions held at a pressure of 50 kb, and that the  $\text{CO}_2$  must have been trapped at even greater pressure in the hot mantle (Schrauder and Navon, 1993). This result has important implications for the redox conditions and speciation of volatiles present in the mantle during diamond growth. The presence of  $\text{CO}_2$  in approximately 10, 50, and 70 % of George Creek large, medium and small diamonds respectively was determined spectroscopically, and is discussed in detail in this chapter.

#### *4.1.1. Infra-red classification of diamonds*

The symmetry of perfect diamond crystal structure prohibits absorption in the IR region, yet the presence of defects allows phonon-assisted absorption (Lax and Burstein, 1955). All diamonds exhibit intrinsic lattice absorption from 4000 - 1500  $\text{cm}^{-1}$  due to two- and three-

phonon transitions (Collins and Fan, 1954; Sutherland *et al.*, 1954; Lax and Burstein, 1955). This is the only IR absorption recognized in nitrogen-free Type IIa diamonds, and is illustrated in Fig. 4.1a. Substitutional nitrogen impurities in Type Ia diamonds destroy local lattice symmetry and allow one-phonon transitions which are responsible for IR absorption at wavenumbers below  $1332\text{ cm}^{-1}$ .

Differences in the IR absorption spectra of diamonds facilitate their classification into Type I and Type II categories (Robertson *et al.*, 1934). Many specimens exhibit heterogeneity and may contain zones of Type I and Type II diamond (Berman, 1965; Takagi and Lang, 1964; Evans, 1976; Hanley *et al.*, 1977). A number of characteristic absorption features of diamonds permits their further subdivision into Type IaA, IaAB, IaB, Ib, IIa and IIb categories, as indicated in Table 4.1 which lists the defects responsible for these absorption features. Representative spectra of nitrogen-free Type IIa and IIb diamonds are shown in Figs. 4.1a and 4.1b respectively. Spectra from nitrogen-bearing Type Ib, IaA, IaAB and IaB diamonds are illustrated in Fig. 4.2 in order of increasing nitrogen aggregation state. Some diamonds exhibit absorption peaks at  $3107$  and  $1405\text{ cm}^{-1}$  (see Fig. 4.1c) which are attributed to the presence of hydrogen (Woods and Collins, 1983).

Type Ia diamonds owe their one-phonon IR absorption to the presence of aggregated substitutional nitrogen defects, whereas singly substituted nitrogen atoms give rise to Ib absorption, characteristic of most synthetic diamonds. It is believed that natural diamonds incorporate nitrogen as dispersed atoms during growth, and that annealing during mantle residence at elevated temperatures promotes aggregation of nitrogen atoms, first to form A defects and then to form B defects (Evans and Qi, 1982). A very small proportion of nitrogen atoms aggregates during annealing to form N<sub>3</sub> defects; clusters of 3 nitrogen atoms on (111) planes (Davies *et al.*, 1978; Bursill and Glaisher, 1985). The presence of N<sub>3</sub> defects in diamonds causes yellow colouration due to absorption of light in the visible and UV region, but does not contribute to the IR absorption (Davies *et al.*, 1978).

Kaiser and Bond (1959) demonstrated a positive correlation between the A defect absorption peak at  $1282\text{ cm}^{-1}$  and nitrogen content determined by mass spectrometry. Interpretations of symmetry properties, UV absorption and lattice constant measurements (Kaiser and Bond, 1959; Davies, 1976) are consistent with A defects comprising pairs of substitutional nearest-neighbour nitrogen atoms, as first proposed by Sobolev *et al.* (1968). The presence of B defects results in IR absorption at  $1174\text{ cm}^{-1}$ , and also contributes to the absorption peak at  $1282\text{ cm}^{-1}$ . Loubser and van Wyk (1981) have proposed that B defects comprise four substitutional nitrogen atoms surrounding a vacancy.

A further consequence of the nitrogen aggregation process is the development on cubic planes of planar structures (platelets) which give rise to anomalous spikes observed in X-ray diffraction patterns (Raman, 1944). Platelets may range in size from a few nm up to several  $\mu\text{m}$  in their maximum dimension and are visible in Transmission Electron Microscopy (TEM) and cathodoluminescence (Evans and Phaal, 1962). Absorption at  $1359 - 1378 \text{ cm}^{-1}$  has been shown to correlate with the X-ray spike intensity from platelets (Sobolev *et al.*, 1968) and is referred to as the B' peak.

The composition of platelets has been the subject of much debate between models invoking mainly nitrogen atoms as the major constituent (e.g. Lang, 1964) and models favouring carbon (e.g. Evans, 1976; Woods, 1986). Although nitrogen has been detected in platelets using Electron Energy Loss Spectroscopy (EELS), concentrations are lower than required by the Lang (1964) model for platelets (Berger and Pennycook, 1982). In addition, thermal conductivity studies (Turk and Klemens, 1974; Berman *et al.*, 1975) indicate that only 3 % of the nitrogen in diamonds is located in planar features, whereas 97 % is contained in small "point-like" aggregates.

The proposal that B aggregates consist of four nitrogen atoms around a vacancy (Loubser and van Wyk, 1981) provides a mechanism for the formation of platelets composed dominantly of carbon. For every B aggregate formed, a vacancy is generated by release of a carbon atom into the lattice as an interstitial. Woods (1986) suggests that it is these interstitial carbon atoms which aggregate to form platelets, with occasional incorporation of nitrogen atoms. Most diamonds, termed "regular" (Woods, 1986), show a positive correlation between the B and B' absorption peaks due to the presence of B aggregates and platelets respectively. This is consistent with nucleation and growth of platelets concurrent with (and as a consequence of) the aggregation of A defects to form B defects, as described above. However, "irregular" diamonds have been identified with lower B' (platelet) absorption than expected on the basis of their B defect absorption (Woods, 1986).

Electron microscopy of "irregular" diamonds revealed that partial degradation of the platelets has occurred to form dislocation loops (Woods, 1976). The presence of {111}-faceted nitrogen-bearing defects of nanometre size called voidites was also noted in "irregular" diamonds (Hirsch *et al.*, 1986; Barry *et al.*, 1987). Pure Type IaB diamonds studied by Van Tendeloo *et al.* (1990) contain voidites, yet lack any spectral or microscopic evidence of whole or degraded platelets. The authors therefore suggest that platelets do not develop in some diamonds (possibly because of extreme mantle residence temperatures) and that platelets are not directly related to the formation of voidites, but merely provide sites for their nucleation. Factors which influence platelet development are discussed in more detail in section 4.3.3.

## 4.2. METHODS

Dichloromethane was used to remove surface organic contamination from diamonds prior to spectroscopic analysis. Specimens were then mounted on adhesive tape along the edge of a glass microscope slide to allow uninterrupted transmission of IR radiation from the spectrometer. Spectra were determined using a Bruker IFS45 FTIR (Fourier Transform Infra-red) spectrometer with microscope attachment and MCT detector in the Crystallography and Mineral Physics Unit at University College, London. A sample aperture of 120  $\mu\text{m}$  was used for all analyses and liquid nitrogen was used to cool the detector. Spectra were acquired from 200 scans at a resolution of 8  $\text{cm}^{-1}$  over the range 4000 - 650  $\text{cm}^{-1}$ .

Quantitative determinations of nitrogen defect content and aggregation state were computed for selected spectra. These results were then used to estimate time-averaged equilibration temperatures ( $T_{\text{NA}}$ ) using an assumed mantle residence time ( $t_{\text{MR}}$ ) of 1.25 Ga. The assumption of a  $t_{\text{MR}}$  of 1.25 Ga is discussed in section 4.3.2. Quantitative analysis necessitated baseline correction of spectra and visual estimation of the percentage of A and B nitrogen defects. The nitrogen aggregation states of corrected spectra were determined by comparison with reference spectra from synthetic mixtures of pure A and B spectral end-members (Mendelsohn and Milledge, in prep., 1995; see Appendix 2.1). Errors in estimation of aggregation states may be of the order of 5 %, especially for very low and very high proportions of B defect content, or in the case of spectra which deviate significantly from the reference spectra.

Absorption in the one-phonon region (corresponding to wavenumbers below 1332  $\text{cm}^{-1}$ ) may be resolved into six components termed A - F (Clark and Davey, 1984a). The detailed structures and origins of E and F spectral components are unknown, and are not considered further in the spectral deconvolution. George Creek diamonds show spectral evidence of A, B and D components due to the presence of A and B nitrogen aggregates, and platelets respectively. Synthetic diamonds (and a very small percentage of natural diamonds, i.e. Type Ib) are characterized by C component absorption in the one-phonon region caused by isolated substitutional nitrogen atoms (Clark and Davey, 1984a). No diamonds from George Creek contained C component absorption in their spectra.

Considerable debate exists (Kaiser and Bond, 1959; Evans and Qi, 1982; Clark and Davey, 1984a; Woods *et al.*, 1990; Gibson *et al.*, 1992, 1993; Kiflawi *et al.*, 1993, 1994) as to the magnitude of the A, B and D absorption coefficients at 1282  $\text{cm}^{-1}$ . Differences in nitrogen content measured by nuclear techniques and mass spectrometry (Madiba *et al.*, 1994) are partly responsible for differences in calculated absorption coefficients. However, discrepancies in

temperatures of geological interest calculated using different absorption coefficients are of the order of only a few °C and are thus not considered to be significant.

Absorption values were normalized to a constant pathlength of 1 mm, by using the ratio of absorption at 1992 cm<sup>-1</sup> to 1.23, the known absorption value due to lattice vibrations of a 1 mm diamond slab at this wavenumber. Total nitrogen contents were calculated without correction for D component absorption according to the following equation (W. R. Taylor, pers. comm., 1993):

$$N_{(\text{tot})}/\text{at. ppm} = \mu_{(\text{tot})}^{1282} \cdot \alpha(\text{A})^{-1} + x(\text{B}) \cdot \mu_{(\text{tot})}^{1282} \cdot [\alpha(\text{B})^{-1} - \alpha(\text{A})^{-1}], \quad (1)$$

where:

$$\mu_{(\text{tot})}^{1282} = (\text{absorption at } 1282 \text{ cm}^{-1})/(\text{absorption at } 1992 \text{ cm}^{-1}) \cdot 1.23$$

$$\alpha(\text{A})^{-1} = \text{reciprocal absorption coefficient for the A defect} \\ = 152 \text{ at. ppm.mm (Gibson } et al., 1992)$$

$$\alpha(\text{B})^{-1} = \text{reciprocal absorption coefficient for the B defect based on mass} \\ \text{spectrometric determination of nitrogen content of specimens with well} \\ \text{characterized spectra} \\ = 652 \text{ at. ppm.mm (H. J. Milledge, pers. comm., 1993)}$$

$$x(\text{B}) = \text{spectral proportion of B defect}$$

Assuming that the aggregation of A defects to form B defects is a second order kinetic process, time-averaged estimates of mantle residence temperature may be calculated from nitrogen aggregation state using the following equation:

$$T_{\text{NA}}(^{\circ}\text{C}) = -E_a/R \cdot \{\ln([N_{(\text{tot})}/N_{(\text{A})} - 1] / [t_{\text{MR}} \cdot N_{(\text{tot})} \cdot A])\}^{-1} - 273.15, \quad (2)$$

where:

$$E_a/R = \text{activation energy/gas constant} = 81160 \text{ K,}$$

$$E_a = 7.03 \text{ eV (Taylor } et al., 1990)$$

$$N_{(\text{A})} = \text{nitrogen content in A defect form (at. ppm)}$$

$$A = \text{Arrhenius constant} = 2.94181 \times 10^5 \text{ s}^{-1} \cdot \text{ppm}^{-1}$$

$$t_{\text{MR}} = \text{diamond mantle residence time in seconds from crystallization to kimberlite} \\ \text{eruption}$$

## 4.3. RESULTS

### 4.3.1. Nitrogen content

The majority of George Creek diamonds contain substantially less than 1000 atomic ppm nitrogen, as seen in Fig. 4.3. Diamond plates, large, medium and small size categories show negatively skewed distributions. Spectral data relevant to nitrogen content and aggregation state for the diamond categories are summarized statistically in Table 4.2. Average nitrogen concentrations of diamond plates, large, medium and small diamonds are 295, 174, 286 and 359 at. ppm respectively. In some instances (especially inhomogeneous large specimens and CO<sub>2</sub>-bearing diamonds) the spectrally determined nitrogen content may reflect "dilution" by zones of Type II diamond.

Multiple spectra of individual plates reveal significant zonation of the specimens with variation in nitrogen content of up to 1427 at. ppm from 91 - 1518 at. ppm. Significant variation of nitrogen content of up to 334 at. ppm from 254 - 588 at. ppm was also determined for small diamonds of ~1 mm diameter. Plates allow for greater spatial resolution in the determination of spectra and this is obviously necessary for heterogeneous specimens such as these, but the spectra still represent the average absorption through the thickness of the plate.

### 4.3.2. Nitrogen aggregation state

As nitrogen aggregation state is a function of temperature, nitrogen concentration and mantle residence time, it is convenient to plot nitrogen concentration versus aggregation state (% of total nitrogen present in B defects) on graphs with temperature contours representing the aggregation state resulting from mantle residence times of 1 and 3 Ga. In this way diamond sub-populations of different ages and thermal histories may be recognized. Diamond populations of the same age and time-averaged mantle residence temperature ( $T_{NA}$ ) should define trends parallel to the isotherms. Any differences in diamond age and  $T_{NA}$  are reflected in the nitrogen aggregation state, but independent information of either diamond age or equilibration temperature is required from mineral inclusions for differences in nitrogen aggregation state to be interpreted geologically.

The choice of isotherms for 1 and 3 Ga is appropriate as radiogenic dating of eclogitic and peridotitic diamond inclusions from several localities indicates ages of 1.0 to 3.2 Ga, with eclogitic diamonds ranging in age from 1.0 to 1.7 Ga (Richardson, 1986; Richardson *et al.*, 1984, 1990, 1993; Smith *et al.*, 1986). Although no conclusive age data are available for

diamonds from the State Line district, a mantle residence time ( $t_{MR}$ ) of 1.25 Ga was used to calculate values for  $T_{NA}$  to compare with inclusion thermobarometric results. This would imply diamond growth in the mantle at 1.6 Ga following continent-island arc collision and prior to post-tectonic magmatism at 1.4 Ga. The Pb isotopic composition of a zircon inclusion encapsulated in a diamond from the Sloan kimberlite is consistent with a Proterozoic age (Otter, 1990). At least three diamond generations with different origins ( $CO_2$ -bearing, eclogitic and websteritic  $CO_2$ -free generations) are present at George Creek, so assumption of a  $t_{MR}$  of 1.25 Ga is obviously an over simplification, but the absolute age of these growth episodes is not known.

The choice of  $t_{MR}$  does not introduce significant error into temperature calculations as aggregation state is much more dependent on temperature than time. Assuming a nitrogen content of 328 at. ppm and aggregation state of 85 % B defects which is representative for George Creek diamonds, a  $t_{MR}$  of 1 Ga would require a  $T_{NA}$  of 1211 °C, whereas a  $t_{MR}$  of 3 Ga would require a  $T_{NA}$  of 1182 °C. This difference in  $T_{NA}$  (29 °C) is within the error limits of geothermometric calibrations for mineral inclusions and hence is not geologically significant.

Most individual diamond plates define nitrogen aggregation state trends which are sub-parallel to the isotherms constructed on Fig. 4.4. This is indicative of single-stage growth. Plates which exhibit wider scatter (GC028, GC036 and GC042) are characterized by extreme deformation features in cathodoluminescence. The extent to which plastic deformation influences aggregation state has not been quantified, but aggregation processes are thought to be enhanced by deformation (Evans, 1992). The trend defined by GC101 implies a younger age or cooler equilibration temperature for this specimen than for the other plates. The insensitivity of equation (2) to large differences in mantle residence time (as illustrated in the previous paragraph) suggests that it is more likely that diamond GC101 experienced cooler time-averaged mantle residence temperatures than the other diamond plates, as opposed to having a younger age.

The distribution of data from 28 large diamonds in Fig. 4.5 is similar to that of the plates in Fig. 4.4, as the eight diamonds polished into plates were all selected from the large size category. In addition to the well-aggregated specimens seen in Fig. 4.4, seven of the large diamonds contain nitrogen defects with an aggregation state of less than 50 %. These specimens are characterized by nitrogen concentrations of less than 60 at. ppm. Although some of these specimens extend the trend defined by most of the plates and well-aggregated large diamonds, the aggregation state of most of the less-aggregated large diamonds is consistent with mantle residence at cooler time-averaged temperatures than those experienced by the well-aggregated specimens.

Of particular note is GC001; two well-aggregated spectra and one poorly-aggregated spectrum was obtained for this diamond. This may imply that growth of this diamond was interrupted and continued at a later stage. A less likely possibility is that a substantial decrease in equilibration temperature occurred during prolonged growth. Older zones of well-aggregated nitrogen defects would reflect their greater age and higher temperature of formation than younger zones. Unfortunately the etching and great thickness exhibited by this specimen prevented accurate spatial correlation of nitrogen aggregation state with temperature estimates from mineral inclusions.

Diamonds from the medium and small size categories (see Figs. 4.6 and 4.7 respectively) show similar distributions to the plates and large diamonds in terms of nitrogen content and aggregation state. However, the nitrogen aggregation state of many of the small diamonds is slightly more advanced and conforms less to the 1200 °C isotherm than the distribution for the diamond plates, large and medium diamonds. This is seen in Fig. 4.8 which illustrates the relationship between nitrogen content and aggregation state for diamond plates and all the size categories, discriminated by the presence or absence of CO<sub>2</sub>.

Wherever possible spectra showing absence or minimal influence of the CO<sub>2</sub> absorption peaks were chosen from CO<sub>2</sub>-bearing diamonds, with strong evidence of CO<sub>2</sub> in other spectra. This was necessary to prevent "dilution" of the nitrogen content of the CO<sub>2</sub>-free zones by CO<sub>2</sub>-bearing zones which proved to be Type II. The CO<sub>2</sub>-free zones of CO<sub>2</sub>-bearing diamonds do not appear to have hydrogen and nitrogen contents or nitrogen aggregation states distinct from CO<sub>2</sub>-free diamonds.

Figures 4.4 to 4.8 show that the majority of George Creek diamonds contain highly-aggregated nitrogen defects in spite of the relatively low nitrogen concentrations. Average aggregation states (% of total nitrogen present as B defects) of 81, 63, 79 and 81 % were calculated for diamond plates, and large, medium and small diamonds respectively (see Table 4.2). Similar nitrogen contents and advanced aggregation states have been reported for eclogitic paragenesis diamonds of Proterozoic age from the Argyle lamproite, Australia (Harris and Collins, 1985; Taylor *et al.*, 1990). The well-aggregated nature of eclogitic diamonds from Argyle and George Creek are consistent with the generally higher temperatures calculated for coexisting eclogitic diamond inclusions worldwide than for peridotitic diamond inclusions (see Table 7.7).

The well-aggregated nature of nitrogen defects in most of the George Creek diamonds is indicative of prolonged mantle residence (~1.25 Ga) at calculated temperatures of the order of 1220 °C. Problems in determining an absolute value for T<sub>NA</sub> include uncertainties in the

activation energy, absorption coefficients and mantle residence time used in the calculation. However a much more significant error is introduced by processing of Type Ia spectra “diluted” by the presence of Type II diamond. The apparent aggregation state in such cases is relatively unaffected, but the apparent nitrogen concentration is lower than that of the Type Ia zones responsible for the one-phonon absorption. This leads to erroneously high calculated values for  $T_{NA}$  and proved to be a particular problem for CO<sub>2</sub>-bearing diamonds. Nevertheless, several spectra without evidence of the CO<sub>2</sub> absorption peaks are considered to be relatively unaffected by Type II “dilution” and were obtained from CO<sub>2</sub>-bearing diamonds by careful spectroscopic analysis of these specimens.

Histograms of  $T_{NA}$  for diamond plates and large, medium and small diamonds are presented in Fig. 4.9. The average value calculated for  $T_{NA}$  is higher than the average temperature calculated for non-touching inclusions (see Table 7.6). If this is not an artefact of the relatively large uncertainties associated with the calculations used to calculate  $T_{NA}$ , this result has implications for the thermal evolution of the Colorado-Wyoming mantle, as discussed below.

Temperature estimates from nitrogen aggregation state are strongly influenced by the highest temperature experienced by the diamonds, and cooling episodes do not have a significant effect on the aggregation state (Taylor *et al.*, 1990). Therefore, diamonds which have undergone significant cooling from their formation temperatures during mantle residence should yield values for  $T_{NA}$  intermediate between temperatures calculated from touching and non-touching inclusions, but biased towards the higher temperatures (W. R. Taylor, pers. comm., 1994).

A discrepancy of ~200 °C between temperatures calculated for touching and non-touching inclusions (see Table 7.6) provides strong evidence of cooling of the lithospheric mantle between diamond formation and kimberlite eruption. However, values of  $T_{NA}$  calculated for individual diamonds are consistently higher than temperatures indicated by inclusion geothermometry. This relationship is unlikely to be due to an underestimate for  $t_{MR}$  used in the computations as the degree of nitrogen aggregation has been shown to be much more dependent on temperature than time. Alternatively, the diamonds may have experienced a heating event subsequent to formation, before cooling to the mantle temperatures prevailing at the time of kimberlite eruption (which are recorded by the non-touching inclusions).

However, the discrepancy in temperature estimates from non-touching inclusions and nitrogen aggregation state is most likely to be related to the large uncertainties associated with the kinetics of the nitrogen aggregation sequence. The aggregation state of nitrogen defects in George Creek diamonds is likely to have been enhanced (Evans, 1992) by the extreme plastic

deformation which has affected many specimens. The equation used to calculate  $T_{NA}$  values does not take into account the D component absorption which is generally significant in well-aggregated diamonds such as the George Creek specimens (Clark and Davey, 1984a). These factors must be taken into account when comparing temperature estimates from nitrogen aggregation state with temperature estimates from geothermobarometric calculations based on inclusion compositions.

If an average mantle residence temperature of 1138 °C is assumed from inclusion thermometry, calculated mantle residence times for George Creek diamonds are considerably greater than the age of the earth. For example, if a  $T_{NA}$  of 1138 °C is assumed for diamond GC833, the nitrogen aggregation state of this diamond would require an implausible  $t_{MR}$  of 22 Ga. Similar age estimates are obtained for other diamonds, and this indicates the futility of age determination of diamonds from nitrogen aggregation state until the kinetic processes which enhance nitrogen aggregation are fully understood. Equally, this result places limitations on the absolute values of  $T_{NA}$  estimates for assumed mantle residence times.

#### 4.3.3. Platelet development

As discussed in section 4.1.1, platelets form as a result of the progressive aggregation of nitrogen defects and this process is dependent on nitrogen concentration, temperature and mantle residence time. However, the relationship between temperature and the development of platelets is not simple. In addition, plastic deformation is thought to have a detrimental effect on platelet development and preservation, and consequently the relative intensity of the platelet peak for a given nitrogen defect concentration and aggregation state is thought to reflect the thermal and deformation history of the diamond.

Experimental aggregation of A defects to form B defects at extreme temperatures of ~2500 °C decreased the ratio of the platelet peak relative to the B peak (Cooper, 1990), contrary to the Woods (1986) model favouring platelet development as a consequence of nitrogen aggregation. The relationship between the strength of the platelet peak and aggregation state thus appears to be dependent on temperature. Furthermore, Van Tendeloo *et al.* (1990) proposed that at the very high temperatures which enhance the aggregation of nitrogen defects, diamonds contain high concentrations of mobile vacancies which annihilate interstitial carbon atoms produced by the formation of B defects. Platelet formation from interstitial carbon atoms released by the formation of B aggregates would thus be suppressed by the presence of mobile vacancies. Accordingly, high temperature mantle residence conditions may prevent platelet development in some diamonds, whereas platelet degradation may occur in other specimens, possibly in

response to deformation or an increase in temperature. Platelet development and preservation in diamonds is therefore controlled in a complex manner by the thermal and deformation conditions which existed during mantle residence time.

The precise frequency of the platelet absorption correlates inversely with their size (Sobolev *et al.*, 1968; Clackson *et al.*, 1989) and hence the position of the platelet peak shows some dependence on total nitrogen content, as seen in Fig. 4.10. The platelet peak occurs at low values of 1358 - 1363  $\text{cm}^{-1}$  (characteristic of large platelets) for diamonds with low nitrogen content. This is consistent with suppressed nucleation and slow growth of platelets to a large size, as a consequence of slow aggregation of nitrogen defects in diamonds with low nitrogen content. Greater variation in nitrogen content is recognized in specimens with platelet peak positions from 1364 - 1372  $\text{cm}^{-1}$ .

The width of the platelet peak is dependent on wavenumber (Woods, 1986). Hence the integrated area of the platelet peak normalized in terms of diamond thickness,  $I(B')/\mu^{1992}$ , is a more reliable estimate of platelet peak strength than platelet peak absorption. "Regular" diamonds show a well defined negative correlation on a plot of  $I(B')/\mu^{1992}$  versus percentage of total nitrogen present in A aggregates, whereas "irregular" diamonds which experienced inhibited platelet growth or platelet degradation are distributed below the trend defined by "regular" diamonds (Woods, 1986). A broad increase in the integrated platelet peak absorption with decreasing proportion of nitrogen residing in A defect sites is seen in Fig. 4.11.

Plates GC036 and GC101 differ from the general trend of platelet evolution defined in Fig. 4.11 and may be classed as "irregular". Some of the data points for plate GC101 conform to the average platelet evolution trend defined by the other plates, but the others fall below this trend as a consequence of suppressed platelet formation or platelet degradation. This suggests a different growth history for this diamond which may be correlated with the unusual cubo-octahedral morphology and growth sector zonation revealed by the cathodoluminescence photomicrograph of this plate (see section 5.3.7).

In contrast, a decrease in  $I(B')/\mu^{1992}$  with decreasing proportion of nitrogen remaining in A defects is seen in Fig. 4.11 for plate GC036. Evidence of severe plastic and possible brittle deformation is recognized from the cathodoluminescence of this plate (see section 5.3.6). During crystallization this diamond may have incorporated an unusually high number of vacancies which would have compensated most of the interstitial carbon atoms generated by the aggregation of A defects to form B defects. Thus platelet growth may have been inhibited, facilitating relatively unimpeded migration of dislocations during deformation.

Alternatively, release of hydrogen from rutile inclusions may have accompanied their transition from rutile-type structure to  $\alpha$ -PbO<sub>2</sub>-type structure with decreasing temperature as discussed in section 5.3.6. The release of hydrogen impurities into the lattice may have had an adverse effect on platelet development. As discussed below, diamonds which do not show good correlation between the two absorption peaks attributed to hydrogen, are distinguished by unusual platelet development. Platelet evolution may thus be influenced primarily by temperature, nitrogen content and aggregation, but further investigation of the relationship between platelet development and hydrogen content is required.

#### 4.3.4. *Hydrogen content*

Diamonds with elevated hydrogen contents are invariably rich in nitrogen (Blinova *et al.*, 1988), but the inverse relationship does not hold (H. J. Milledge, pers. comm., 1993). The presence of hydrogen in diamonds may be detected from absorption peaks at 3107 and 1405 cm<sup>-1</sup> (Woods and Collins, 1983). Excellent correlation between the normalized areas under the 3107 and 1405 cm<sup>-1</sup> absorption peaks is shown in Fig. 4.12. The single specimen which lies above the trend in Fig. 4.12 shows extreme degradation of the platelet peak, whereas the two specimens which lie below the trend are characterized by unusually strong platelet peak absorption. Although hydrogen-rich specimens do show some degree of elevation in nitrogen content, there is no obvious relationship between hydrogen and nitrogen content in George Creek diamonds (see Fig. 4.13). The absence of IR absorption peaks at 3107 and 1405 cm<sup>-1</sup> in spectra with evidence of CO<sub>2</sub> absorption peaks suggests that hydrogen impurities are negligible in this diamond growth generation, although hydrogen may be present in some as yet unknown form.

#### 4.3.5. *Possible spectral evidence of deformation*

A very small component of IR absorption at 2443 cm<sup>-1</sup> was recognized in diamonds which lack interference from high pressure CO<sub>2</sub> absorption at this wavenumber. It is believed that this absorption is a result of the extreme deformation which affected a large proportion of George Creek diamonds during residence in the lithospheric mantle. Distortion of the diamond lattice by plastic deformation may have resulted in a lowering of lattice symmetry, enhancing phonon-assisted absorption. The wavenumber of this absorption corresponds to that of the TO + LO phonon assignment (i.e. transverse optic plus longitudinal optic) of Hardy and Smith (1961).

#### 4.3.6. CO<sub>2</sub>-bearing diamonds

Reports of macroscopic fluid and gas inclusions in diamonds abound in the early literature (e.g. Brewster, 1862; Bauer and Spencer, 1904; Schlossmacher, 1932), but recent investigations of a number of these and other specimens purported to contain such inclusions have refuted these claims (Roedder, 1984; pp: 507). Mass spectrometric analysis of gases released from diamonds by crushing or graphitization under high vacuum have indicated the presence of CO<sub>2</sub> and other volatile components such as H<sub>2</sub>O, CO<sub>2</sub>, CH<sub>4</sub>, Ar and possible H<sub>2</sub> and CO (Melton *et al.*, 1972; Melton and Giardini, 1974, 1975, 1981; Giardini and Melton, 1975). The possibility of contamination from the crushing apparatus and lack of reproducibility in these experiments casts doubt on these results (Roedder, 1984; pp: 509 - 511). Moreover, thermodynamic modelling of the stability fields of the volatile species reported from crushing or graphitization experiments indicates that these species are not stable in the proportions reported, at the temperatures, pressures and redox conditions necessary for diamond growth (Taylor, 1988; Fedorov *et al.*, 1991).

The presence of anomalous IR absorption properties in several George Creek diamonds was first observed by Robinson and Swash (1990). Similar anomalous IR features detected for a diamond of unknown origin were convincingly ascribed to the presence of sub-microscopic inclusions of solid CO<sub>2</sub> at a pressure of 50 kb (Schrauder and Navon, 1993). No evidence of other IR-active volatiles such as H<sub>2</sub>O, CH<sub>4</sub> or CO is found in spectra of CO<sub>2</sub>-bearing diamonds. The presence of CO<sub>2</sub> in diamonds appears to be an exceedingly rare phenomenon for most localities, except for George Creek where approximately half of the diamonds are CO<sub>2</sub>-bearing.

Very few diamonds containing spectral evidence of solid CO<sub>2</sub> have been recognized amongst diamonds from Siberia, Australia and from the Sloan kimberlite which is also located in the State Line kimberlite district (H. J. Milledge, pers. comm., 1993). Several diamonds from Jagersfontein kimberlite in South Africa contain "cloud-like" inclusions which give rise to IR absorption typical of liquid CO<sub>2</sub> at relatively low pressure (H. J. Milledge, pers. comm., 1993). Infra-red spectroscopy has indicated the presence of CO<sub>2</sub> in yakutite, an impact-generated mixture of cubic diamond and hexagonal diamond (lonsdaleite) recovered from the Popigai astrobleme in Yakutia, Russia (Milledge *et al.*, 1994). Representative examples of CO<sub>2</sub>  $\nu_3$  absorption peaks characteristic of the IR spectra obtained for diamonds from George Creek and Jagersfontein are compared with those from yakutite and atmospheric CO<sub>2</sub> in Fig. 4.14.

#### 4.3.6a. Variability of the CO<sub>2</sub> absorption peaks

Evidence of the IR absorption peaks at 650, 2376, 3620 and 3752 cm<sup>-1</sup>, attributed to the presence of CO<sub>2</sub> (Schrauder and Navon, 1993), was found in George Creek diamonds characterized by some degree of yellow, brown or red-brown colour. Strong absorption bands at 650 and 2376 cm<sup>-1</sup> are ascribed to the  $\nu_2$  orthogonal bending vibration modes and  $\nu_3$  asymmetric stretching mode of CO<sub>2</sub> respectively (Alberty, 1987; pp: 511; Schrauder and Navon, 1993). Weak absorption at 3620 and 3752 cm<sup>-1</sup> results from  $\nu_3 + 2\nu_2$  and  $\nu_3 + \nu_1$  combination bands respectively (Schrauder and Navon, 1993).

The frequencies of the fundamental modes of solid CO<sub>2</sub> are sensitive to pressure changes and may be used to estimate the pressure of CO<sub>2</sub> encapsulated within sub-microscopic inclusions in the diamond lattice (Hanson and Jones, 1981; Schrauder and Navon, 1993). Experimental evidence indicates that the wavenumber of the  $\nu_2$  bending vibration of CO<sub>2</sub> decreases with increasing pressure, whereas the wavenumber of the  $\nu_3$  asymmetric stretching vibration increases with increasing pressure (Hanson and Jones, 1981). The  $\nu_3$  absorption peak is subject to greater pressure dependence and provides more reliable pressure estimates than the  $\nu_2$  absorption peak which shows considerable anharmonicity (Hanson and Jones, 1981). The relationship between pressure and wavenumber of the  $\nu_3$  absorption peak of solid CO<sub>2</sub>, determined experimentally by Hanson and Jones (1981), is shown in Fig. 4.15.

The nature of the  $\nu_3$  absorption in George Creek diamonds is investigated in greater detail as this band proved to be the strongest in all spectra. Correlation with the  $\nu_2$  peak proved to be a problem as this peak was often beyond the lower wavenumber limit (650 cm<sup>-1</sup>) of the spectrometer. Several variants (including single peaks, doublets and triplets) of the characteristic CO<sub>2</sub>  $\nu_3$  absorption peak may be recognized in expanded IR spectra from George Creek CO<sub>2</sub>-bearing diamonds which are presented in Fig. 4.16. Expanded spectra show that many of the  $\nu_3$  peaks which appear to be single in unexpanded spectra are resolvable into two or three components (see Fig. 4.17 and Appendix 2.6).

Considerable variation in the intensity and shape of the CO<sub>2</sub>  $\nu_3$  absorption peak(s) exists within single specimens as seen in Fig. 4.18. In this and several other specimens, the nature of the CO<sub>2</sub>  $\nu_3$  absorption peak(s) correlates with diamond colour, although this correlation is not consistent for all specimens. In the multi-coloured diamond depicted in Fig. 4.18, red-brown areas are characterized by a single CO<sub>2</sub>  $\nu_3$  absorption peak, dark brown areas are characterized by doublets with the lower shoulder at the higher wavenumber side, and the CO<sub>2</sub> doublets detected in yellow areas have the lower shoulder at the lower wavenumber side.

Although spectra with CO<sub>2</sub> absorption peaks are restricted to areas of yellow, brown-yellow, yellow-brown, brown or red-brown colour in all the George Creek diamonds, there is no consistent correlation between peak morphology or height with diamond colour. However, as noticed by Schrauder and Navon (1993), there is generally a positive correlation between the height of CO<sub>2</sub> absorption peaks and the intensity of diamond colour for diamonds with variable yellow or brown colouration, but this relationship does not hold for red-brown diamonds. In fact, some of the darkest red-brown diamonds (e.g. Plate GC151) have weaker CO<sub>2</sub> absorption peaks than yellow CO<sub>2</sub>-bearing diamonds, and show variations in CO<sub>2</sub> absorption peak height which are unrelated to the intensity of red-brown colour.

In order to facilitate discussion,  $\nu_3$  peaks characterized by wavenumbers  $\geq 2400$  cm<sup>-1</sup> are referred to as  $\nu_{3a}$  peaks, whereas peaks in the 2365 - 2399 and 2339 - 2364 cm<sup>-1</sup> ranges are referred to as  $\nu_{3b}$  and  $\nu_{3c}$  peaks respectively. Plots of  $\nu_{3a}$  and  $\nu_{3b}$  peak height versus  $\nu_2$  peak height (see Figs. 4.19a and 4.19b) show reasonable positive correlation, whereas the plot of  $\nu_{3c}$  peak height versus  $\nu_2$  peak height shows considerable scatter without a positive correlation (see Fig. 4.19c). A possible cause for the lack of correlation between  $\nu_{3c}$  and  $\nu_2$  peak height is discussed below.

#### 4.3.6b. Investigation of interference from background atmospheric CO<sub>2</sub> and possible orientation effects

The good agreement between  $\nu_{3c}$  peak wavenumbers with data from reference spectra showing positive and negative CO<sub>2</sub> backgrounds (see Fig. 4.20) suggests that the  $\nu_{3c}$  peaks may be caused by CO<sub>2</sub> at atmospheric pressure. Attempts were made to compensate for fluctuations in the background levels of atmospheric CO<sub>2</sub> by taking multiple spectra at the same location with background references of variable atmospheric CO<sub>2</sub> content. This had no significant effect on the CO<sub>2</sub> absorption peaks, nor was any orientation effect detected in multiple spectra taken from approximately the same location, with the diamond in different orientations (see Fig. 4.21). Any limited variations in spectra of differently oriented diamonds are possibly due to small-scale spatial heterogeneity of CO<sub>2</sub> inclusions in terms of concentration and pressure, as it is impossible to analyse the same volume of diamond in different orientations. The  $\nu_{3c}$  peaks are thus believed to be caused by low pressure CO<sub>2</sub> from partially decrepitated inclusions or within fractures in the diamonds. This is consistent with the poor correlation of the  $\nu_{3c}$  peak height with the high pressure CO<sub>2</sub>  $\nu_2$  peak height seen in Fig. 4.19c.

#### 4.3.6c. Pressure estimates from CO<sub>2</sub> absorption peaks

Comparison of the frequencies recorded for  $\nu_{3a}$  peaks with Fig. 4.15 implies that extreme pressures (in excess of 200 kb at room temperature) exist in the CO<sub>2</sub> inclusions found in specimens with  $\nu_{3a}$  peaks. Extrapolation to mantle temperatures would necessitate even greater pressures which seem geologically unreasonable, particularly as no evidence of inclusions associated with great depth (e.g. majoritic garnet) have been identified. The shift of the  $\nu_{3a}$  and  $\nu_{3b}$  peaks to high wavenumbers may be due to interaction of the CO<sub>2</sub> molecules with carbon atoms of the diamond lattice as described below.

Re-equilibration and annealing of CO<sub>2</sub>-bearing fluid inclusions in mantle xenoliths at lower temperatures and pressures may result in precipitation of graphite or amorphous carbon around the margins of inclusion cavities (Pasteris, 1988). A consequence of the large molar volume of graphite is that such precipitation would increase the pressure within the inclusions. Thus, graphite precipitation from CO<sub>2</sub> inclusions in some specimens may give rise to high wavenumber  $\nu_3$  peaks in their spectra. Evidence that graphitization has affected CO<sub>2</sub>-bearing diamonds is provided by visible graphite rosettes of up to ~400  $\mu\text{m}$  in diameter which are commonly associated with coloured zones of CO<sub>2</sub>-bearing diamond. Precipitation of thin films of graphite on the walls of sub-microscopic CO<sub>2</sub> inclusions may have formed in response to the same conditions which resulted in the development of graphite rosettes. The positive correlation of  $\nu_{3a}$  peak height with  $\nu_{3b}$  and  $\nu_2$  peak height (see Figs. 4.22 and 4.19a) suggests that the degree of secondary graphitization is proportional to the concentration of high pressure CO<sub>2</sub> inclusions in the diamond lattice. It is not known what factors would control precipitation of graphite, but deformation and/or prolonged equilibration at conditions within the stability field of graphite seem likely.

Based on the equation of state for solid CO<sub>2</sub> (Liu, 1984) which predicts a molar volume of  $21 \pm 0.4 \text{ cm}^3 \cdot \text{mol}^{-1}$  for CO<sub>2</sub> at room temperature and 50 kb pressure, Schrauder and Navon (1993) propose that intersection of CO<sub>2</sub> isochores with a typical shield geotherm would require crystallization of CO<sub>2</sub>-bearing diamonds at pressures of 70 - 85 kb, at depths of 220 - 270 km. This is considerably higher than most geothermobarometric estimates for diamond growth (see Table 7.7). However, these pressure and depth estimates may be reconciled with the crystallization of CO<sub>2</sub>-bearing diamond at temperatures and pressures appropriate to the lithospheric mantle if the elevated pressures are a consequence of secondary graphitization.

Unfortunately, an independent estimate of pressure from geothermobarometric calibrations is prevented by the absence of coexisting mineral phases such as garnet and orthopyroxene in the

CO<sub>2</sub>-bearing growth generation. Estimates of the pressure of CO<sub>2</sub> contained in sub-microscopic inclusions from the wavenumber of the  $\nu_3$  absorption peak, are therefore subject to limitations, as it is well known that annealing processes and crystallization of daughter minerals and/or graphite may alter the composition and pressure of fluid inclusions (Roedder, 1984). Moreover, partial decrepitation due to changes in temperature and pressure results in a decrease in pressure of the CO<sub>2</sub> inclusions.

Decrepitation of fluid inclusions occurs when the difference between external pressure and internal pressure of an inclusion exceeds the yield strength of the enclosing diamond. The ability of inclusions to withstand decrepitation may be modelled as a function of inclusion diameter (Taylor, 1988). The internal pressure of the inclusion decreases rapidly during growth of an ellipsoidal crack around the inclusion. The energy required to break carbon-carbon bonds to form the crack and compress the adjacent lattice atoms is compensated by that released by expansion of the fluid (Taylor, 1988).

For an initial fluid pressure of 55 kb, C-O-H inclusions of 1 and 10  $\mu\text{m}$  diameter would generate cracks with equilibrium radii of 6 and 170  $\mu\text{m}$  and final internal fluid pressures of 9.6 and 2.0 kb respectively (Taylor, 1988). Hence it is thought that inclusions greater in size than 10  $\mu\text{m}$  would not survive diamond entrainment and ascent to the surface in kimberlite magma. The calculations of Taylor (1988) indicate that there is a negative correlation between original inclusion size and the final pressure maintained after partial decrepitation, and thus the smallest sub-microscopic inclusions are most likely to survive and provide the most accurate estimate of the pressures which existed in the fluid at the time of entrapment. Prolonged residence in the hot mantle would have promoted the annealing of CO<sub>2</sub> inclusions to produce planar arrays of more evenly spaced pseudo-secondary inclusions of smaller size, as described by Roedder (1984). The survival of CO<sub>2</sub> inclusions in George Creek diamonds may have been promoted by annealing to sub-microscopic size during mantle residence time.

Infra-red spectroscopy and thermodynamic considerations have revealed that CO<sub>2</sub> inclusions in George Creek diamonds have undergone a number of modifications in response to changes in pressure and temperature. Caution must therefore be exercised in the interpretation of the present spectral features associated with CO<sub>2</sub>-bearing diamond, and extrapolations of estimates of pressure and other physical properties of the inclusions to mantle conditions are limited by these considerations. The sub-microscopic size of the inclusions is responsible for their preservation, but precludes the use of conventional fluid inclusion analysis techniques such as homogenization experiments using microscope hot- and cold-stage attachments, or Laser Raman Microthermometry.

## **5. CATHODOLUMINESCENCE PROPERTIES** **OF GEORGE CREEK DIAMONDS**

### **5.1. INTRODUCTION**

Under electron-beam bombardment many substances, including diamond, emit electromagnetic radiation referred to as cathodoluminescence. This phenomenon is caused by the excitement of electrons from a valence band to a conduction band, followed by their relaxation and the emission of light (Davies, 1979). Properties of cathodoluminescence such as wavelength, polarization and decay time provide information on the electronic transitions involved, and can be useful in identifying the defects responsible for the luminescence. Reviews by Davies (1979) and Walker (1979) indicate that the origin of cathodoluminescence is extremely complex, hence a comprehensive discussion is beyond the scope of this thesis.

Cathodoluminescence in diamond is generated by point defects such as substitutional impurities (e.g. nitrogen, boron, hydrogen, aluminium), intrinsic defects (vacancies and interstitial sites) and dislocation defects (Zezin *et al.*, 1990). However, the intensity of luminescence in diamond is not directly related to the concentration of luminescence centres (Davies, 1979). In addition, the strong temperature-dependence of emission intensities is not linear (Zezin *et al.*, 1990) and electron-donor centres may be gettered (compensated for) by the presence of elements which act as electron-acceptors. Milledge *et al.* (1989) suggest that aluminium associated with diamond inclusions such as garnet may getter nitrogen, resulting in dark or non-luminescent areas surrounding garnet inclusions.

The defects responsible for many of the peaks in cathodoluminescence spectra are still unknown. On account of the above factors, the potential of cathodoluminescence as a quantitative analytical technique has yet to be developed. The qualitative information and high spatial resolution provided by cathodoluminescence images has nevertheless proved to be invaluable in the interpretation of IR spectroscopy and X-ray diffraction patterns. The ability of cathodoluminescence to discriminate between growth zones or growth sectors with very slight differences in defect concentration has extended the understanding of synthetic and natural diamond growth processes, particularly the growth sector dependence of impurity incorporation.

Planar aggregates (platelets) on (100) lattice planes which are visible in TEM and are responsible for anomalous X-ray diffraction "spikes", may be recognized by their strongly polarized yellow-green cathodoluminescence (Evans and Phaal, 1962). Cathodoluminescence studies of polished diamond plates have revealed exceptionally complex growth zonation in certain specimens.

Variation of up to 4 ‰  $\delta^{13}\text{C}$  in carbon isotope composition between growth zones has been recognized in integrated cathodoluminescence and carbon isotope studies (Wilding *et al.*, 1990; Otter *et al.*, 1991). The distribution of defects such as platelets and small nitrogen aggregates may vary considerably between different growth zones. The occurrence of multiple resorption events during diamond growth is indicated by the truncation of growth zonation (Wilding, 1990; Zevin *et al.*, 1990; Otter *et al.*, 1991; Bulanova, 1995).

## 5.2. METHODS

George Creek diamonds were investigated using Technosyn and Nuclide Luminoscope cathodoluminescence attachments for optical microscopes in the Electron Microscope Unit at the University of Cape Town and the Crystallography and Mineral Physics Unit at University College, London respectively. Samples were cleaned by ultrasonic agitation in hydrochloric acid and then dichloromethane before they were mounted on copper plates with water-soluble carbon dag. Accelerating voltages of 12 - 15 kV were used and the electron beam current was maintained at approximately 0.8 mA by adjustment of a sensitive leak valve once vacuum had been achieved. Cathodoluminescence spectra were recorded for selected specimens using the Cambridge S180 SEM in the Crystallography and Mineral Physics Unit at University College, London. Liquid nitrogen was used to cool the specimens, thus increasing spectral resolution.

As cathodoluminescence is a surface phenomenon and the identification of internal zonation was obscured by the severely etched nature of George Creek diamonds, several diamond plates polished parallel to the (100) plane were studied as well as the unpolished specimens. High magnification cathodoluminescence photographs of diamond plates were used for comparison of features recognized in IR spectra with the cathodoluminescence zonation.

## 5.3. RESULTS

### 5.3.1. Plate GC005

Figure 5.1 illustrates the bright blue luminescence and well-developed octahedral growth zonation characteristic of many natural diamonds. This blue Band A luminescence is attributed to the interaction of electron-donor and electron-acceptor defect pairs (Davies, 1979). The presence of a macle twin plane is marked by the angular intersection of octahedral growth zones to define a “herringbone” pattern.

Considerable variation in nitrogen content and aggregation state was determined on the basis of IR absorption. Substitutional nitrogen content varies between 90 and 1518 at. ppm, and 74 - 99 % of the total nitrogen is present in B aggregates. Elevated nitrogen content and significant platelet development is restricted to the inner zone which is devoid of slip planes. This suggests that an abrupt change in growth conditions occurred between the inner and outer zones, with a substantial decrease in nitrogen available for substitution in the diamond lattice during growth of the outer zone. There is no evidence for resorption of the inner zone prior to growth of the outer zone, as the contact between the two zones is planar. The systematic decrease in nitrogen content towards the exterior of the outer zone implies a continual depletion of the diamond growth medium in nitrogen during the later period of crystallization.

Yellow-green lines marking (111) slip planes produced by plastic deformation are restricted to the outer zone of the diamond. As the inner zone is older, and hence must have been exposed to the same strain as the outer zone, the lack of slip lines in the region characterized by platelet development supports the proposal (Evans, 1976) that platelets increase the resistance of diamonds to plastic deformation. Experiments conducted by Evans and Wild (1965) at atmospheric pressure and 2100 K demonstrated that extreme deformation of Type II diamond resulted from the application of shear stresses of  $5 \times 10^8 - 6 \times 10^8 \text{ N.m}^{-2}$ , whereas no deformation of Type Ia platelet-rich diamonds was observed at double this stress. The presence of platelets may impede the movement of dislocations during plastic deformation.

### 5.3.2. Plate GC006

Weak blue luminescence and poorly developed octahedral growth zonation (see Fig. 5.2) is found in GC006 which was sawn in half and polished along the (001) plane. The centre of the diamond is occupied by a small diamond "seed" distinguished by slightly paler luminescence. The external curvature of the "seed" implies that it experienced resorption before renewed growth occurred. Similar indications of intermittent diamond growth around small mineral inclusions and diamond nuclei are common in diamonds from Yakutia (Bulanova, 1995). The lack of significant platelet development is consistent with the IR spectra obtained for this specimen which indicate low concentrations (80 - 479 at. ppm) of well-aggregated nitrogen defects.

### 5.3.3. Plate GC028

This specimen is characterized by weak blue luminescence and abundant yellow-green slip lines (see Fig. 5.3) caused by intense plastic deformation during mantle residence. The almost total lack of characteristic platelet absorption in IR spectra from this specimen is consistent with the

proposal that diamonds without platelets are easily deformed (Evans, 1976). The scarcity of platelets in this diamond is a consequence of the low nitrogen content and moderate aggregation state of < 31 - 76 at. ppm nitrogen and 43 - 63 % respectively.

#### *5.3.4. Plate GC037*

In contrast to the previous specimen, this plate (see Fig. 5.4) shows significant development of platelets and well-defined octahedral growth zones. Variation in platelet size is a function of nitrogen defect concentration, with larger platelets of up to ~15  $\mu\text{m}$  corresponding to areas of lower nitrogen concentration, as determined from IR spectra. This suggests that rapid nucleation of platelets was promoted in zones of elevated substitutional nitrogen content, leading to development of abundant small platelets; whereas nucleation was suppressed resulting in slow growth of large platelets in zones deficient in nitrogen.

A general decrease in nitrogen content and aggregation state from the innermost regions to the edges is observed from IR spectra (see Fig. 5.4). Nitrogen content determined spectroscopically varies from 537 at. ppm in the inner zone to < 300 at. ppm in the outer rim (e.g. points 7 and 8). The corresponding nitrogen defect aggregation state ranges from as much as 94 % aggregation in the older inner regions to 84 - 90 % in the outer rim. The presence of yellow-green slip planes indicates that this specimen was subject to plastic deformation during mantle residence.

#### *5.3.5. Plate GC042*

Further evidence of extreme plastic deformation is provided by the intersecting slip planes in plate GC042 (see Fig. 5.5). An IR mapping traverse was undertaken perpendicular to bright blue octahedral growth planes in order to reveal any variation in nitrogen content or aggregation. No systematic variation was encountered, although the possible presence of an older inner region containing lower concentrations of more highly-aggregated nitrogen defects is deduced from thermal modelling of selected spectra. A less likely alternative is that the variation in aggregation state could be explained by a significant decrease in the crystallization temperature of outer growth zones. Nitrogen content varies from < 23 - 147 at. ppm and the aggregation state of the nitrogen defects ranges from approximately 56 - 82 %.

Cathodoluminescence reveals a curved crack connected to the exterior of the diamond. A number of small yellow-green haloes are associated with the crack. These haloes were produced by radiation damage from the decay of radioactive elements within secondary inclusions which crystallized in the crack. Investigation of the diamond plate in the SEM indicated that the

inclusions have been lost, either during the polishing process, or during ultrasonic agitation to clean the specimen.

### 5.3.6. Plate GC036

The complexities of diamond growth and deformation are illustrated to dramatic effect by the cathodoluminescence photomicrograph of plate GC036 in Fig. 5.6. In contrast to the central monocrystalline “seed” which acted as a nucleus to growth in diamond GC006, this specimen contains a polycrystalline “seed” of several “nested octahedra”. During the initial growth conditions which prevailed during nucleation of diamond GC036, localized carbon saturation levels were high enough to permit the formation of several closely-spaced nucleation centres. The longest dimension of the polycrystalline “seed” is approximately 800  $\mu\text{m}$ . Octahedral growth zonation, variable platelet distribution and evidence of resorption are clearly evident in the high magnification photomicrograph of this feature (see Fig. 5.7a).

Intensive development of parallel yellow-green slip lines provides evidence of extreme plastic deformation in an external region of the diamond plate. However, the cathodoluminescence is dominated elsewhere by a “brecciated” texture consisting of irregular curvilinear fragments which are delineated by subtle variation in blue, pink and violet cathodoluminescence. This texture resembles sub-grain boundaries formed during plastic deformation (B. Harte, pers. comm., 1995), but has not been reported in studies of plastically deformed diamonds from other localities. The “brecciation” texture may be attributed to brittle deformation processes, or complex events of growth and dissolution (J. W. Harris, pers. comm., 1995). The preservation of octahedral zonation in the polycrystalline “seed” in close proximity to the “brecciated” zone indicates different lattice responses to growth, dissolution and deformation processes, possibly as a result of variable lattice yield strength owing to disparate defect contents of the zones.

The extreme heterogeneity and thickness of this sample frustrated attempts to correlate features recognized in the surface cathodoluminescence image with spectra derived from the entire thickness of the plate. Limited variation in nitrogen content and aggregation state of 55 - 232 at. ppm and 79 - 86 % respectively was determined spectroscopically. A correlation between low nitrogen content and plastically deformed zones was found, although degradation of the platelet absorption peak in IR spectra appeared to be relatively uniform throughout the plate.

The inclusion content (see Fig. 5.7b) of the plastically deformed zone is lower than that of the region characterized by the most intense “brecciation”. A large garnet inclusion (~300  $\mu\text{m}$  in length) of irregular morphology and several smaller garnet inclusions are found in this diamond.

Also present are a sulphide inclusion surrounded by a graphite rosette, graphite rosettes and disseminated graphite along fractures, and rutile inclusions. A single rutile inclusion exposed at the surface of the plate was positively identified by semi-quantitative electron microprobe analysis.

As discussed in section 7.3.7, IR spectroscopy of the rutile inclusions indicated their hydrous nature. It is possible that loss of hydrogen from the rutile inclusions as a result of cooling and depressurization may have caused the “brecciation” of the diamond. Alternatively, deformation may have been produced by an increase in the molar volume of the rutile inclusions accompanying the transition from rutile-type structure to  $\alpha$ -PbO<sub>2</sub>-type structure (Bendeliani *et al.*, 1967) with decreasing temperature. A decrease of approximately 200 °C in final equilibration temperature from crystallization temperatures of approximately 1138 °C is indicated by geothermometry of non-touching and touching garnet and clinopyroxene inclusions (see section 7.3). Such a temperature decrease is consistent with the transition of rutile-type structure to  $\alpha$ -PbO<sub>2</sub>-type structure.

A single halo caused by radiation damage is seen at the irregular interface between the “brecciated” zone and an external zone characterized by the presence of slip lines and visible platelets. The central cubo-octahedral cavity within the halo is empty, precluding identification of the mineral which it once contained, although perovskite or zircon are suitable candidates on the basis of radioactive element content. The presence of localized carbonate material was deduced from IR absorption peaks at 877, 1045 and 1448 cm<sup>-1</sup> (W. R. Taylor, pers. comm., 1993). In some instances cracks could be identified in regions containing spectral indications of carbonate. This material is therefore believed to be of secondary origin, possibly introduced into fractures during the intense “brecciation” event.

### 5.3.7. Plate GC101

The variable blue cathodoluminescence of this plate provides insight into the IR spectral heterogeneity. The inner region of this diamond (see Fig. 5.8) comprises a cubo-octahedral core which is distinguished by subtle growth sector zonation characteristic of synthetic diamonds (see Fig. 5.9). Growth sectoral dependence of unpaired nitrogen defect concentration in synthetic diamonds has been demonstrated; {111} growth sectors incorporate the highest concentrations of substitutional nitrogen, followed by {113} and {110} sectors, whereas {100} sectors may contain extremely variable nitrogen contents (Woods and Lang, 1975).

Minor variation in nitrogen content and aggregation state from 224 - 412 at. ppm and 81 - 89 % respectively was determined spectroscopically. A positive correlation between nitrogen

concentration, nitrogen aggregation state and the normalized area for the platelet peak was found. However, greater spatial resolution was required to establish the relationships between growth zonation and defect distribution.

Contour plots of characteristic platelet, nitrogen and hydrogen defect absorption peaks were generated from IR mapping (P. H. Turner, pers. comm., 1994). A comparison of the resultant plots presented in Fig. 5.10 illustrates the relationships between substitutional defects. No platelets are visible in the cathodoluminescence image, but variable platelet distribution and development is evident from IR spectroscopy. The most intense platelet development corresponds to an outer region of elevated hydrogen and B aggregate content, whereas correlation with A aggregate content is less distinct.

A general correlation between hydrogen and nitrogen content is consistent with previous investigations (Blinova *et al.*, 1988). The greatest similarity between the contour plots and cathodoluminescence image is seen in the plot of absorption at  $3107\text{ cm}^{-1}$  due to the presence of hydrogen; in which central contour lines suggest radial growth sectors.

### 5.3.8. Plate GC008

This plate is dominated by anomalous pink-violet cathodoluminescence (see Fig. 5.11) attributed to the presence of sub-microscopic  $\text{CO}_2$ -bearing inclusions within the diamond lattice. No evidence of inclusions was found during high magnification SEM investigation of  $\text{CO}_2$ -bearing diamonds. The anomalous luminescence is consistent with this result as no discrete features of similar size to platelets are seen, and thus the defects responsible for the luminescence are likely to be sub-microscopic.

Areas of dull blue-grey luminescence within the anomalous pink luminescence (see Fig. 5.12) define a texture akin to that generated by the annealing fluid inclusions within fractures in quartz crystals (A. H. Rankin, pers. comm., 1993). This texture may represent a stage in the healing of fractures which contained  $\text{CO}_2$  fluid. The mechanisms involved in fracture healing are comprehensively discussed and illustrated in Roedder (1984). Dissolution occurs preferentially at unstable fracture surfaces with irrational Miller indices until they are replaced by crystal faces with low Miller indices (Roedder, 1984). In this way planar arrays of small well-faceted secondary inclusions are produced.

Zones of diamond exhibiting the more normal cathodoluminescence colours associated with  $\text{CO}_2$ -free diamond are also present in this specimen. Intensive development of yellow-green slip

planes testifies that these zones have been subjected to significant plastic deformation during mantle residence. Nitrogen content in this plate is below the detection limit of the IR spectrometer.

#### *5.3.9. Plate GC030*

Complex intergrowth relationships between CO<sub>2</sub>-bearing and CO<sub>2</sub>-free diamond growth generations are revealed by the cathodoluminescence photomicrograph of this plate (see Fig. 5.13). Anomalous orange and orange-brown luminescence correlates with areas which show spectral evidence of CO<sub>2</sub> absorption in the IR region. The origin of the feathery grey detail in the zones with anomalous cathodoluminescence is unknown.

Areas exhibiting the customary blue luminescence of diamond generally lack the variable IR absorption peak(s) at 2350 - 2424 cm<sup>-1</sup> attributed to the  $\nu_3$  asymmetric stretching vibration of crystalline CO<sub>2</sub> (Schrauder and Navon, 1993). However, owing to the considerable heterogeneity of the diamond, overlap of the different generations results in "mixed" spectra with contributions from the CO<sub>2</sub>-bearing and CO<sub>2</sub>-free diamond. Low concentrations (88 to ~110 at. ppm) of moderately-aggregated (72 - 85 %) nitrogen defects were calculated from IR spectra showing no (or very minor) CO<sub>2</sub> absorption. Significant absorption indicative of the presence of hydrogen correlates with nitrogen content and is found only in spectra obtained from CO<sub>2</sub>-free diamond.

#### *5.3.10. Plate GC150*

This plate is characterized by zones of anomalous orange and brown luminescence, intergrown with zones of blue luminescence which are crosscut by abundant yellow-green slip planes (see Fig. 5.14). No evidence of nitrogen defects was found in IR spectra lacking the characteristic CO<sub>2</sub> absorption peak(s). In agreement with results for other specimens, CO<sub>2</sub>-bearing zones with anomalous luminescence lack IR absorption peaks indicative of nitrogen defects.

#### *5.3.11. Plate GC151*

This diamond plate is notable for its particularly intense red-brown colouration, but relatively low CO<sub>2</sub> absorption peaks in IR spectra. In contrast to the other polished plates, no blue luminescence is found in this plate which is characterized by anomalous green-brown luminescence. Curved and linear features with a greater component of red luminescence can be

identified from the background green-brown luminescence in Fig. 5.15, and are suggestive of hummocky growth zonation. Possible octahedral growth zonation may also be detected from subtle variations in cathodoluminescence colour. The presence of CO<sub>2</sub> absorption peaks and absence of peaks from nitrogen defects was recognized in every spectrum from this plate.

### *5.3.12. Plate GC171*

This plate is similar to plate GC150, with complex intergrowth relationships between different growth generations. Anomalous brown-orange luminescence demarcates CO<sub>2</sub>-bearing diamond, whereas CO<sub>2</sub>-free diamond is characterized by blue luminescence transected by yellow-green slip planes (see Fig. 5.16). Spectroscopic investigations failed to identify any significant nitrogen defect absorption, although this may have been obscured by broad absorption in this region attributed to the presence of silicate inclusions.

### *5.3.13. Unpolished diamonds*

The severe etching and irregular morphology exhibited by most of the unpolished George Creek diamonds limits the extent to which their cathodoluminescence can be related to growth zonation, deformation processes and the other features discussed previously. Nevertheless, cathodoluminescence was used in conjunction with IR spectroscopy to detect the presence of CO<sub>2</sub>-bearing diamond, and was also useful in the identification of diamonds which have been subjected to radiation damage.

Comparison of the cathodoluminescence of two diamonds illustrated in Figs. 5.17a and 5.17b suggests that the CO<sub>2</sub>-bearing diamond is younger than the CO<sub>2</sub>-free diamond. A large etched cavity is observed in diamond GC753, which lacks spectroscopic evidence of CO<sub>2</sub>, or the anomalous cathodoluminescence associated with CO<sub>2</sub>-bearing diamond. This diamond may have fractured as a result of differential expansion between an inclusion and the diamond host; subsequent etching and resorption would have enlarged this cavity to its present size. Diamond GC755 is believed to have had a similar history, but experienced a further episode of growth which filled its central cavity with CO<sub>2</sub>-bearing diamond distinguished by anomalous cathodoluminescence.

Evidence of resorption is seen in Figs. 5.17c and 5.17d. Diamond GC863 is characterized by the intergrowth of blue-luminescent CO<sub>2</sub>-free diamond with a minor component of CO<sub>2</sub>-bearing diamond. Resorption of both diamond growth generations resulted in well-rounded morphology. Intense resorption has also modified the morphology of diamond GC872. This specimen exhibits

bright blue cathodoluminescence and a “chemically polished” surface texture attributed to the action of dry CO<sub>2</sub> (Phaal, 1965).

The effects of radiation damage on the cathodoluminescence of diamonds GC870 and GC874 are seen in Figs. 5.17e and 5.17f respectively. Discrete radiation haloes are discernible amongst yellow-green slip lines on the surface of the former specimen, whereas the latter specimen exhibits uniform yellow-green cathodoluminescence characteristic of diamonds which have experienced annealing at elevated temperatures subsequent to irradiation (H. J. Milledge, pers. comm., 1994).

#### *5.3.14. Cathodoluminescence Spectra*

A brief discussion of cathodoluminescence spectra obtained for four CO<sub>2</sub>-bearing diamonds follows. The IR spectra of these diamonds indicate the lack of (or negligible) nitrogen defect content. Two of the diamonds exhibit anomalous orange to orange-brown and minor blue cathodoluminescence when observed with the luminoscope microscope attachment, whereas the other specimens are characterized by violet-pink and yellow-green luminescence.

Broad Band A luminescence generated by electron donor-acceptor transitions is observed in all the spectra as a strong peak with maximum intensity at ~400 nm. The exact position of this luminescence is dependent on the separation between electron-donor and electron-acceptor pairs, and excitation conditions (Dean, 1965). In addition, luminescence peaks at 445, 453, 461 and 471 nm characterize a spectrum (Fig. 5.18a) obtained for diamond GC814 which has orange-brown and blue luminescence. Broad luminescence bands are also detected at 480 - 575 and 625 - 700 nm.

Diamond GC837 exhibits similar blue and orange cathodoluminescence to that of GC814, and has similar spectral features (see Fig. 5.18b). In addition to the Band A luminescence and peaks at 445, 453, 461 and 471 nm, peaks at 480, 493 and 503 nm are evident superimposed on a broad luminescence band from 445 to 575 nm. A broad band of weak luminescence is also detected between 625 - 700 nm.

Yellow-green and pink cathodoluminescence zones characterize diamond GC821. The yellow-green cathodoluminescence is indicative of plastically deformed CO<sub>2</sub>-free diamond, whereas IR spectra obtained from regions of pink luminescence contain CO<sub>2</sub> absorption peaks. Band A luminescence and minor peaks at 480, 493, 503 and 511 nm may be recognized in the spectra shown in Fig. 5.19a. Peaks at 567 nm are present in two of the spectra from this specimen.

The Band A luminescence in one of the spectra from diamond GC771 is resolved into peaks at 409, 422, 432 and 445 nm (see Fig. 5.19b). Peaks are also detected at 498, 506 and 513 nm. A single spectrum reveals a peak at 379 nm superimposed on the Band A luminescence, as well peaks at 572, 583 and 595 nm. The pink and yellow-green cathodoluminescence colours of this diamond are similar to those of diamond GC821, and indicate the presence of CO<sub>2</sub>-bearing diamond and plastically deformed CO<sub>2</sub>-free diamond growth generations respectively.

The presence of sub-microscopic CO<sub>2</sub> inclusions in diamonds appears to generate a number of distinct cathodoluminescence absorption peaks in addition to the common Band A luminescence. The similarities in the spectra of the two diamonds with blue and orange-brown cathodoluminescence contrast with the more variable nature of spectra recorded for diamonds with areas of pink and green luminescence. In all the CO<sub>2</sub>-bearing diamonds studied, anomalous pink-violet cathodoluminescence appears to be limited to those diamonds with yellow-green luminescence caused by intensive development of slip planes in CO<sub>2</sub>-free regions. CO<sub>2</sub>-bearing diamonds with blue cathodoluminescence and limited evidence of plastic deformation in CO<sub>2</sub>-free regions appear to be characterized by orange-brown cathodoluminescence in their CO<sub>2</sub>-bearing regions. Further investigation of the cathodoluminescence spectra of CO<sub>2</sub>-bearing diamonds may indicate correlations with variables such as diamond colour, position and shape of CO<sub>2</sub> absorption peak in IR spectra and the content of other defects. In addition, the interpretation of electronic transitions indicated by the cathodoluminescence spectra may provide insight into the relationship between CO<sub>2</sub> defects and the diamond lattice.

## **6. GEOLOGICAL IMPLICATIONS OF** **CO<sub>2</sub>-BEARING DIAMONDS**

### **6.1. INTRODUCTION**

The presence of sub-microscopic inclusions, composed dominantly of high pressure CO<sub>2</sub>, in many diamonds from George Creek provides information on many aspects of diamond growth and related mantle processes. The composition and distribution of fluids in the mantle has long been an enigma, only partly resolved by thermodynamic considerations, evidence from fluid inclusions in mantle xenoliths, and the compositions of magmatic products generated by mantle melting. Sampling of pristine mantle fluids is problematic because most minerals are not strong enough to prevent decrepitation of fluid inclusions caused by pressure release and entrainment in the hot magmas which carry mantle minerals to the surface (Roedder, 1984). Furthermore, secondary processes which occur during high temperature annealing may alter the composition and pressure of fluid inclusions, although this may provide further insight to changing conditions during mantle residence.

Fluids present in the mantle exert a strong control on such important processes as partitioning of elements between solid and fluid phases, and the metasomatic transport of elements. The composition of fluids is buffered in the stability fields of minerals such as amphibole and phlogopite which may accommodate a significant amount of water, and carbonates which provide a reservoir for CO<sub>2</sub>. The stability fields of minerals with buffering capacities are strongly dependent on bulk composition, temperature, pressure and oxygen fugacity. This suggests that the presence and composition of fluids is depth-dependent and is a function of the regional geotherm.

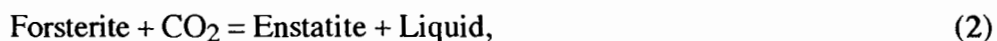
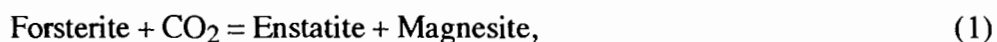
Mantle rheology, melting, and magma generation is influenced by the presence of fluids. Partial melting in the seismic low-velocity zone is attributed to the presence of CO<sub>2</sub> and water (Lambert and Wyllie, 1968; Wyllie and Huang, 1975a, b). In addition, the depth-dependent effects of CO<sub>2</sub> and water on experimentally-determined peridotite solvi have been invoked to explain the composition and formation of basaltic, kimberlitic and carbonatitic magmas (Wyllie and Huang, 1975a, b). Dehydration of oceanic lithosphere, recycled into the mantle by subduction, is believed to release fluids which generate zones of melting, magmatism and metasomatism (e.g. Fyfe and McBirney, 1975; Kesson and Ringwood, 1989a). Knowledge of the nature and effects of mantle fluids would assist in the understanding of the spatial, temporal and compositional controls of magmatism, as well as the degassing history of the earth.

## 6.2. THE STABILITY OF CO<sub>2</sub> IN MANTLE ASSEMBLAGES

Experimental investigations using natural peridotites and simpler synthetic analogues indicate that CO<sub>2</sub> may exist as a free phase in the mantle only once carbonation reactions have proceeded to completion, or at very high temperatures (Newton and Sharp, 1975; Wyllie and Huang, 1975a, b). Total carbonation of mantle assemblages requires the addition of > 30 wt % CO<sub>2</sub> to peridotite and > 10 wt % CO<sub>2</sub> to eclogite (Schrauder and Navon, 1993). The stability and composition of C-O-H fluids and their effect on mantle assemblages as a function of temperature and pressure is discussed below. The discussion is based mostly on experimental observations from simple systems which approximate lherzolitic and harzburgitic bulk compositions. Some disagreement exists over the exact topology of the relevant reactions in temperature-pressure space, but the broad implications for the nature of mantle fluids remain largely unaffected by such experimental discrepancies.

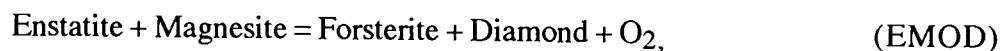
At pressures below ~22 kb, mildly reducing and more oxidizing fluids are buffered to CO<sub>2</sub>-rich compositions because water is accommodated in amphibole (Eggler, 1978; Wyllie, 1978, 1979). Water may also be accommodated in phlogopite, but the presence and buffering capacity of this mineral is controlled by the K content of the surrounding mantle. A free fluid phase may only exist at pressures greater than ~22 kb if water is present in excess of that required to hydrate all potential phlogopite, and if the CO<sub>2</sub> content exceeds the buffering capacity of carbonate minerals (Eggler, 1987). Carbonation of peridotite requires pressures in excess of ~16 kb (Olafsson and Eggler, 1983; Eggler, 1987), thus CO<sub>2</sub>-rich fluids may exist in the shallower regions of the mantle, as indicated by the presence of CO<sub>2</sub>-bearing fluid inclusions in peridotite xenoliths from numerous localities (Andersen *et al.*, 1984; Roedder, 1984; and references therein).

Figure 6.1. depicts the most important reactions involved in the carbonation of common mantle assemblages. At relatively low temperatures and pressures olivine reacts with CO<sub>2</sub> according to the following reactions (Eggler, 1978; Wyllie *et al.*, 1983) :



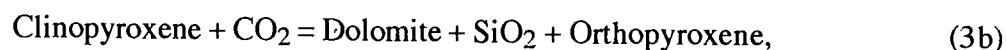
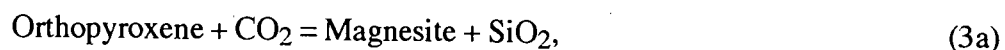
These reactions occur at pressures well below the diamond stability field and CO<sub>2</sub> fluid is thus unlikely to exist in uncarbonated mantle lithologies rich in olivine at pressures in excess of ~16 kb. Experimental investigations of reactions appropriate to carbonated graphite-bearing

peridotite (Eggler *et al.*, 1980) may be combined with thermodynamic data (Robie *et al.*, 1978) to yield an equation which defines the temperature, pressure and redox conditions at which diamond exists in equilibrium with enstatite, magnesite and olivine (Eggler and Baker, 1982). The relevant equation is referred to as the EMOD buffer:



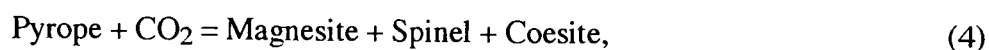
Oxygen fugacities buffered by the EMOD assemblage are mildly reducing and lie close to the MW (magnetite-wüstite) oxygen fugacity buffer for a wide range of pressure and temperature conditions (Eggler and Baker, 1982). At a temperature and pressure (1050 °C and 55 kb) considered typical of diamond formation any fluid present in equilibrium with the EMOD assemblage would consist of CO<sub>2</sub> and water (Eggler and Baker, 1982).

Pyroxenes may coexist with CO<sub>2</sub> fluid to higher pressures than olivine, but react to form carbonates and coesite/quartz (Wyllie *et al.*, 1983; Mäder and Berman, 1991) in the following manner:



The carbonation reactions of orthopyroxene and clinopyroxene occur at very similar temperature and pressure conditions and are represented by a single curve in Fig. 6.1. This curve intersects the graphite-diamond phase boundary of Kennedy and Kennedy (1976) at ~52 kb and permits the existence of CO<sub>2</sub> fluids in pyroxene-rich diamondiferous lithologies.

The stability field of garnet in the presence of CO<sub>2</sub> fluid is inferred from low-pressure data (Brown *et al.*, 1989) for the reaction:



As seen in Fig. 6.1, reaction 4 intersects the graphite-diamond phase boundary (Kennedy and Kennedy, 1976) at ~46 kb, and garnet resists carbonation to higher pressures than olivine or pyroxene.

Temperature-pressure relationships of the above experimentally-determined carbonation reactions limit the presence of CO<sub>2</sub> fluids to mildly reduced or relatively oxidized regions of the sub-continental lithospheric mantle characterized by the abundance of garnet (and pyroxene). Thus CO<sub>2</sub> fluids are more likely to exist in environments comprising eclogite, websterite or pyroxenite than in olivine-rich peridotitic environments.

Subduction of carbonaceous sediments may result in the presence of unusual assemblages containing carbonates and coesite in localized regions of the mantle (Schrauder and Navon, 1993). Synthetic CaO-SiO<sub>2</sub>-CO<sub>2</sub> and MgO-SiO<sub>2</sub>-CO<sub>2</sub> analogues of such assemblages melt at temperatures in excess of 1400 °C and release CO<sub>2</sub> according to the following reactions (Wyllie and Huang, 1976; Huang *et al.*, 1980):



Raman spectroscopy and experimental studies at high pressures and temperatures indicate that magnesite is stable in the mantle and may act as a source of CO<sub>2</sub> and carbon to depths of at least 1000 km (Canil and Scarfe, 1990; Gillet, 1993). Examples of carbonates in mantle xenoliths are extremely rare (McGetchin and Besançon, 1973; Berg, 1986) since dissociation of magnesite occurs explosively during kimberlite eruption (Eggler, 1975; Wyllie, 1978). The abundance of disaggregated sub-calcic garnets in kimberlites located in the Kaapvaal craton is attributed to violent dissociation of magnesite-bearing harzburgite xenoliths during kimberlite ascent (Boyd and Gurney, 1982). Indirect evidence of the presence of carbonate in the mantle is provided by the unusual LREE enrichment in sub-calcic garnet macrocrysts and diamond inclusions from the Kimberley and Finsch kimberlites (Shimizu and Richardson, 1987). The trace element patterns of these garnets are thought to have been caused by metasomatism of the sub-continental lithospheric mantle by alkali carbonate fluid(s) (Shimizu and Richardson, 1987).

Figure 6.1 shows that the solidus of lherzolite is considerably lower than that of harzburgite in the presence of moderate amounts of H<sub>2</sub>O and CO<sub>2</sub> (Wyllie, 1978; Ellis and Wyllie, 1980). Under these conditions all peridotites would be solid at depths less than ~175 km (Wyllie, 1987). In the restricted depth interval of 175 - 195 km lherzolite would be partly melted, whereas carbonated harzburgite would remain unmelted in the presence of free CO<sub>2</sub> (Wyllie, 1987). Distinction between lherzolite and harzburgite becomes meaningless at temperatures above ~1050 °C because of the melting of clinopyroxene. At depths in excess of ~195 km peridotite of harzburgitic and lherzolititic bulk composition would be melted (Wyllie, 1987).

Schrauder and Navon (1993) propose two mechanisms by which CO<sub>2</sub> may be stabilized as a free volatile phase in the mantle. It may be possible for total carbonation of mantle assemblages to occur locally, e.g. in highly metasomatized veins where CO<sub>2</sub> may then exist as a supercritical fluid phase. Reaction of CO<sub>2</sub>-bearing fluids with wall rocks may result in localized development of sufficient carbonate to stabilize CO<sub>2</sub> as a free phase. Alternatively, high temperature melting (at ~1300 - 1400 °C) of siliceous and carbonaceous sediments subducted into the mantle may release large amounts of CO<sub>2</sub>. Melting of carbonated lherzolite and harzburgite may also liberate CO<sub>2</sub> in the mantle if the local geotherm intersects the volatile-present solidi of lherzolite and harzburgite.

### 6.3. IMPLICATIONS FOR DIAMOND GENESIS

The presence of CO<sub>2</sub> inclusions in a sub-population of diamonds from George Creek provides unequivocal evidence that at least some diamonds crystallize from fluids and are not the products of subsolidus crystallization. Most models for diamond genesis (e.g. Deines, 1980; Haggerty, 1986) favour their formation in the presence of strongly reducing fluids rich in methane, rather than less reducing fluids dominated by CO<sub>2</sub>. However, spectroscopic studies of cubic and coated stones suggest that fluids comprising water and CO<sub>2</sub> are associated with their crystallization (Navon *et al.*, 1988; Schrauder and Navon, 1994). This does not, however, preclude the involvement of CH<sub>4</sub>-rich fluid in the formation of diamonds with octahedral growth forms.

The nature of fluids in equilibrium with diamond or graphite has been investigated as a function of oxygen fugacity, temperature and pressure (Taylor, 1988). Thermodynamic modelling of C-O-H fluids using a Modified Redlich-Kwong equation of state indicates that relatively oxidizing fluids in equilibrium with diamond or graphite are restricted to variable CO<sub>2</sub>-H<sub>2</sub>O compositions. Reducing fluids contain variable proportions of CH<sub>4</sub>, H<sub>2</sub>, H<sub>2</sub>O and C<sub>2</sub>H<sub>6</sub> and change with decreasing oxygen fugacity from H<sub>2</sub>O > CH<sub>4</sub> > H<sub>2</sub> compositions at the most oxidizing conditions permitted, to CH<sub>4</sub> > H<sub>2</sub> > C<sub>2</sub>H<sub>6</sub> compositions below the IW (iron-wüstite) buffer (Taylor, 1988). Taylor and Green (1989) suggest a "redox-melting" model for the formation of diamonds in response to the interaction of reducing CH<sub>4</sub>-H<sub>2</sub>O fluids of asthenospheric origin with more oxidized peridotite of the lithospheric mantle.

The restricted stability field permitting the coexistence of olivine and CO<sub>2</sub>-bearing fluid implies that peridotitic diamonds are unlikely to have grown from CO<sub>2</sub>-bearing fluids. Unlike CO<sub>2</sub>, CH<sub>4</sub> does not form volatile-bearing products by reaction with silicate minerals, and hence under mildly reducing conditions CH<sub>4</sub>-H<sub>2</sub>O fluids may be associated with peridotitic mantle

assemblages. Thus, CH<sub>4</sub>-H<sub>2</sub>O fluids are likely to characterize peridotitic diamond growth environments, whereas the absence of olivine and abundance of garnet and pyroxene in mantle of eclogitic composition may stabilize CO<sub>2</sub>-bearing fluids at pressures in the diamond stability field.

The coexistence of olivine - spinel ± orthopyroxene in mantle xenoliths allows the estimation of oxygen fugacity, based on the thermodynamic properties of the mineral phases present (O'Neill and Wall, 1987). Reduced oxygen fugacities between the WM (wüstite-magnetite) and IW (iron-wüstite) buffers for olivine - spinel ± orthopyroxene inclusion assemblages contained within diamonds from southern African kimberlites have been calculated using this method (Daniels and Gurney, 1991). Under these redox conditions CH<sub>4</sub> would be the dominant volatile species in the diamond growth region. Calculated oxygen fugacities between the FMQ (fayalite-magnetite-quartz) and WM buffers for non-diamondiferous lherzolitic assemblages would stabilize the presence of CO<sub>2</sub>-H<sub>2</sub>O fluids (Daniels and Gurney, 1991). Thus, heterogeneity of the redox conditions and volatile phases existed in the peridotitic mantle sampled by southern African kimberlites, and such heterogeneity is likely to have characterized the oxygen fugacity of the lithospheric mantle in other localities such as the State Line district.

## 7. MINERAL INCLUSIONS RECOVERED FROM GEORGE CREEK DIAMONDS

### 7.1. INTRODUCTION

The study of minerals trapped within diamonds during their growth has contributed greatly to the understanding of diamond genesis. The perfect crystal structure of diamond is reflected by its extremely hard and chemically inert nature (Field, 1979; pp: 641 - 649). In most cases these properties have protected diamond inclusions from re-equilibration, resulting in the preservation of isotopic, trace, minor and major element compositions which existed in these minerals during diamond growth. Identification of mineral inclusions by various researchers using refractive index measurements and X-ray diffraction techniques was followed by the first quantitative analyses using an electron microprobe (Meyer and Boyd, 1968). The advent of ion probes, sensitive mass spectrometers and laser fluorination techniques has facilitated the study of trace elements, stable and radiogenic isotope ratios in diamond inclusions.

Table 7.1 lists the minerals identified as inclusions in diamonds thus far. An important distinction is made between syngenetic (and possibly protogenetic) inclusions and epigenetic inclusions which may invade the diamond along fractures subsequent to growth (Meyer and Tsai, 1976a, b). Mineral inclusions which may be primary, but which are generally regarded as not being stable at the temperature, pressure and redox conditions necessary for diamond growth, are assigned to a category of uncertain origin in Table 7.1. It was recognised that diamond inclusion minerals could be divided into two parageneses (Meyer and Boyd, 1968; Meyer and Tsai, 1976) and that these parageneses occur in dissimilar ratios in different kimberlite occurrences (Harris and Gurney, 1979).

#### *7.1.1. Peridotitic paragenesis*

The peridotitic paragenesis comprises inclusions similar in composition to minerals found in ultramafic xenoliths recovered from kimberlites and lamproites. Diamond inclusions of the peridotitic paragenesis are dominated by sulphides, forsteritic olivines, chrome-pyropes, chrome-diopside clinopyroxenes, magnesian orthopyroxenes, and chromites. Further subdivision of the peridotitic paragenesis into harzburgitic, lherzolitic and wehrlitic sub-parageneses appears to be necessary for a better characterization of diamond source regions in the upper mantle and for the interpretation of the carbon isotope distributions of diamond populations (Kirkley *et al.*, 1991; van Heerden *et al.*, 1995).

### 7.1.2. *Eclogitic paragenesis*

Sulphides, pyrope-almandine garnets, and omphacitic clinopyroxenes are the most common diamond inclusions of the eclogitic paragenesis. Minerals which are found as accessory phases in eclogite xenoliths (rutile, kyanite, sanidine, coesite and corundum) form a minor proportion of eclogitic paragenesis inclusions (Harris and Gurney, 1979, and references therein). Rare diamond inclusions belonging to a websteritic sub-paragenesis have been reported (Gurney *et al.*, 1984b; Moore and Gurney, 1989, and this dissertation). Websteritic inclusions may inadvertently be classified as eclogitic because of the difficulty in distinguishing orthopyroxene inclusions from clinopyroxenes prior to cracking of the diamond host. Colourless or pale green orthopyroxene inclusions may also be mistaken for olivine during visual assessment of inclusion content, and assigned to the peridotitic paragenesis. Analysis of orthopyroxene inclusions is needed to distinguish between magnesian peridotitic inclusions and iron-rich websteritic inclusions. The abundance and origin of diamonds of the websteritic sub-paragenesis thus requires further investigation.

Sobolev *et al.* (1984) have suggested the presence of a third calc-silicate sub-paragenesis in placer-derived diamonds from the Copeton area of New South Wales, Australia. Diamonds from this locality contain grossular-rich garnets, omphacitic pyroxenes with low Al<sub>2</sub>O<sub>3</sub> content, and coesite, and would thus appear to belong to an eclogitic sub-paragenesis. The low Al<sub>2</sub>O<sub>3</sub> content of the pyroxenes precludes the coexistence of kyanite with the minerals reported, and the authors suggest the term “grospyte” to distinguish this paragenesis from grospydite which contains kyanite. The <sup>13</sup>C enrichment in Copeton diamonds of the “grospyte” paragenesis (Sobolev *et al.*, 1979, 1981) contrasts with the <sup>13</sup>C depletion reported for many eclogitic diamonds (Kirkley *et al.*, 1991).

### 7.1.3. *Mineral inclusions from cubic diamonds and fibrous diamond coat*

The suite of minerals included in cubic diamonds and fibrous diamond coat differs from the peridotitic and eclogitic paragenesis minerals associated with diamonds of the octahedral growth form. Sub-micrometer inclusions of apatite (Lang and Walmsley, 1983), biotite (Walmsley and Lang, 1992a), carbonates including ankerite (Walmsley and Lang, 1992b), and polyphase assemblages of quartz, carbonate, apatite and phyllosilicates (Navon *et al.*, 1988; Guthrie *et al.*, 1991) have been recognized in turbid diamond coat by means of TEM, electron diffraction and energy-dispersive X-ray spectroscopy (EDS) techniques. The use of IR spectroscopy has indicated the presence of sub-microscopic fluid inclusions containing variable proportions of H<sub>2</sub>O, CO<sub>2</sub> and carbonate in diamond coat and fibrous cubic diamonds (Chrenko *et al.*, 1967;

Navon *et al.*, 1988; Schrauder and Navon, 1994). The composition of the fluid inclusions varies between a “carbonatitic” endmember rich in carbonate, K, Ca, Fe, Mg and P, and a “hydrous” endmember rich in H<sub>2</sub>O, K, Si and Al (Schrauder and Navon, 1994).

#### 7.1.4. Radiometric dating of diamond inclusions

The ancient and xenocrystic nature of diamonds erupted by kimberlites (and lamproites) was first confirmed by the study of uranium and lead isotopes in composites of sulphide inclusions from the Premier, Finsch and Kimberley mines of South Africa (Kramers, 1979) and samarium and neodymium isotope ratios in composites of harzburgitic garnet inclusions from the Finsch and Kimberley mines (Richardson *et al.*, 1984). The model lead age of Premier sulphide inclusions proved to be indistinguishable from the emplacement age of the kimberlite, whereas the results for Finsch and Kimberley indicated the much greater (> 2 Ga) age of the inclusions compared to the kimberlite ages. Richardson *et al.* (1984) determined a model age of 3.2 Ga for diamonds of the harzburgitic sub-paragenesis from the latter kimberlites. The authors attributed the rare earth element distributions in these harzburgitic garnets to an ancient metasomatic event which affected lithosphere which had been previously depleted by extraction of komatiitic magmas.

Subsequently peridotitic and eclogitic diamond inclusion populations from many localities have been radiometrically dated using composites of diamond inclusions (Richardson, 1986; Richardson *et al.*, 1990, 1993; Smith *et al.*, 1986), laser probe <sup>40</sup>Ar/<sup>39</sup>Ar dating techniques (Burgess *et al.*, 1989, 1992; Phillips *et al.*, 1989), and lead isotope dating of zircon inclusions using a high resolution ion probe (Kinny and Meyer, 1994). Table 7.2 (updated and modified from Harris, 1992) presents reported diamond inclusion and host kimberlite emplacement ages and contrasts the ancient (Archaean) nature of diamonds of the peridotitic paragenesis with the wider range of generally younger (Proterozoic) ages obtained for diamonds of the eclogitic paragenesis.

## 7.2. METHODS

Mineral inclusions were liberated from George Creek diamonds after detailed description of the host diamond, the nature of inclusions and presence of any fractures leading to the surface. In addition to obvious fractures in the host diamond, a mottled inclusion colour and the lack of well-faceted crystal faces is often indicative of an epigenetic (secondary) origin. In cases where minerals recovered had not been reported before as syngenetic diamond inclusions and had not been seen before cracking, or the possible presence of cracks could not be discounted

due to severe etching, the paragenesis and primary nature of inclusions was classified as uncertain. The prevalence of well-faceted cubo-octahedral morphology in the majority of syngenetic mineral inclusions is caused by the higher free energy of diamond relative to other minerals crystallizing during coeval growth (Harris and Gurney, 1979).

Detailed descriptions of the spatial relationships of inclusions are required if an attempt is to be made to correlate temperature estimates from element partitioning between mineral inclusions with temperature estimates from the nitrogen aggregation state determined by IR spectroscopy. Equilibrium crystallization of mineral inclusions used to calculate equilibration temperatures is essential for meaningful interpretation of geothermometric results. For diamonds with several inclusions, geothermometric calibrations were applied to mineral pairs most closely located in the host diamond, and therefore most likely to have crystallized within the shortest time interval.

Disequilibrium between mineral inclusions within single diamonds is not common, yet the coexistence of minerals of the eclogitic and peridotitic parageneses within single diamonds has been reported (Prinz *et al.*, 1975; Hall and Smith, 1984; Griffin *et al.*, 1988; Moore and Gurney, 1989; Otter, 1990). Crosscutting tie-lines between coexisting minerals on ternary diagrams indicate minor disequilibrium (Rickard *et al.*, 1989), whereas the presence of quartz and olivine in a diamond from the River Ranch kimberlite in Zimbabwe (M. G. Kopylova, pers. comm., 1994) is a further example of extreme disequilibrium. Disequilibrium between coexisting diamond inclusions may result from very slow and intermittent diamond growth in environments of changing lithology, fluid composition, oxygen fugacity, temperature and pressure. Inclusions encapsulated by early diamond growth will not re-equilibrate with inclusions trapped by later growth unless cracks within the diamond facilitate mass transfer between inclusions.

After cleaning overnight in 30 % hydrofluoric acid, diamonds were cracked in a steel diamond cracker designed by S. H. Richardson. Diamond fragments and the liberated inclusions were transferred to a clean glass petri dish for examination under a binocular microscope. Inclusions were mounted individually in "Petropox" epoxy on frosted glass slides. Further descriptions of inclusion size, morphology and birefringence were made at this point, to eliminate the possibility of mistaking as inclusions any silicon carbide grains from the abrasive paper used to polish the inclusions. The epoxy was cured for approximately 30 minutes on a hot plate, and allowed to harden further overnight. Inclusions were initially polished using 200 grit silicon carbide paper in a stainless steel tray filled with distilled water. Slides were then cleaned with ethanol and hand-polished on 3  $\mu\text{m}$  and 1  $\mu\text{m}$  polishing laps with the appropriate industrial diamond paste.

The slides were cleaned with ethanol and then coated with carbon in a Varian vacuum coater before electron microprobe analysis. Major element compositions were determined using the Cameca/Camebax electron microprobe in the department of Geological Sciences at the University of Cape Town. Counting times of 10 seconds were used for all elements except for Na in garnet and K in clinopyroxene where counting times of 30 and 60 seconds respectively were used to ensure lower limits of detection and  $2\sigma$  of 0.01 wt. %. Matrix effects were corrected on-line using the method of Bence and Albee (1968). Further analytical conditions are described in Appendix 3. Inclusion compositions are plotted in terms of cations per formula unit rather than the more conventional weight percent method, to facilitate recognition of coupled substitutions and inter-element relationships.

In instances when more than one inclusion was recovered from a diamond, all fragments large enough for electron microprobe analysis were analysed to investigate any potential disequilibrium. However, if the analyses varied by less than  $2\sigma$ , only the best analysis was used for further work. A difference in inclusion composition greater than  $2\sigma$  was encountered in only one diamond (GC010), an aggregate that contained two clinopyroxenes in separate octahedra.

### 7.3. MINERALOGY

As recorded for the nearby Sloan kimberlite (Otter, 1990), inclusions from George Creek are dominantly of the eclogitic paragenesis. Websteritic paragenesis assemblages were also recovered from three diamonds. Websteritic inclusions recovered include a polymineralic orthopyroxene-clinopyroxene-phlogopite inclusion which coexisted with graphite rosettes, a biminerally orthopyroxene-clinopyroxene inclusion which coexisted with discrete clinopyroxene inclusions, and a green garnet which was surrounded by a rosette of graphite. The websteritic garnet and clinopyroxene inclusions show compositional affinities with the more refractory Group GC1 inclusions defined on the basis of compositional variations in eclogitic garnet and clinopyroxene inclusions. Unlike the compositionally more variable Group GC2 inclusions, Group GC1 inclusions define compositional trends which may have been inherited from fractionated igneous protoliths.

An enigmatic feature of the diamonds from the George Creek kimberlite provided for this study is the apparent lack of peridotitic inclusions, despite the presence of subcalcic chrome-pyrope garnets in the heavy mineral concentrate (McCallum and Waldman, 1991). Purple peridotitic garnet inclusions have been identified in other George Creek diamonds which were examined by M. E. McCallum and J. A. Carlson (pers. comm., 1995).

Visual inspection indicated that black rosettes are the most abundant inclusions in George Creek diamonds. Silicate minerals recovered (in order of decreasing abundance) include omphacitic clinopyroxene, pyrope-almandine garnet, orthopyroxene and titanian phlogopite (see Table 7.3). Rutile, ilmenite and rare pure silicon oxide (coesite?) inclusions comprise the oxide minerals encapsulated in the diamonds. A single grain of moissanite (SiC) was recovered.

### 7.3.1. Black rosettes

Figure 7.1a illustrates a diamond containing a large black graphite inclusion. The graphite was intergrown with brown diamond which may indicate that graphitization resulted from deformation, as discussed in section 3.3.4. Although varying in size up to 800  $\mu\text{m}$  in diameter, black rosettes proved difficult to recover, often shattering into fragments too small for mounting, or adhering as thin films on the diamond surface. In most cases the morphology and lustre of rosettes was consistent with that of graphite, but pyrrhotite inclusions were recovered from diamond GC080 (see Appendix 3.11). Pyrrhotite inclusions appeared homogeneous without evidence of exsolution under reflected light at 100 $\times$  magnification. The low (< 0.5 wt %) Ni content is consistent with classification of these sulphides as eclogitic, following the recognition of high Ni content in sulphides of peridotitic paragenesis and low Ni content in diamonds of eclogitic paragenesis recovered from Russian diamonds (Yefimova *et al.*, 1983).

Graphite is commonly found as rosettes around syngenetic silicate and sulphide inclusions, but the mechanisms promoting this graphitization are not fully understood. Graphitization of diamond requires a volume increase which is difficult to reconcile with an origin due to pressure release during eruption. In addition, graphitization *in vacuo* does not proceed rapidly at temperatures below 1700 °C (Davies and Evans, 1972), suggesting that graphitization occurs during mantle residence. Orlov (1959) proposed that graphitization occurs as a result of internal stresses around inclusions or along lattice planes. Almost all CO<sub>2</sub>-bearing diamonds from George Creek contain black rosette inclusions.

### 7.3.2. Clinopyroxene

Pale green clinopyroxene inclusions recovered from George Creek diamonds commonly exhibit well-faceted, elongated cubo-octahedral morphology and bright second order birefringence colours. Inclusions vary in size from ~10 to ~280  $\mu\text{m}$  in diameter. A pale green clinopyroxene inclusion is depicted *in situ* in Fig. 7.1b.

Enrichment of K in eclogitic clinopyroxene inclusions has been reported by several workers (Sobolev *et al.*, 1972; Gurney *et al.*, 1979; Tsai *et al.*, 1979; Gurney *et al.*, 1984b; Moore and Gurney, 1985; Jaques *et al.*, 1989; Rickard *et al.*, 1989; Otter and Gurney, 1989). Diamondiferous eclogites are less enriched in K than eclogitic diamond inclusions (e.g. Sobolev *et al.*, 1972) and this may be the result of partial melting or metasomatism of the xenoliths (Switzer and Melson, 1969; Mysen and Griffin, 1973; Reid *et al.*, 1976). McCandless and Gurney (1989) suggested that concentrations of  $\geq 0.08$  wt. %  $K_2O$  in clinopyroxenes (and  $\geq 0.09$  wt %  $Na_2O$  in garnets) characterize the Group I eclogites from the Roberts Victor kimberlite which were defined on textural criteria by MacGregor and Carter (1970). The formation of diamondiferous and Group I eclogites thus appears to occur under similar conditions, and all diamondiferous eclogites studied by McCandless and Gurney (1989) are classified chemically and texturally as Group I.

Incorporation of K into the clinopyroxene lattice is pressure dependent, with a minimum pressure of 32 kb required (Erlank and Kushiro, 1970). Recent experiments (Harlow, 1992; Edgar and Vukadinovic, 1993) indicate that significant K solubility in clinopyroxene exists at temperatures of 1200 - 1500 °C and pressures of 50 - 60 kb, and that under these conditions K solubility decreases systematically with temperature, but increases with pressure. With progressively decreasing temperature clinopyroxene coexists with garnet, garnet + coesite (?), garnet + coesite (?) + phlogopite and rutile (Edgar and Vukadinovic, 1993).

George Creek clinopyroxene inclusions contain elevated K contents of up to 0.05 cations per formula unit (p.f.u.) and two compositional groups can be distinguished in Fig. 7.2. Group GC1 clinopyroxenes are characterized by lower K, Na, Al, Fe and Ti contents than those of Group GC2. The contents of both Mg and Ca in the more refractory Group GC1 pyroxenes are in excess of 0.70 cations per formula unit, and except for one inclusion (GC039C) all contain trace quantities of Cr. Except for a single  $CO_2$ -bearing diamond, no Cr was detected by electron microprobe analysis using 10 s counting times for Group GC2 clinopyroxenes. Figure 7.2 illustrates the broader compositional range defined by Group GC2 inclusions in comparison to Group GC1 inclusions.

Clinopyroxene end-member calculations made using the method of Hatton (1978) are listed in Appendix 3.3. A strong positive correlation between the atomic Na and Al content of George Creek clinopyroxenes (see Fig. 7.3a.) is consistent with enrichment of the pyroxenes in the jadeite component as has been reported for eclogitic diamond inclusions worldwide (Meyer, 1987). The molecular proportion of jadeite decreases with increasing  $Mg^\#$  [ $Mg^\# = 100 \times Mg/(Mg+Fe)$ ] and Ca content of the clinopyroxenes (see Figs. 7.3b. and 7.3c.). A positive correlation between jadeite and Ti content is seen in Fig. 7.3d., but the relationship between

jadeite and Fe (see Fig. 7.3e.) is obscured due to the lack of distinction between Fe<sup>2+</sup> and Fe<sup>3+</sup> in electron microprobe analyses. However, calculated acmite content increases with increasing jadeite content for clinopyroxenes with > 7 mol. % acmite (see Fig. 7.3f.). The Ca content of clinopyroxenes increases with increasing Mg<sup>#</sup> (see Fig. 7.4a.), whereas the relationship between Fe and Mg<sup>#</sup> is more complex, as illustrated in Fig. 7.4b.

George Creek clinopyroxene inclusions plot within the worldwide field for diamond inclusions on a ternary Ca:Mg:Fe plot, as depicted in Fig. 7.5. The distributions of clinopyroxenes belonging to Group GC1 and GC2, and those recovered from CO<sub>2</sub>-bearing diamonds are compared in Fig. 7.5. Group GC1 clinopyroxenes have a more limited compositional scatter than those of Group GC2, and are slightly richer in Mg and poorer in Fe.

### 7.3.3. Orthopyroxene

Diamonds GC022 and GC057 contained orthopyroxene inclusions, which existed in the former diamond as a bimineralic orthopyroxene-clinopyroxene inclusion coexisting with monomineralic clinopyroxene inclusions, and in the latter diamond as a trimineralic orthopyroxene-clinopyroxene-phlogopite inclusion coexisting with black rosettes. These orthopyroxene inclusions are assigned to a websteritic paragenesis, due to their coexistence with clinopyroxene and the lack of olivine inclusions in George Creek diamonds.

Websteritic orthopyroxene diamond inclusions from Orapa (Gurney *et al.* 1984b), Monastery (Moore and Gurney, 1989) and Jagersfontein (Rickard *et al.*, 1991) are characterized by lower enstatite and Cr contents than peridotitic orthopyroxene inclusions. Orthopyroxenes recovered from diamonds GC022 and GC057 contain 0.003 and 0.000 Cr cations p.f.u. and have low Mg<sup>#</sup>'s of 82.97 and 82.31 respectively. In contrast, the range in Mg<sup>#</sup> for worldwide peridotitic orthopyroxene inclusions is 91 - 95 (Meyer, 1987).

Aluminium and Ca contents are lower (0.018, 0.020 Al cations p.f.u and 0.017, 0.019 Ca cations p.f.u.) for George Creek orthopyroxene inclusions than for websteritic orthopyroxene inclusions from the Monastery mine. Elevated Al and Ca contents in orthopyroxene inclusions from Monastery are attributed to their crystallization in the absence of garnet (Moore and Gurney, 1989). In the George Creek websteritic paragenesis, Al is accommodated in phlogopite (in diamond GC057) and possibly also in garnet, as a single green garnet (in diamond GC376) is assigned to the websteritic paragenesis.

#### 7.3.4. Garnet

Numerous translucent pale-to-medium orange, isotropic garnet inclusions were recovered from George Creek diamonds. The garnet inclusions are predominantly of slightly rounded cubo-octahedral form, with noticeable curvature of larger crystal faces. Some of the larger garnets show considerable irregularity of their crystal faces and may represent protogenetic inclusions that crystallized prior to diamond growth. The garnet inclusions range in size from ~10 to ~350  $\mu\text{m}$  along the longest dimension. Several garnet inclusions contain very small black ilmenite inclusions which are discussed in section 7.3.6.

As is the case for clinopyroxenes, two compositionally distinct groups are recognized for George Creek garnet inclusions. To achieve optimum separation of the groups in inter-element plots, all garnets with  $\text{Mg}^\#$ 's exceeding 50 are classified as Group GC1. A line representing 60 mol. % Mg effectively separates the more magnesian Group GC1 garnet inclusions from the Group GC2 garnet inclusions. The distribution of George Creek garnet inclusions on a ternary Ca:Mg:Fe diagram is depicted in Fig. 7.6. Group GC1 garnet inclusions define a linear trend of Mg enrichment with decreasing Fe and Ca, whereas no such trend is recognized for Group GC2 garnet inclusions.

Except for two diamonds, all garnets which coexisted with Group GC1 clinopyroxene inclusions are classified as Group GC1 according to this criterion, and all garnets which coexisted with Group GC2 clinopyroxenes are assigned to Group GC2. Group GC1 garnets coexist with Group GC2 clinopyroxene inclusions in diamonds GC166 and GC538. This inconsistency may be explained by crystallization of diamond over an extended period of time, as inclusions encapsulated at different growth stages are not able to re-equilibrate. Multi-stage growth under variable physical and chemical conditions occurred for diamond GC166 which comprises  $\text{CO}_2$ -bearing and  $\text{CO}_2$ -free growth zones.

Compositions of orange garnet inclusions are similar to those of eclogitic garnet inclusions reported from other localities, with elevated Na contents of up to 0.050 cations p.f.u. The Ca and Fe contents of George Creek garnet inclusions decrease with increasing  $\text{Mg}^\#$  as seen in Figs. 7.7a. and 7.7b. Similarly, a decrease in Na with increasing  $\text{Mg}^\#$  is seen in Fig. 7.7c. Group GC1 garnets define a trend of increasing Na with increasing Ca content, whereas for the majority of Group GC2 garnets Na correlates negatively with Ca (see Fig. 7.7d.). The compositional trends exhibited by Group GC1 garnet inclusions are consistent with igneous fractionation trends.

The common occurrence of biminerally garnet-ilmenite inclusions and the presence of a single triminerally garnet-rutile-ilmenite inclusion is unique to diamonds from George Creek. Crystallization of garnets at high pressures and temperatures may have accommodated elevated Fe and Ti levels which would have subsequently exsolved as ilmenite crystals at lower pressures and temperatures. Ringwood and Major (1971) proposed that Ti is accommodated in the garnet structure at high pressure by coupled substitution of  $Ti + Na$  for  $Ca + Al$ . Fig. 7.8a. illustrates the excellent positive correlation between  $Ti_{gar}$  and  $Na_{gar}$ , but the positive correlation between  $(Ti + Na)_{gar}$  vs  $(Ca + Al)_{gar}$  in Fig. 7.8b. is inconsistent with this substitution mechanism. The relationship between  $(Ti + Na)_{gar}$  and  $(Mg + Al)_{gar}$  shown in Fig. 7.8c. is more consistent with coupled substitution of  $Ti + Na$  for  $Mg + Al$  during crystallization at high temperatures and pressures. Alternatively, ilmenite and rutile may have been stabilized on the solidus during diamond crystallization because of the Fe and Ti rich nature of the diamond growth region, and the prevailing temperature, pressure and oxygen fugacity conditions. The presence of discrete rutile inclusions in a number of diamonds is consistent with this suggestion.

A single green garnet was recovered from the  $CO_2$ -bearing diamond GC376 which also contained black rosettes of graphite. The green garnet proved to be enriched in Fe, and depleted in Ca (1.273 and 0.383 cations p.f.u. respectively). The absence of coexisting silicate phases precludes the unambiguous classification of the paragenesis of this inclusion, but the low Na content is inconsistent with an eclogitic origin. The low Mg and Cr content of 1.367 and 0.006 cations p.f.u. respectively precludes classification of the green garnet as peridotitic. Hatton (1978) reported an Fe-enrichment trend in garnet websterite xenoliths from Roberts Victor, accordingly the green garnet is classified as websteritic.

### 7.3.5. Phlogopite

Phlogopite has been reported as an intergrowth with omphacitic clinopyroxene and rutile in a diamond of unknown African origin (Prinz *et al.*, 1975), in association with omphacitic clinopyroxene in a diamond from Finsch kimberlite, South Africa (Gurney *et al.*, 1979), and coexisting with epigenetic richterite amphibole in a diamond from the Sloan kimberlite, (Meyer and McCallum, 1986). The phlogopite inclusion reported by Prinz *et al.* (1975) is similar in composition to that of a phlogopite inclusion recovered from diamond GC057. The red-brown phlogopite lath was contained in a polymineralic inclusion of clinopyroxene and orthopyroxene which was assigned to the websteritic paragenesis. These phlogopites are characterized by low Mg and high Ti contents (see Table 7.4 for comparison of phlogopite diamond inclusion compositions).

The solubility of Ti in phlogopite has been shown to be independent of bulk composition, but increases with increasing temperature and oxygen fugacity, and decreases with increasing pressure (Arima and Edgar, 1981). Phlogopite crystallization is promoted by high H<sub>2</sub>O activity and is suppressed by high CO<sub>2</sub> activity (Edgar and Arima, 1983) which implies that any fluid(s) present during crystallization of the websteritic phlogopite-clinopyroxene-orthopyroxene inclusions in diamond GC057 could not have been dominated by CO<sub>2</sub>.

Phlogopite may have constituted a substantial reservoir for H<sub>2</sub>O, K and Ti in the Colorado-Wyoming lithospheric mantle. Metasomatic aqueous fluids, released by dehydration reactions in subducted oceanic crust, are believed to promote the formation of phlogopite (Fyfe and McBirney, 1975). The development of metasomatic zones composed mostly of phlogopite, orthopyroxene and omphacitic clinopyroxene ( $\pm$  coesite) is believed to follow the hybridization of hydrous, siliceous fluids/melts with hotter peridotite in the mantle wedge (Wyllie and Sekine, 1982). The association of phlogopite with orthopyroxene and omphacitic clinopyroxene in diamond GC 057 indicates that crystallization of diamond may have occurred in subduction-generated metasomatic zones in the Colorado-Wyoming mantle.

#### 7.3.6. Ilmenite

Ilmenite inclusions occur as black rod-shaped inclusions, or more rarely as elongate octahedra, enclosed within eclogitic garnet inclusions (see Fig. 7.1c). Small ilmenite fragments are also encountered attached to the edges of garnet inclusions, and a single ilmenite inclusion was seen in a rutile inclusion at the edge of a garnet inclusion. The ilmenite inclusions exhibit shiny brassy lustre in reflected light and no evidence of exsolution is seen at 100  $\times$  magnification.

Polishing of these inclusions proved to be exceptionally difficult as the tiny ( $\sim 10 \times \sim 25 \mu\text{m}$ ) ilmenite crystals tended to pluck out of the enclosing garnet or epoxy. At least 9 of the 28 diamonds from which eclogitic garnets were recovered contained ilmenite inclusions associated with the garnet inclusions. Ilmenite inclusions were present in garnet inclusions of both Group GC1 and Group GC2. The compositions of two ilmenite inclusions large enough for electron microprobe analysis are presented in Appendix 3.11. A further inclusion similar in appearance to the ilmenite inclusions shows evidence of alteration, and electron microprobe analysis yielded a low total, dominated by Ti and Fe.

Magnesium-rich ilmenites have been recovered from diamonds from Yakutia (Sobolev *et al.*, 1976), South Africa (Tsai, 1978), Zaire (Mvuemba Ntanda *et al.*, 1982) and the Colorado-Wyoming State Line district (Meyer and McCallum, 1986). The compositions of these and the

George Creek ilmenite inclusions are presented in Table 7.5. Ilmenite inclusions from George Creek and Brazilian diamonds (Meyer and Svisero, 1975) appear to belong to the eclogitic paragenesis on the basis of their Fe-enrichment and low Mg and Cr contents. Recovery of diamondiferous lherzolite xenoliths containing Mg-rich ilmenite (Pokhilenko *et al.*, 1977) implies that the Mg-rich ilmenite diamond inclusions reported in Table 7.5 belong to the peridotitic paragenesis.

The composition of ilmenite inclusions is strongly dependent on redox conditions, the influence of metasomatic fluids and the diamond paragenesis. The positioning of the George Creek ilmenite analyses on a ternary plot with  $f_{O_2}$  contours after Haggerty and Tompkins (1983), is indicative of reducing conditions during crystallization at roughly  $10^{-9}$  bars oxygen fugacity (see Fig. 7.9.).

### 7.3.7. Rutile

The most abundant oxide mineral present in eclogite xenoliths is rutile (Haggerty, 1989). Inclusions of rutile have been reported in eclogitic paragenesis diamonds (Meyer and Svisero, 1975; Prinz *et al.*, 1975; Mvuemba Ntanda *et al.*, 1982; Hall and Smith, 1984; Meyer and McCallum, 1986; Daniels and Gurney, 1989) and were also found in George Creek diamonds (see Fig. 7.1d.).

Rutile inclusions recovered from George Creek diamonds vary in colour from orange-brown to red-brown, brown or black. A relationship between inclusion colour and morphology was noted. Smaller ( $\sim 50 \mu\text{m}$  diameter) well-faceted, elongate, cubo-octahedral and cubo-octahedral inclusions are generally darker in colour than rutile inclusions of larger size and/or rounded or irregular morphologies. No correlation between colour and minor element composition was found for the rutile inclusions.

Four sizeable rutile inclusions (up to  $120 \mu\text{m}$  in maximum dimension) and several smaller rutile inclusions were recovered from the central  $\text{CO}_2$ -bearing zone of diamond GC050. This association may imply that Ti metasomatism accompanied crystallization of the  $\text{CO}_2$ -bearing diamond growth generation. However, large rutile inclusions are also found in  $\text{CO}_2$ -free diamonds, and the growth of younger  $\text{CO}_2$ -bearing diamond in the centre of GC050 may have been facilitated by fractures surrounding rutile inclusions which had crystallized in  $\text{CO}_2$ -free diamond.

A single trimineralic garnet-rutile-ilmenite inclusion, which coexisted with clinopyroxene and a black rosette inclusion, was also recovered. The planar nature of the contact between the rutile and garnet crystals is suggestive of equilibrium crystallization of the minerals, as discussed in section 7.3.4, rather than subsequent exsolution of the rutile from the garnet. In contrast, the presence of fine rods of rutile in garnets in three eclogite xenoliths from Jagersfontein kimberlite, South Africa (Haggerty, 1994) is consistent with exsolution of rutile on cooling and depressurization of the garnets from crystallization conditions of high temperature and pressure.

MARID rutiles and those found as diamond inclusions do not exhibit elevated contents of Nb and Cr which characterize metasomatized xenoliths (Haggerty, 1989). As seen in Appendix 3.9 and Fig 7.10, the only elements to occur in minor quantities in George Creek rutile inclusions are Fe, Al and low levels of Cr and Ca. The possible presence of Nb, Ta and V was investigated using the electron microprobe, but the concentrations of these elements were found to be negligible.

Infra-red spectroscopy indicated the hydrous nature of the rutile inclusions, as has been documented previously for rutiles of upper mantle origin (Rossman and Smyth, 1990; Bell and Rossman, 1992; Vlassopoulos *et al.*, 1993). The presence of hydrogen is thought to compensate for charge deficiencies caused by the substitution of trivalent Fe, Al, Cr and V cations which are only partially compensated by substitution of pentavalent Nb and Ta cations (Vlassopoulos *et al.*, 1993). Hydrogen may thus have been accommodated in George Creek rutile inclusions to balance charge deficiencies caused by incorporation of minor amounts of Fe, Al, Cr and Ca, uncompensated by the negligible Nb and Ta contents.

### 7.3.8. Coesite

A colourless, rounded inclusion of pure silicon oxide (presumably coesite, the high pressure polymorph of quartz) was recovered from CO<sub>2</sub>-bearing diamond GC778. Coesite was first identified as a diamond inclusion in synthetic diamonds (Milledge, 1961), but has subsequently been recognized in eclogitic diamonds from numerous localities (Sobolev *et al.*, 1976, Gurney *et al.*, 1984a; Hall and Smith, 1984; Sobolev *et al.*, 1984; Daniels and Gurney, 1989; Jaques *et al.*, 1989; Novgorodov *et al.*, 1990; Otter, 1990).

CO<sub>2</sub>-rich fluid reacts with normal mantle minerals such as olivine, enstatite, diopside and pyrope to produce carbonates (e.g. Wyllie *et al.*, 1983). However, the presence of highly siliceous material such as subducted sedimentary rocks would expand the stability field of CO<sub>2</sub>-rich fluid (Schrauder and Navon, 1993). The occurrence of a silicon oxide inclusion in a CO<sub>2</sub>-

bearing diamond therefore provides support for the proposal of Schrauder and Navon (1993) that CO<sub>2</sub> may exist as free volatile phase in areas of the mantle where subduction processes have resulted in an unusually siliceous bulk composition.

### 7.3.9. *Moissanite*

A single blue-green, isotropic moissanite fragment was recovered from a diamond which also contained a clinopyroxene inclusion. Both inclusions were observed before the diamond was cracked and the moissanite inclusion was embedded in epoxy before polishing with silicon carbide paper, eliminating the possibility of laboratory contamination.

Moissanite has been recovered from several localities, both from kimberlite heavy mineral concentrate (Bobrievich *et al.*, 1957; He, 1984; Jaques *et al.*, 1986 and Leung *et al.*, 1990) and as diamond inclusions (Moore *et al.*, 1986; Jaques *et al.*, 1989; Leung, 1990; Wilding, 1990). As the formation of this mineral requires extremely reducing conditions (Woermann and Rosenhauer, 1985), and it is commonly used as an abrasive, the identification of moissanite as a diamond inclusion is questioned by some workers (Otter, 1990).

### 7.3.10. *Epigenetic inclusions*

In this study inclusions which appeared to be of epigenetic origin were not investigated in any great detail. Epigenetic minerals identified by electron microprobe include haematite, carbonates and sellaite (MgF<sub>2</sub>). All these minerals have been reported before as secondary inclusions, due to their association with cracks in the enclosing diamonds and/or because they are not stable at the extreme temperatures and pressures of diamond crystallization (Harris, 1968).

## 7.4. THERMOBAROMETRY

The partitioning of elements between silicate and oxide minerals is controlled by the presence and speciation of any fluid phase present, bulk composition, oxygen fugacity, and temperature and pressure of crystallization. Experimental and theoretical investigations have advanced the understanding of temperature and pressure effects, and many geothermobarometers applicable to upper mantle assemblages have been calibrated. Comprehensive reviews of commonly-used geothermobarometers have been published by Finnerty and Boyd (1984, 1987) and Carswell and Gibb (1980, 1987).

Application of geothermobarometry to diamond inclusions has been hampered by the lack of suitable coexisting phases and the possibility that the inclusions do not represent equilibrium assemblages. Disequilibrium between diamond inclusions has been identified and can be as extreme as the coexistence of eclogitic and peridotitic minerals in a single diamond (Prinz *et al.*, 1975; Hall and Smith, 1984; Moore and Gurney, 1989; Otter, 1990). Plots of coexisting discrete and touching inclusions from George Creek diamonds are presented in Figs. 7.11 and 7.12 respectively. Cross-cutting tie lines indicative of disequilibrium assemblages (Rickard *et al.*, 1989) are apparent. Cathodoluminescence, IR spectroscopy and stable isotope studies have demonstrated that complex zoning and heterogeneity exists in many diamonds (Swart *et al.*, 1983; Wilding, 1990; Bulanova, 1995). Hence, caution is required in the interpretation of diamond inclusion thermobarometry and the inherent limitations of the methods should be recognized.

The lack of olivine and orthopyroxene in eclogitic assemblages precludes the use of existing geobarometers. However, pressure estimates can be made with reference to relevant experimentally-determined phase relationships such as the diamond-graphite boundary (Kennedy and Kennedy, 1976). Temperatures and pressures were calculated using a computer program PT.For written by W. R. Taylor which utilizes the commonly used geothermobarometric calibrations.

Pressure estimates may be made from the Al content of two websteritic orthopyroxene inclusions, if they are assumed to have crystallized in equilibrium with garnet. The composition of the garnet used in the calculations does not affect the pressure estimates significantly. The garnet composition chosen for pressure estimates is that of the green garnet believed to be websteritic on the basis of its Fe-enrichment. As the orthopyroxene inclusions enclosed in the diamond lattice were unable to re-equilibrate with garnet during residence in the mantle, the aluminium content of the orthopyroxene inclusions should reflect the pressures of diamond formation if the calculations are made at temperatures which are assumed to have prevailed during diamond crystallization. A diamond formation temperature of 1138 °C was assumed from the mean temperature estimate for non-touching eclogitic inclusion pairs (see below). Application of the Nickel and Green (1985) barometer yields pressure estimates of 52 kb and 56 kb for the formation of websteritic diamonds GC057 and GC022 respectively at a temperature of 1138 °C. These values are in good agreement, but differ from corresponding pressure estimates of 60 kb and 62 kb obtained from the MacGregor (1974) barometer. Pressure estimates of 52 - 62 kb fall within the diamond stability field (see Fig. 6.1) at a temperature of 1138 °C believed to be representative of diamond formation conditions.

Calculated temperatures for discrete and touching diamond inclusion pairs are listed in Table 7.6. A pressure of 50 kb, as adopted by most workers, is assumed for thermometry calculations for consistency and comparison of results. Separation of coexisting minerals by the diamond host prevents re-equilibration of discrete inclusions. Hence, geothermometry reveals temperatures of diamond formation, provided the inclusions are syngenetic not protogenetic, and that they crystallized in chemical equilibrium. The temperatures calculated for discrete garnet-clinopyroxene pairs, using the Ellis and Green (1979) thermometer, are within the range reported for eclogitic diamonds from localities worldwide and are most similar to temperature estimates for eclogitic diamonds from Sloan and Orapa (see Table 7.7). The range in temperatures calculated for discrete garnet-clinopyroxene pairs is from 1071 - 1178 °C, with a mean value of 1138 °C, and a standard deviation of 29 °C. Use of the Powell (1985) and Krogh (1988) thermometers, produces similar average temperatures (1125 and 1148 °C respectively), but with greater scatter of results.

Temperature estimates, from the aggregation state of nitrogen impurities (assuming a mantle residence period of 1.25 Ga) determined by IR spectroscopy, are included in Table 7.6 for comparison with thermometric estimates. Histograms of temperatures calculated from inclusion thermometry and nitrogen aggregation state are contrasted in Fig. 7.13. A well-defined mode occurs at 1125 - 1150 °C for discrete mineral pairs, whereas the mode for temperatures calculated on the basis of nitrogen aggregation state is at 1200 - 1225 °C. This discrepancy is discussed further in section 4.3.2.

The mean temperature calculated for three touching garnet-clinopyroxene pairs (bimineralic inclusions), using the Ellis and Green (1979) thermometer, is 955 °C. This value compares remarkably well with the mean temperature of 915 °C for two touching clinopyroxene-orthopyroxene pairs, calculated according to the method of Bertrand and Mercier (1985). As touching inclusions were able to re-equilibrate in response to changing temperature and pressure conditions, the temperatures calculated for these inclusions indicate the temperature of the diamondiferous mantle lithosphere at the time of kimberlite eruption.

Thermometric data for George Creek inclusions are thus consistent with cooling of the mantle lithosphere by approximately 200 °C after diamond formation. Gurney *et al.*, (1984b) report that the final equilibration temperatures for diamondiferous xenoliths from the Roberts Victor kimberlite in South Africa are at least 200 °C cooler than the temperatures calculated for minerals encapsulated in diamonds. Similar thermal evolution for the Siberian mantle is suggested by inclusion geothermometry for Yakutian diamonds (Bulanova, 1995; W. R. Taylor, pers. comm., 1994). These results support the suggestion (Griffin *et al.*, 1992) that diamond formation is associated with a short-lived "thermal pulse", associated with K, Rb, Sr

and REE metasomatism of the mantle, before cooling to a conductive shield geotherm of approximately  $40 \text{ mW.m}^{-2}$  (Pollack and Chapman, 1977).

## 7.5. IMPLICATIONS OF GEORGE CREEK INCLUSION MINERALOGY

The dominance of eclogitic paragenesis inclusions (except for rare websteritic paragenesis inclusions) is unique to George Creek. It is thought that kimberlite eruptions preferentially sample metasomatized and fractured zones in the mantle (Eggler, 1989). Accordingly, it is impossible to make accurate estimates of the relative abundance of eclogite, harzburgite, lherzolite and websterite which existed in the mantle at the time of diamond formation or kimberlite eruption, based on xenolith and diamond inclusion paragenesis proportions. Nevertheless, the majority of diamond inclusions from the Sloan kimberlite are also of the eclogitic paragenesis (Otter, 1990) and this indicates the important role of eclogitic mantle for diamond genesis in the Colorado-Wyoming State Line District. However, diamond growth was not restricted to mantle of eclogitic composition, as diamondiferous peridotites and diamonds with peridotitic inclusions have been recovered from Colorado-Wyoming (Eggler and McCallum, 1975; McCallum and Eggler, 1976; Meyer and McCallum, 1986; Otter, 1990).

### 7.5.1. Evidence of subduction

Recycling of oceanic material into the mantle by subduction is proposed by many workers to account for the formation of eclogite xenoliths (e.g. Helmstaedt and Doig, 1975; Helmstaedt and Schulze, 1979; Schulze, 1986). Magmatic features of eclogites may be reconciled with a subduction origin if basaltic melts, derived from subducted oceanic crust, are trapped and solidify near the lithosphere-asthenosphere boundary (Hofmann and White, 1982; Ringwood, 1982). The carbon isotopic distribution of diamonds of the eclogitic paragenesis may have been inherited from organic carbon contained in sediments which were subducted into the mantle (Koval'skiy and Cherskiy, 1972; Javoy *et al.*, 1986; Jaques *et al.*, 1989; Kirkley *et al.*, 1991).

Ater *et al.* (1984) suggest that the petrology and geochemical relationships of non-diamondiferous eclogite and grosspydrite xenoliths from the Colorado-Wyoming State Line District are consistent with their derivation from subducted oceanic crust. Extreme depletion in  $^{13}\text{C}$  of a sub-population of diamonds from the Sloan kimberlite is attributed to crystallization of these diamonds from organic carbon recycled into the mantle (Otter, 1990). Preliminary  $\delta^{13}\text{C}$  data (see Table 1.1 and Fig. 1.1) indicate that a sub-population of diamonds from the George Creek K1 kimberlite dyke shows similar extreme depletion in  $^{13}\text{C}$ .

The composition of certain inclusions from George Creek diamonds may also reflect the effects of subduction-related processes. The presence of a single inclusion of pure silicon oxide in a CO<sub>2</sub>-bearing diamond may provide evidence that subduction of siliceous sediments stabilizes CO<sub>2</sub> as a free volatile phase in the mantle, as proposed by Schrauder and Navon (1993). In particular, phlogopite is believed to form in metasomatic zones in response to the subduction of oceanic lithosphere (Fyfe and McBirney, 1975).

The extreme Ti enrichment in the phlogopite inclusion recovered from a George Creek diamond exceeds even that of MARID phlogopites (Erlank *et al.*, 1987). Metasomatic replacement of garnet and clinopyroxene by phlogopite has been reported for eclogites from Roberts Victor kimberlite (Hatton, 1978), but the phlogopite is not enriched in Ti. The enrichment in Ti in the phlogopite recovered from a websteritic George Creek diamond reflects an unusual bulk composition which may have been caused by the subduction of Ti-rich mafic intrusions in the oceanic crust into the mantle, or by metasomatic processes.

#### 7.5.2. Evidence of mantle metasomatism

The extremely variable effects of mantle metasomatism have been investigated in great detail and are reviewed by Harte (1987) and Menzies and Hawkesworth (1987). Considerable changes in modal proportions, major, minor and trace element contents of mantle assemblages may result from metasomatic processes. In many instances overprinting of more than one metasomatic episode complicates understanding of the reactions involved and the causes of metasomatism. Most metasomatized xenoliths described in the literature are of peridotitic composition, and clear evidence of metasomatism in eclogitic assemblages is scarce.

Metasomatic enrichment of the mantle in Ti and Fe by magmatic intrusions of pyroxene-rich rocks has been reported from Matsoku (e.g. Harte *et al.*, 1987). Ilmenite is commonly found in these metasomatized xenoliths (Harte *et al.*, 1987). Similar metasomatic enrichment of Ti and Fe is recognized in minerals from ilmenite peridotites from the Colorado-Wyoming State Line District (Eggler *et al.*, 1987a). The authors interpret lherzolite xenoliths enriched in basaltic components as the reaction products of intrusive dykes, veins and layers of websterite and pyroxenite with depleted peridotite wall-rocks of the mantle (Eggler *et al.*, 1987a). The relationship between enriched lherzolite xenoliths and eclogite xenoliths is not known, but the abundance of Ti and Fe in rutile and ilmenite inclusions in eclogitic diamonds may indicate that an affiliation existed between these lithologies in the Colorado-Wyoming mantle. Fluids released by dehydration reactions in subducted oceanic lithosphere may have initiated partial melting in the mantle, resulting in the intrusion of pyroxenite and websterite dykes and layers

into the peridotitic mantle wedge, and the crystallization of eclogite from melts of basaltic composition.

The presence of a CO<sub>2</sub>-bearing diamond generation from George Creek provides unequivocal evidence of the influx of metasomatic fluids into the diamondiferous mantle in the Colorado-Wyoming region. In diamond GC050, rutile inclusions are clearly restricted to the CO<sub>2</sub>-bearing portion of the diamond, which suggests that Ti metasomatism may have accompanied crystallization of the CO<sub>2</sub>-bearing diamond generation.

### *7.5.3. Significance of K-rich inclusions*

George Creek clinopyroxene inclusions are notable for their extreme enrichment in K. Accommodation of significant K in the pyroxene lattice is only possible at elevated pressures (Erlank and Kushiro, 1970), and K content increases with pressure of crystallization (Harlow, 1992; Edgar and Vukadinovic, 1993). Comparison of K contents of George Creek and worldwide clinopyroxene inclusions suggests higher crystallization pressures for George Creek diamonds than for diamonds containing inclusions assumed to have formed at approximately 50 kb on the basis of geothermobarometric calibrations. The relationship between K content and crystallization pressure for clinopyroxenes is also strongly influenced by bulk composition and temperature of crystallization. The elevated K contents of George Creek clinopyroxene inclusions reflect relatively high pressures and K enrichment of the Colorado-Wyoming mantle during diamond genesis. Recovery of a phlogopite inclusion provides further evidence of the elevated K content of the mantle sampled by eruption of the George Creek kimberlite.

### *7.5.4. Compositional heterogeneity of the Colorado-Wyoming mantle*

Considerable heterogeneity of the lithospheric mantle has been illustrated by the highly variable nature of xenoliths recovered from discrete kimberlite phases at numerous localities. In particular, xenoliths from the Colorado-Wyoming Kimberlite Province exhibit a wide range in composition (e.g. Egger, 1988). The compositional distinctions between George Creek Group GC1 and Group GC2 inclusions may be a result of diamond crystallization in environments characterized by different composition, temperature, pressure, oxygen fugacity and metasomatic history.

Group GC1 inclusions are more refractory and exhibit less compositional variation than Group GC2 inclusions. Temperature estimates using the method of Ellis and Green (1979) for the two Group GC1 garnet and clinopyroxene pairs are lower than estimates for Group GC2 pairs

(see Table 7.6). The lowest calculated temperature was obtained for a diamond which contained coexisting Group GC1 garnet and Group GC2 clinopyroxene inclusions. Disequilibrium between these mineral inclusions is not surprising, considering the coexistence of CO<sub>2</sub>-free and CO<sub>2</sub>-bearing generations in this diamond.

Oceanic lithosphere which is subducted into the mantle comprises compositionally variable rock types such as pelagic sediments, basalts with variable hydrothermal alteration, sheeted dykes and differentiated plutonic intrusions. Metamorphosed sequences representing subducted oceanic material at great depths in the mantle should reflect the heterogeneity of the original oceanic lithosphere. The Group GC1 and Group GC2 inclusions may have crystallized in different regions of metamorphosed oceanic lithosphere which had chemically distinct compositions. Trends of increasing Fe and Ca with decreasing Mg content, and increasing Na with Ca in Group GC1 garnets are consistent with igneous fractionation trends which may have been inherited from subducted oceanic protoliths.

Alternatively, the compositional variations between Group GC1 and Group GC2 inclusions are the result of slow and intermittent diamond growth in a region of the mantle subject to changing physical and chemical conditions. The coexistence of Group GC1 and Group GC2 inclusions may be explained in this way. Recycling of oceanic material into the diamond growth region by subduction would still be envisaged to explain the composition of George Creek mineral inclusions. Investigation of the trace element compositions and relative ages of the two groups of inclusions may possibly elucidate the relationship between the two compositional groups of inclusions.

## **8. A MODEL FOR THE GENESIS AND MANTLE RESIDENCE OF GEORGE CREEK DIAMONDS**

Physical and chemical properties of diamonds from George Creek record a complex mantle history of changing conditions which were alternately favourable and unfavourable to diamond growth and preservation. At least two distinct periods of diamond growth under different physical and chemical conditions resulted in the crystallization of CO<sub>2</sub>-free and CO<sub>2</sub>-bearing diamond sub-populations in the Colorado-Wyoming mantle. Both diamond generations were subsequently resorbed and etched by oxidizing fluids.

On the basis of morphological relationships in some diamonds, the CO<sub>2</sub>-free diamond growth generation is believed to be older than the CO<sub>2</sub>-bearing diamond growth generation. Crystallization of CO<sub>2</sub>-free diamonds took place dominantly in regions of the mantle comprising eclogitic assemblages, with a minor websteritic component. Visual inspection and inclusion recovery failed to identify any peridotitic inclusions in the George Creek diamonds which were studied.

The recognition of two compositionally distinct groups of eclogitic clinopyroxene and garnet inclusions suggests that diamond growth occurred in two eclogitic environments with different compositional characteristics, or that the inclusions reflect prolonged crystallization under changing chemical conditions. The latter proposal is favoured because of the coexistence of Group GC1 garnet inclusions with Group GC2 clinopyroxene inclusions in two diamonds. Separation of the inclusions by the inert diamond lattice would have prevented their re-equilibration in response to variations in bulk composition.

Estimates of pressures for diamond formation between 52 - 56 kb (Nickel and Green, 1985) and 60 - 62 kb (MacGregor, 1974) were made from the Al content of websteritic orthopyroxene inclusions assumed to be in equilibrium with garnet at a temperature of 1138 °C. The temperature of 1138 °C is the mean temperature calculated using the Ellis and Green (1979) method for coexisting eclogitic garnet and clinopyroxene inclusion pairs at an assumed pressure of 50 kb. The bulk composition of the eclogitic diamond growth region and the high pressures of crystallization facilitated the accommodation of elevated contents of K and the jadeite end-member in clinopyroxene inclusions. Similarly, elevated contents of Na and Ti in eclogitic garnet inclusions are thought to have been controlled by high pressure crystallization.

Evidence of extreme plastic deformation is provided by the presence of lamination lines on resorption surfaces of many George Creek diamonds. Intensive development of yellow-green

slip planes, caused by plastic deformation, may be recognized from cathodoluminescence photomicrographs of many CO<sub>2</sub>-free diamonds (e.g. GC028) and the CO<sub>2</sub>-free zones of CO<sub>2</sub>-bearing diamonds (e.g. GC008). A unique example of a diamond which has experienced severe brittle deformation, or a complex history of growth and dissolution in addition to extreme plastic deformation, is revealed by the cathodoluminescence photomicrograph of GC036.

It is likely that the episodes of plastic deformation played a significant role in the enhancement of nitrogen aggregation processes in George Creek diamonds. Large uncertainties are associated with the kinetics of the nitrogen aggregation reaction used to calculate equilibration temperatures and the spectra were not corrected for D component absorption. In addition, the exact age of the George Creek diamonds is unknown, and hence a mantle residence time of 1.25 Ga was assumed from tectonomagmatic considerations and the Pb isotopic composition of a zircon inclusion from the Sloan kimberlite (Otter, 1990). These factors may explain discrepancies between temperature estimates from nitrogen aggregation state and those from inclusion geothermometry. A heating episode after diamond crystallization is less likely to be responsible for the higher temperatures estimated from the nitrogen aggregation state, but may provide a mechanism for the release of CO<sub>2</sub> into the diamond growth region.

Thermal perturbation may have been responsible for melting of carbonated mantle to release metasomatic CO<sub>2</sub>-bearing fluids which were responsible for the crystallization of CO<sub>2</sub>-bearing diamonds. Renewed crystallization of diamond occurred under conditions of carbon saturation following the influx of CO<sub>2</sub>-bearing fluids into the diamondiferous mantle. Small volumes of the CO<sub>2</sub> fluid were trapped as fluid inclusions during renewed diamond crystallization, which in many instances occurred along fractures and in etched embayments in older CO<sub>2</sub>-free diamonds. The incorporation of CO<sub>2</sub> fluid inclusions would have been promoted by relatively rapid crystallization, and the irregular, etched morphology of the CO<sub>2</sub>-free diamonds on which renewed growth was occurring.

Prolonged annealing of the CO<sub>2</sub> inclusions during mantle residence time, which resulted in the formation of smaller pseudo-secondary inclusions, may have increased the ability of the inclusions to withstand decrepitation. The anomalous cathodoluminescence colours associated with CO<sub>2</sub>-bearing diamonds are consistent with the location of CO<sub>2</sub> in sub-microscopic inclusions. Further evidence that annealing of CO<sub>2</sub>-bearing inclusions took place during prolonged mantle residence may be provided by the extremely high pressures indicated by the position of the CO<sub>2</sub>  $\nu_3$  absorption peak in the IR spectra of many CO<sub>2</sub>-bearing diamonds. Precipitation of minimal amounts of graphite on the inclusion walls in response to changing

pressure and temperature conditions may have decreased the volume, and hence increased the pressure of the CO<sub>2</sub> fluid.

The unique abundance of CO<sub>2</sub>-bearing diamonds from George Creek needs to be explained. Mineral inclusions recovered from George Creek diamonds suggest that the diamonds sampled by kimberlite eruption were almost entirely derived from mantle domains of eclogitic composition. Total carbonation of eclogite requires addition of 20 wt % less CO<sub>2</sub> than is required for the complete carbonation of peridotite (Schrauder and Navon, 1993). The preponderance of eclogite in the mantle sampled by the George Creek kimberlite may thus have provided optimum compositional conditions for the stabilization of CO<sub>2</sub> as a free fluid phase.

Preliminary carbon isotope data for George Creek diamonds, as well as the compositions of diamond inclusions from the Colorado-Wyoming State Line District, are consistent with the subduction of oceanic material into the diamond growth region (J. M. Gibson, pers. comm., 1994). The wide range in the carbon isotopic composition of George Creek diamonds (see Table 1.1 and Fig. 1.1) is believed to have been inherited from subducted carbon which was derived from heterogeneous oceanic material comprising organic matter, marine carbonates, pelagic sediments, basalts of variable hydrothermal alteration, sheeted dykes, fractionated ultramafic and mafic sequences, and mantle peridotite. Variations in garnet and clinopyroxene inclusion compositions, particularly those of Group GC1, represent possible igneous fractionation trends preserved in igneous protoliths subducted into the mantle.

Subduction of siliceous sediments into the mantle is suggested by the recovery of a single silicon oxide inclusion from a CO<sub>2</sub>-bearing diamond. Localized mantle domains containing carbonate and coesite are thus inferred to have existed at depth in the Colorado-Wyoming mantle. Melting of these domains due to thermal perturbation may have released CO<sub>2</sub>-bearing fluid which is assumed to have migrated into zones of cooler diamondiferous eclogite where renewed diamond crystallization may then have occurred.

Carbonation of mantle harzburgite may be invoked to explain the presence of sub-calcic garnets in heavy mineral concentrate from George Creek. Pyrope resists carbonation in comparison with olivine and orthopyroxene, and thus sub-calcic garnets present in harzburgite may have survived partial carbonation of peridotitic regions of the mantle. Explosive dissociation of magnesite in carbonated harzburgitic xenoliths during kimberlite ascent would account for the abundance of sub-calcic garnet xenocrysts in the George Creek kimberlite.

In view of the abundance of sub-calcic garnets in the heavy mineral concentrate, the scarcity of peridotitic diamonds in the George Creek kimberlite needs to be explained. Diamond crystallization in the peridotitic mantle may have been suppressed by unfavourable oxygen fugacity conditions, or the lack of sufficient carbon necessary for diamond crystallization. Alternatively, the influx of CO<sub>2</sub>-bearing fluids into the mantle resulted in the formation of magnesite and total resorption of any diamonds in the regions of peridotitic mantle sampled by the George Creek kimberlite.

The highly-etched nature of most CO<sub>2</sub>-free and CO<sub>2</sub>-bearing diamonds from George Creek is thought to reflect the presence of oxidizing CO<sub>2</sub>-H<sub>2</sub>O fluids in the hypabyssal kimberlite during eruption. However, at least one episode of etching must have occurred earlier, prior to crystallization of the CO<sub>2</sub>-bearing diamond growth generation, as intergrowth relationships revealed by cathodoluminescence suggest that CO<sub>2</sub>-bearing diamond crystallized in etched cavities and embayments in many CO<sub>2</sub>-free diamonds. The great variability and intensity of etch features (even on different surfaces of single diamonds) suggests a complex history of repeated etching and resorption of George Creek diamonds by oxidizing fluids.

Cooling of the lithospheric mantle by ~200 °C between diamond formation and kimberlite eruption in the Devonian is suggested by the temperatures of 912 - 977 °C calculated for touching inclusions which were able to re-equilibrate during mantle residence time. Lithospheric cooling may have taken place during uplift and erosion of the Colorado-Wyoming region at 1.5 - 1.3 Ga, following cessation of Proterozoic magmatism.

## **ACKNOWLEDGEMENTS**

I am extremely grateful for the support and encouragement of many colleagues and friends who were always ready to assist in times of emergency and stress. It was a privilege and a pleasure have John Gurney as my supervisor, and it was an excellent opportunity to learn from his wide knowledge of all things related (and unrelated!) to the mantle, diamonds and kimberlites. John proved to be an astute and patient supervisor, even when faced with a wild-eyed student bearing the umpteenth muddled draft... I truly appreciate his generosity and confidence in me, particularly for allowing me the opportunity to spend several months in London working with Judith Milledge and Wayne Taylor.

Although not officially a supervisor, Judith Milledge provided much valued assistance and information during my sojourns at University College, London. Many a dark and dingy winter's day in the basement was lightened by her sharp wit, and this thesis would have been impossible without her guidance in the interpretation of the IR and CL results.

Wayne Taylor was a fountain of inspiration and energy. His help and interest, particularly in the quantitative spectral analysis is much appreciated. I'd like to thank Wayne for his prompt response to innumerable frantic e-mail messages, as this provided a vital link for the exchange of ideas and information.

The staff and post-graduate students of the Crystallography and Mineral Physics Unit, and Department of Geological Science at University College London offered warm friendship and help. In particular, Pete Woods provided expert technical assistance, and Adrian Jones provided stimulating discussion and experimental assistance.

Mal McCallum was instrumental in providing the diamonds studied in this project. He proved to be a veritable mine of information on the State Line district, and his help and interest were invaluable, especially at the outset of the project.

Herb Helmstaedt is thanked for his advice and constructive comments on the thesis. I would also like to thank Michael Seal for organising the polishing of diamond plates and Paul Turner for undertaking the IR mapping.

Many staff members of the department of Geological Sciences at UCT provided assistance in this project. Dick Rickard is thanked for his technical wizardry in keeping an aged probe running, Steve Richardson kindly lent me his diamond cracker, David Wilson kept up a steady supply of epoxy, frosted slides and good humour, Nicky Wilson-Harris, Isobel Lathwaite and Jean Lamb provided competent administrative assistance.

Dane Gerneke, Charles Brintjies and William Williams of the Electron Microscope Unit at UCT are thanked for sparing their valuable time to assist in obtaining SEM and CL photomicrographs. Special thanks must go to the Matthews family; David, Ewalda, Lachlan, Caellum and especially Thalassa were more than just friends and served as my surrogate family. The progress of this thesis was smoothed along by many a fine bottle of wine shared in their company... Thank you also to my close friends: Susan (and trusty guillotine), Norma, Else, Stuart, Trish, Jude, Alan, Sean, Petra, Protea and Leon for putting up with my antisocial behaviour and coping with my minor crises. Thank you Leon for the editing, advice, computing help and friendship.

Most importantly; Mom and Dad, Shirley and Mark have supported me in many ways throughout my education. Thank you for being a vital source of encouragement and for always showing an interest in my studies.

## REFERENCES

- Akaishi, M. 1993. New non-metallic catalysts for the synthesis of high pressure, high temperature diamond. *Diamond and Related Materials*, **2**: 183-189.
- Akaishi, M., Kanda, H. and Yamaoka, S. 1993. Phosphorous: an elemental catalyst for diamond synthesis and growth. *Science*, **259**: 1592-1594.
- Alberty, R. A. 1987. *Physical Chemistry*, 7th edn, John Wiley & Sons, New York: 934 pp.
- Andersen, T., O'Reilly, S. Y. and Griffin, W. L. 1984. The trapped fluid phase in upper mantle xenoliths from Victoria, Australia: implications for mantle metasomatism. *Contrib. Mineral. Petrol.*, **88**: 72-85.
- Anthony, T. R. 1994. The behavior of gas inclusions in diamond generated by temperature changes. *Diamond and Related Materials*, **4**: 83-94.
- Arima, M. and Edgar, A. D. 1981. Substitution mechanism and solubility of titanium in phlogopites from rocks of probable mantle origin. *Contrib. Mineral. Petrol.*, **77**: 288-298.
- Ater, P. C. 1982. Petrology and geochemistry of mantle eclogite xenoliths from Colorado-Wyoming kimberlites. Unpubl. M.Sc. Thesis, Colorado State University, Fort Collins.
- Ater, P. C., Egger, D. H. and McCallum, 1984. Petrology and geochemistry of mantle eclogite xenoliths from Colorado-Wyoming kimberlites: Recycled ocean crust? *In*: Kornprobst, J., ed., *Kimberlites II: The Mantle and Crust-Mantle Relationships*, Elsevier, Amsterdam: 309-318.
- Barry, J. C., Bursill, L. A., Hutchinson, J. L. 1987. Measurement of lattice displacement of {100} platelets in diamond. *Phil. Mag.*, **A48**: 109-121.
- Bauer, M. and Spencer, L. J. 1904. *Precious Stones*, Charles Griffin & Co., London: 627 pp.
- Bell, D. R. and Rossman, G. R. 1992. Water in the earth's mantle: The role of nominally anhydrous minerals. *Science*, **255**: 1391-1397.
- Bence, A. E. and Albee, A. L. 1968. Empirical correction factors for the electron microanalysis of silicates and oxides. *J. Geol.*, **76**: 382-403.
- Bendeliani, N. A., Popova, S. V. and Vereschagin, L. F. 1967. About new modifications of ZrO<sub>2</sub> and HfO<sub>2</sub> prepared under high pressure. *Geokhimiya*, **6**: 677-683 (in Russian).
- Bennett, V. C. and De Paolo, D. J. 1987. Proterozoic crustal history of the western United States as determined by neodymium isotope mapping: *Geol. Soc. Am. Bull.*, **99**: 674-685.
- Berg, G. W. 1986. Evidence for carbonate in the mantle. *Nature*, **324**: 50-51.
- Berger, S. D. and Pennycook, S. J. 1982. Detection of nitrogen at {100} platelets in diamond. *Nature*, **298**: 635-637.
- Berman, R. 1965. Ed., *The Physical Properties of Diamond*. Clarendon Press, Oxford.
- Berman, R., Hudson, P.R.W. and Martinez, M. 1975. Nitrogen in diamond: evidence from thermal conductivity. *J. Phys. C*, **8**: L430-L434.
- Bertrand, P. and Mercier, J.-C. C. 1985. The mutual solubility of coexisting ortho- and clinopyroxene: towards an absolute geothermometer for the natural system? *Earth Planet. Sci. Lett.*, **76**: 109-122.
- Bezrukov, G. M., Butuzov, V. P. and Gorokhov, S. S. 1970. Some aspects of the genesis of natural diamonds in the light of experimental data. *Dokl. Akad. Nauk. S.S.S.R.*, **193**: 131-135.
- Blinova, G. K., Gurkina, G. A. and Sinakov, S. K. 1988. Some chemical properties of the medium from which natural diamonds crystallize. *Dokl. Akad. Nauk. S.S.S.R.*, **301**: 207-209.
- Bobrievich, A. P., Kalyuzhnyi, V. A. and Smirnov, G. I. 1957. Moissanite in the kimberlites of the eastern Siberian Platform. *Dokl. Akad. Nauk. S.S.S.R.*, **115**: 1189-1192.
- Bovenkerk, H. P. 1961. Some observations on the morphology and physical characteristics of synthetic diamond. *Am. Mineral.*, **46**: 952-963.
- Boyd, F. R. and Finnerty, A. A. 1980. Conditions of origin of natural diamonds of peridotitic affinity. *J. Geophys. Res.*, **85**: 6911-6918.
- Boyd, F. R. and Gurney, J. J. 1982. Low-calcium garnets: keys to craton structure and diamond crystallization. *Carnegie Inst. Wash. Yearbook*, **81**: 261-267.
- Boyd, F. R. and Gurney, J. J. 1986. Diamonds and the African Lithosphere. *Science*, **232**: 472-477.
- Brewster, D. 1862. On the pressure cavities in topaz, beryl, and diamond, and their bearing on geological theories. *Roy. Soc. Edinburgh Trans.*, **23**: 39-44. (pub. 1864).

- Deines, P. 1980. The carbon isotopic composition of diamonds: relationship to diamond shape, colour, occurrence and vapour composition. *Geochim. Cosmochim. Acta.*, **44**: 943-961.
- Deines, P., Gurney, J. J. and Harris, J. W. 1984. Associated chemical and carbon isotopic composition variations in diamonds from Finsch and Premier kimberlite, South Africa. *Geochim. Cosmochim. Acta.*, **48**: 325-342.
- De Vries, R. C. 1975. Plastic deformation and "work-hardening" of diamond. *Mat. Res. Bull.*, **10**: 1193-1200.
- Divis, A. F. 1976. Geology and geochemistry of the Sierra Madre Range, Wyoming. *Colo. Sch. Mines Q.*, **71**: 1-127.
- Edgar, A. D. and Arima, M. 1983. Conditions of phlogopite crystallization in ultrapotassic volcanic rocks. *Mineral. Mag.*, **47**: 11-19.
- Edgar, A. D. and Vukadinovic, D. 1993. Potassium-rich clinopyroxene in the mantle: An experimental investigation of a K-rich lamproite up to 60 kbar. *Geochim. Cosmochim. Acta.*, **57**: 5063-5072.
- Eggler, D. H. 1975. Peridotite-carbonate relations in the system CaO-MgO-SiO<sub>2</sub>-CO<sub>2</sub>. *Carnegie Inst. Wash. Yearbook*, **74**: 468-474.
- Eggler, D. H. 1978. The effect of CO<sub>2</sub> upon partial melting of peridotite in the system Na<sub>2</sub>O-CaO-Al<sub>2</sub>O<sub>3</sub>-MgO-CO<sub>2</sub> to 35 kb, with an analysis of melting in a peridotite-H<sub>2</sub>O-CO<sub>2</sub> system. *Am. J. Sci.*, **278**: 305-343.
- Eggler, D. H. 1987. Solubility of major and trace elements in mantle metasomatic fluids: Experimental constraints. In: Menzies, M. A. and Hawkesworth, C. J., eds., *Mantle Metasomatism*, Academic Press, London: 21-41.
- Eggler, D. H. 1989. Kimberlites: how do they form? In: *Kimberlites and Related Rocks, Vol. 1. Their Composition, Occurrence, Origin and Emplacement*. Geol. Soc. Aust., Spec. Publ. No. 14, Blackwell: 489-504.
- Eggler, D. H. and Baker, D. R. 1982. Reduced volatiles in the system C-O-H: Implications to mantle melting, fluid formation, and diamond genesis. In: Akimoto, S. and Manghnani, M. H., eds., *High-Pressure Research in Geophysics, Advances in Earth and Planetary Sciences*, **12**, Centre for academic Publications, Tokyo: 237-250.
- Eggler, D. H. and McCallum, M. E. 1975. Diamond-bearing peridotite nodule in a Wyoming kimberlite pipe. *Geol. Soc. Am. Abstracts with Programs*, **7**, No. 7: 1065.
- Eggler, D. H., Baker, D. R. and Wendlandt, R. F. 1980. *f*O<sub>2</sub> of the assemblage graphite-enstatite-forsterite-magnesite: experiment and application to mantle *f*O<sub>2</sub> and diamond formation. *Geol. Soc. Am. Abstr. Programs*, **12**, No. 7: 420.
- Eggler, D. H., Dudas, F. O., Hearn, B. C., McCallum, M. E., McGee, E. S., Meyer, H. O. A. and Schulze, D. J. 1987a. Lithosphere of the continental United States: xenoliths in kimberlites and other alkaline magmas. In: Nixon, P. H., ed., *Mantle Xenoliths*, John Wiley & Sons, Chichester: 41-57.
- Eggler, D. H., McCallum, M. E. and Kirkley, M. B. 1987b. Kimberlite-transported nodules from Colorado-Wyoming: A record of enrichment of shallow portions of an infertile lithosphere. *Geol. Soc. Am. Spec. Pap.*, **215**: 77-90.
- Eggler, D. H., Meen, J. K., Welt, F., Dudas, F. O., Furlong, K. P., McCallum, M. E. and Carlson, R. W. 1988. Tectonomagmatism of the Wyoming Province. *Colo. Sch. Mines Q.*, **83**: 25-40.
- Ellis, D. J. and Green, D. H. 1979. An experimental study of the effect of Ca upon garnet-clinopyroxene Fe-Mg exchange. *Contrib. Mineral. Petrol.*, **71**: 13-22.
- Ellis, D. and Wyllie, P. J. 1980. Phase relations and their petrological implications in the system MgO-SiO<sub>2</sub>-H<sub>2</sub>O-CO<sub>2</sub> at pressures of up to 100kbar. *Am. Mineral.*, **65**: 540-556.
- Erlank, A. J. and Kushiro, I. 1970. Potassium contents of synthetic pyroxenes at high temperatures and pressures. *Carneg. Inst. Wash. Yearbook*, **68**: 433-439.
- Erlank, A. J., Waters, F. G., Hawkesworth, C. J., Haggerty, S. E., Allsopp, H. L., Rickard, R. S. and Menzies, M. A. 1987. Evidence for mantle metasomatism in peridotite nodules from the Kimberley pipes, South Africa. In: Menzies, M. A. and Hawkesworth, C. J., eds., *Mantle Metasomatism*, Academic Press, London: 221-311.
- Evans, T. 1976. Diamonds. *Contemp. Phys.*, **17**: 45-70.
- Evans, T. 1992. Aggregation of Nitrogen in Diamond. In: Field, J. E., ed., *The Properties of Natural and Synthetic Diamond*, Academic Press, London: 259-290.
- Evans, T. and Phaal, C. 1962. Imperfections in Type I and Type II diamonds. *Proc. R. Soc. A* **270**: 538-552.
- Evans, T. and Qi, Z. 1982. The kinetics of the aggregation of nitrogen atoms in diamond. *Proc. R. Soc. A* **381**: 159-178.
- Evans, T. and Sauter, D. H. 1961. Etching of diamond surfaces with gases. *Phil. Mag.*, **6**: 429-440.

- Evans, T. and Wild, R. K. 1965. Plastic bending of diamond plates. *Phil. Mag.*, **1**: 479-489.
- Fedorov, I. I., Chepurov, A. I., Osorgin, N. Yu., Sokol, A. G. and Sobolev, N. V. 1991. Experimental modeling and thermodynamic analysis of C-O-H fluid in equilibrium with graphite and diamond at high pressures and temperatures. *Dokl. Akad. Nauk. S.S.S.R.*, **320**: 710-712.
- Field, J. E. 1979. Ed., *The properties of diamond*, Academic Press, London: 674 pp.
- Finnerty, A. A. and Boyd, F. R. 1984. Evaluation of thermobarometers for garnet peridotites. *Geochim. Cosmochim. Acta.*, **48**: 15-27.
- Finnerty, A. A. and Boyd, F. R. 1987. Thermobarometry for garnet peridotites: basis for the determination of thermal and compositional structure of the upper mantle. In: Nixon, P. H., ed., *Mantle Xenoliths*, John Wiley & Sons, Chichester: 381-402.
- Frank, F. C. 1967. Defects in diamond. In: Burls, J., ed., *Science and Technology of Industrial Diamonds*, **1**, Science. Ind. diamond Info. Bur., London: 119-136.
- Frank, F. C. and Puttick, K. E. 1958. Etch pits and trigons on diamond. *Phil. Mag.*, **3**: 1273-1279.
- Frank, F. C., Puttick, K. E. and Wilks, E. M. 1958. Etch pits and trigons on diamond. *Phil. Mag.*, **3**: 1262-1272.
- Fritsch, E. and Scarratt, K. V. G. 1989. Optical studies of one type of natural diamonds with high hydrogen content. Workshop on diamonds, 25th Int. Geol. Cong., July 1989, Washington D.C., *Extended Abstr.* : 21-22.
- Fyfe, W. and McBirney, A. 1975. Subduction and the structure of andesite volcanic belts. *Am. J. Sci.*, **275-A**: 285-197.
- Giardini, A. A. and Melton, C. E. 1975. The nature of cloud-like inclusions in two Arkansas diamonds. *Am. Mineral.*, **60**: 931-933.
- Gibson, J. M., Mendelssohn, M. J., Milledge, H. J. and Pillinger, C. T. 1992. Investigation of the absolute values of the infrared absorption coefficient for different types of diamond. *Diamond Conference Abstracts*, Cambridge (unpublished).
- Gibson, J. M., Mendelssohn, M. J., Milledge, H. J. and Pillinger, C. T. 1993. Further investigation of the absolute values of the infrared absorption coefficient for different types of diamond. *Diamond Conference Abstracts*, Bristol: 9.1-9.4 (unpublished).
- Gillet, P. 1993. Stability of magnesite (MgCO<sub>3</sub>) at mantle pressure and temperature conditions: A Raman spectroscopic study. *Am. Mineral.*, **78**: 1328-1331.
- Gorina, I. F. 1971. Crystal morphology of diamonds in Anabaro-Oleneksky Interfluvium. In: Rabkin, M. I., Milashev, V. A. and Yegorov, L. S., eds, *Kimberlite Volcanism and Prospects for Primary Diamond Content in the North-eastern part of the Siberian Platform*. Arctic Geology Research Institute of the USSR Ministry of Geology, Leningrad (in Russian).
- Griffin, W. L., Jaques, A. L., Sie, S. H., Ryan, C. G., Cousens, D. R. and Suter, G.F. 1988. Conditions of diamond growth: a proton microprobe study of inclusions in West Australian diamonds. *Contrib. Mineral. Petrol.*, **99**: 143-458.
- Gurney, J. J. 1984. A correlation between garnets and diamonds in kimberlites. In: Glover, J. E. and Harris, P. G., eds., *Kimberlite Occurrence and Origin, a basis for conceptual models in exploration*. Geol. Dept. Univ. Ext., Univ. Western Australia. Publ. No. 8: 143-166.
- Gurney, J. J. 1989. Diamonds. In: *Kimberlites and Related Rocks, Vol. 2. Their Mantle/Crust Setting, Diamonds and Diamond Exploration*. Geol. Soc. Aust., Spec. Publ. No. 14, Blackwell: 935-965.
- Gurney, J. J. and Hatton, C. J. 1989. Diamondiferous minerals from the Star Mine, South Africa. In: *Kimberlites and Related Rocks, Vol. 2. Their Mantle/Crust Setting, Diamonds and Diamond Exploration*. Geol. Soc. Aust., Spec. Publ. No. 14, Blackwell: 1023-1028.
- Gurney, J. J. and Moore, R. O. 1990. The development of advanced technology to distinguish between productive diamondiferous and barren diatremes. *Geol. Surv. Canada, open file report* 2124, **1**: 1-90.
- Gurney, J. J. and Switzer, G. S. 1973. The discovery of garnets closely related to diamonds in the Finsch pipe, South Africa. *Contrib. Mineral. Petrol.*, **39**: 103-116.
- Gurney, J. J., Harris, J. W. and Rickard, R. S. 1979. Silicate and oxide inclusions in diamonds from the Finsch kimberlite. In: Boyd, F. R. and Meyer, H. O. A., eds, *Kimberlites, diatremes and diamonds: Their geology, petrology and chemistry*, A.G.U., Washington D.C.: 1-15.
- Gurney, J. J., Harris, J. W. and Rickard, R. S. 1984a. Silicate and oxide inclusions in diamonds from the Orapa Mine, Botswana. In: Kornprobst, J., ed., *Kimberlites II: The Mantle and Crust-Mantle Relationships*, Elsevier, Amsterdam: 3-10.

- Gurney, J. J., Harris, J. W. and Rickard, R. S. 1984b. Minerals associated with diamonds from the Roberts Victor mine. In: Kornprobst, J., ed., *Kimberlites II: The Mantle and Crust-Mantle Relationships*, Elsevier, Amsterdam: 25-33.
- Guthrie, G. D. Jr., Veblen, D. R., Navon, O. and Rossman, G. R. 1991. Submicrometer fluid inclusions in turbid-diamond coats. *Earth Planet. Sci. Lett.*, **105**: 1-12.
- Haggerty, S. E. 1986. Diamond genesis in a multiply-constrained model. *Nature*, **320**: 34-38.
- Haggerty, S.E. 1989. Upper mantle opaque mineral stratigraphy and the genesis of metasomites and alkali-rich melts. In: *Kimberlites and Related Rocks, Vol. 2. Their Mantle/Crust Setting, Diamonds and Diamond Exploration*. Geol. Soc. Aust., Spec. Publ. No. 14, Blackwell: 687-699.
- Haggerty, S. E. 1994. Deep upper mantle and transition zone xenoliths in the Jagersfontein kimberlite, Kaapvaal craton. *Eos Trans., A.G.U. Spring Meeting, Abstracts*: 192.
- Haggerty, S. E. and Tompkins, L. A. 1983. Redox state of the Earth's upper mantle from kimberlitic ilmenites. *Nature*, **303**: 295-300.
- Hall, A. E. and Smith, C. B. 1984. Lamproite diamonds— are they different? In: Glover, J. E. and Harris, P. G., eds, *Kimberlite Occurrence and Origin: a basis for conceptual models in exploration*. Geol. Dept and Univ. Extension, Univ. of Western Australia, Publ. No. 8: 167-212.
- Hancock, S. L. and Rutland, R. W. R. 1984. Tectonics of an early Proterozoic geosuture: the Halls Creek orogenic sub-province, Northwestern Australia. *J. Geodynamics*, **1**: 387-432.
- Hanley, P. L., Kiflawi, I. and Lang, A. R. 1977. On topographically identifiable sources of cathodoluminescence in natural diamonds. *Phil. Trans. R. Soc.*, **A284**: 329-368.
- Hanson, R. C. and Jones, L. H. 1981. Infrared and Raman studies of pressure effects on the vibrational modes of solid CO<sub>2</sub>. *J. Chem. Phys.*, **75**: 1102-1112.
- Hardy, J. R. and Smith, S. D. 1961. Two-phonon Infra-red lattice absorption in diamond. *Phil. Mag.*, **6**: 1163-1172.
- Harlow, G. E. 1992. Potassium clinopyroxene at high pressure. *Geol. Soc. Amer., Session 48-A129* (abstr).
- Harris, J. W. 1968. The recognition of diamond inclusions—Pt 2: Epigenetic mineral inclusions. *Ind. Diam. Rev.*, **28**: 458-461.
- Harris, J. W. 1992. Diamond geology. In: Field, J. E., ed., *The Properties of Natural and Synthetic Diamond*, Academic Press, London: 345-393.
- Harris, J. W. and Collins, A. T. 1985. Studies of Argyle diamonds. *Ind. Diam. Rev.*, **45**: 128-130.
- Harris, J. W. and Gurney, J. J. 1979. Inclusions in diamond. In: Field, J. E., ed., *The Properties of Diamond*, Academic Press, London: 555-591.
- Harris, J. W. and Vance, E. R. 1974. Studies of the reaction between diamond and heated kimberlite. *Contrib. Mineral. Petrol.*, **47**: 237-244.
- Harris, J. W., Hawthorne, J. B., Oosterveld, M. M. and Wehmeyer, E. 1975. A classification scheme for diamond, and a comparative study of South African diamond characteristics. In: Ahrens, L. H., Dawson, J. B., Duncan, A. R. and Erlank, A. J., eds, *Phys. Chem. Earth*, **9**, Pergamon Press, Oxford: 765-783.
- Harris, J. W., Hawthorne, J. B. and Oosterveld, M. M. 1979. Regional and local variations in the characteristics of diamonds from some southern African Kimberlites. In: Boyd, F. R. and Meyer, H. O. A., eds, *Kimberlites, diatremes and diamonds: Their geology, petrology and chemistry*, A.G.U, Washington D.C.: 27-41.
- Harris, J. W., Hawthorne, J. B. and Oosterveld, M. M. 1983. A comparison of diamond characteristics from the De Beers Pool mines, Kimberley, South Africa. In: Kornprobst, J., ed., *Annales Scientifiques de l'Universite de Clermont Ferrand II*, **74**: 1-13, Elsevier, Amsterdam.
- Harte, B. 1987. Metasomatic events recorded in mantle nodules. In: Nixon, P. H., ed., *Mantle Xenoliths*, John Wiley & Sons, Chichester: 625-640.
- Harte, B., Winterburn, P. A. and Gurney, J. J. 1987. Metasomatic and enrichment phenomena in garnet peridotite facies mantle xenoliths from the Matsoku kimberlite pipe, Lesotho. In: Menzies, M. A. and Hawkesworth, C. J., eds., *Mantle Metasomatism*, Academic Press, London: 145-220.
- Hatton, C. J. 1978. The geochemistry and origin of xenoliths from the Roberts Victor mine. Unpubl. Ph.D. Thesis, University of Cape Town, Cape Town.
- He, G-Z. 1984. Kimberlites in China and their major components: A discussion on the physio-chemical properties of the upper mantle. In: Kornprobst, J., ed., *Kimberlites I: Kimberlites and Related Rocks*, Elsevier, Amsterdam: 181-194.

- Helmstaedt, H. and Doig, R. 1975. Eclogite nodules from kimberlite pipes of the Colorado Plateau – samples of subducted Franciscan-type oceanic lithosphere. *In: Ahrens, L. H., Dawson, J. B., Duncan, A. R. and Erlank, A. J., eds, Phys. Chem. Earth, 9*, Pergamon Press, Oxford: 95-111.
- Helmstaedt, H. and Schulze, D. J. 1979. Garnet-clinopyroxenite-chlorite eclogite transition in a xenolith from Moses Rock: further evidence for metamorphosed ophiolites under the Colorado Plateau. *In: Boyd, F. R. and Meyer, H. O. A., eds., The Mantle Sample: Inclusions in Kimberlite and Other Volcanics*, A. G. U., Washington D.C.: 357-365.
- Henoc, J., Heinrich, K. F. K. and Myklebust, R. L. 1973. A rigorous correction procedure for quantitative electron probe microanalysis (COR 2). U.S. Bureau of Standards Technical Note **769**, U.S. Government Printing Office, Washington D.C.
- Hervig, R. L., Smith, J. V., Steele, I. M., Gurney, J. J., Meyer, H. O. A. and Harris, J. W. 1980. Diamonds: Minor elements in silicate inclusions: Pressure-temperature implications. *J. Geophys. Res.*, **85**: 6919-6929.
- Hills, F. A., Gast, P. W., Houston, R. S. and Swainbank, I. 1968. Precambrian geochronology of the Medicine Bow Mountains of southeastern Wyoming. *Geol. Soc. Am. Bull.*, **79**: 1757-1984.
- Hirsch, P. B., Hutchinson, J. L. and Titchmarsh, J. 1986. Voidites in diamond. Evidence for a crystalline phase containing nitrogen. *Phil. Mag.*, **A54**: L49-L54.
- Hoerni, J. A. and Wooster, W. A. 1955. The X-ray anomalous reflexions from diamond. *Acta Crystallogr.*, **8**: 187-194.
- Hofmann, A. W. and White, W. M. 1982. Mantle plumes from subducted oceanic crust. *Earth Planet. Sci. Lett.*, **57**: 421-436.
- Hoffman, P. F. 1988. United plates of America, the birth of a craton: Earth Proterozoic assembly and growth of Proto-Laurentia. *Annual Reviews of Earth and Planetary Science*, **16**: 543-603.
- Houston, R. S., Duebendorfer, E. M., Karlstrom, K. E. and Premo, W. R. 1989. A review of the geology and structure of the Cheyenne belt and Proterozoic rocks of southern Wyoming. *In: Grambling, J. A. and Tewksbury, B. J., eds., Proterozoic Geology of the Southern Rocky Mountains*. Geol. Soc. America Spec. Paper **235**: 1-12.
- Huang, W.-L., Wyllie, P. J. and Nehru, C. E. 1980. Subsolidus and liquidus phase relationships in the system CaO-SiO<sub>2</sub>-CO<sub>2</sub> to 30 kbar with geological applications. *Am. Mineral.*, **65**: 285-301.
- Jaques, A. L., Hall, A. E., Sheraton, J. W., Smith, C. B., Sun, S.-S., Drew, R. M., Foudoulis, C. and Ellingsen, K. 1989. Composition of crystalline inclusions and C-isotopic composition of Argyle and Ellendale diamonds. *In: Kimberlites and Related Rocks Vol. 2. Their Mantle/Crust Setting, Diamonds and Diamond Exploration*. Geol. Soc. Aust., Spec. Publ. No. 14, Blackwell: 966-989.
- Jaques, A. L., Lewis, J. D. and Smith, C. B. 1986. The kimberlitic and lamproititic rocks of Western Australia. *Geol. Surv. West. Aust. Bull.*, **132**.
- Javoy, M., Pineau, F. and Delorme, H. 1986. Carbon and nitrogen isotopes in the mantle. *Chem. Geol.*, **57**: 41-62.
- Kaiser, W. and Bond, W. L. 1959. Nitrogen, a major impurity in common type I diamond. *Phys. Rev.*, **115**: 857-863.
- Kanda, H., Yamaoka, S. and Setaka, N. 1977. Etching of diamond octahedrons by high pressure water. *J. Crystal Growth*, **38**: 1-7.
- Karlstrom, K. E. and Houston, R. S. 1984. The Cheyenne Belt: Analysis of a Proterozoic suture in southern Wyoming. *Precamb. Res.*, **25**: 415-446.
- Kennedy, C. S. and Kennedy, G. C. 1976. The equilibrium boundary between graphite and diamond. *J. Geophys. Res.*, **81**: 2467-2470.
- Kesson, S. E. and Ringwood, A. E. 1989a. Slab-mantle interactions, 1. Sheared and refertilised garnet peridotite xenoliths— samples of Wadati-Benioff zones? *Chem. Geol.*, **78**: 83-96.
- Kesson, S. E. and Ringwood, A. E. 1989b. Slab-mantle interactions, 2. The formation of diamonds. *Chem. Geol.*, **78**: 97-118.
- Kiflawi, I., Boyd, S. R. and Woods, G. S. 1993. Infrared determination of the nitrogen concentration in pure type Ia diamonds. *Diamond Conference Abstracts*, Bristol: 8.1-8.4 (unpublished).
- Kiflawi, I., Mayer, A. E., Spear, P. M., van Wyk, J. A. and Woods, G. S. 1994. Infrared absorption by the single nitrogen and A defect centres in diamond. *Phil. Mag. B*, **69**: 1141-1147.
- Kinny, P. D. and Meyer, H. O. A. 1994. Zircon from the mantle: a new way to date old diamonds. *J. Geol.*, **102**: 475-482.

- Kirkley, M. B. 1980. Peridotite xenoliths in Colorado-Wyoming kimberlites. Unpubl. M.Sc. Thesis, Colorado State University, Fort Collins.
- Kirkley, M. B., Gurney, J. J., Otter, M. L., Hill, S. J. and Daniels, L. R. M. 1991. The application of C isotope measurements to the identification of the sources of C in diamonds. *Appl. Geochem.*, **6**: 447-494.
- Koval'skiy, V. V. and Cherskiy, N. V. 1972. The carbon isotope composition of diamonds. *Geologiya i geofizika*, **9**: 10-15 (in Russian).
- Kramers, J. D. 1979. Lead, uranium, strontium, potassium and rubidium in inclusion-bearing diamonds and mantle-derived xenoliths from Southern Africa. *Earth Planet. Sci. Lett.*, **42**: 58-70.
- Krogh, E. J. 1988. The garnet-clinopyroxene Fe-Mg geothermometer—a reinterpretation of existing experimental data. *Contrib. Mineral. Petrol.*, **99**: 44-48.
- Lambert, I. B. and Wyllie, P. J. 1968. Stability of hornblende and a model for the low velocity zone: *Nature*, **219**: 1240-1241.
- Lang, A. R. 1964. A proposed structure for nitrogen impurity platelets found in diamond. *Proc. Phys. Soc. Lond.*, **84**: 871-876.
- Lang, A. R. and Walmsley, J. C. 1983. Apatite inclusions in natural diamond coat. *Phys. Chem. Mineral.*, **9**: 6-8.
- Lax, M. and Burstein, E. 1955. Infrared lattice absorption in ionic and homopolar crystals. *Phys. Rev.*, **97**: 39-52.
- Leung, I. S. 1990. Silicon carbide cluster entrapped in a diamond from Fuxian, China. *Am. Mineral.*, **75**: 1110-1119.
- Leung, I. S., Guo, W., Friedman, I. and Gleason, J. 1990. Natural occurrence of silicon carbide in a diamondiferous kimberlite from Fuxian. *Nature*, **346**: 352-354.
- Lindsley, D. H. and Dixon, S. A. 1976. Diopside-enstatite equilibria at 850 to 1400 °C, 5 to 35 kbars. *Am. J. Sci.*, **276**: 1285-1301.
- Liu, L. 1984. Compression and phase behavior of solid CO<sub>2</sub> to half a megabar. *Earth Planet. Sci. Lett.*, **71**: 1041-110.
- Loubser, J. H. N. and Wright, A. C. J. 1973. Discussion on the Endor and ESR spectra of diamonds with the N3 optical system. *Diamond Research*, Industrial Diamond Information Bureau 1973: 16-20.
- Loubser, J. H. N. and van Wyk, J. A. 1981. *Diamond Conference Abstracts*, Reading: 35-40 (unpublished).
- MacGregor, I. D. 1974. The system MgO-Al<sub>2</sub>O<sub>3</sub>-SiO<sub>2</sub>: Solubility of Al<sub>2</sub>O<sub>3</sub> in enstatite for spinel and garnet peridotite compositions. *Am. Mineral.*, **59**: 110-119.
- MacGregor, I. D. and Carter, J.L. 1970. The chemistry of clinopyroxenes and garnets of eclogite and peridotite xenoliths from the Roberts Victor mine, South Africa. *Phys. Earth Planet. Int.*, **3**: 391-397.
- Mäder, U. K. and Berman, R. G. 1991. An equation of state for carbon dioxide to high pressure and temperature. *Am. Mineral.*, **76**: 1547-1559.
- Madiba, C. C. P., Smallman, C., Sellschop, J. P. F. and Connell, S. H. 1993. Nitrogen analysis in type Ia diamonds. *Diamond Conference Abstracts*, Bristol: 13.1-13.4 (unpublished).
- McCallum, M. E. 1991. The Sloan 1 and 2 kimberlite complex near the southern boundary of the State Line district of the Colorado-Wyoming Kimberlite Province. *Wyoming Geological Association Guidebook, Forty-second Field Conf.*: 229-250.
- McCallum, M. E. and Egger, D. H. 1976. Diamonds in an upper mantle peridotite nodule from kimberlite in southern Wyoming. *Science*, **192**: 253-256.
- McCallum, M. E., Huntley, P. M., Falk, R. W. and Otter, M. L. 1994. Morphological, resorption and etch feature trends of diamonds from kimberlite populations within the Colorado-Wyoming State Line District, USA. In: Meyer, H. O. A. and Leonardos, O. H., eds, *Diamonds: Characterization, Genesis and Exploration*. CPRM Spec. Publ. No. 1/B, CPRM, Brasilia: 32-50.
- McCallum, M. E. and Waldman, M. A. 1991. The diamond resources of the Colorado-Wyoming State Line District: kimberlite indicator mineral chemistry as a guide to economic potential. *Wyoming Geological Association Guidebook, Forty-second Field Conf.*: 77-90.
- McCallum, M. E., Egger, D. H. and Burns, L. K. 1975. Kimberlitic diatremes in northern Colorado and southern Wyoming. In: Ahrens, L. H., Dawson, J. B., Duncan, A. R. and Erlank, A. J., eds, *Phys. Chem. Earth*, **9**, Pergamon Press, Oxford: 149-161.
- McCandless, T. E. and Collins, D. S. 1989. A diamond-graphite eclogite from the Sloan 2 kimberlite, Colorado, U.S.A. In: *Kimberlites and Related Rocks Vol. 2. Their Mantle/Crust Setting, Diamonds and Diamond Exploration*. Geol. Soc. Aust., Spec. Publ. No. 14, Blackwell: 1063-1069.

- McCandless, T. E. and Gurney, J. J. 1989. Sodium in garnet and potassium in clinopyroxene: criteria for classifying mantle eclogites. *In: Kimberlites and Related Rocks, Vol. 2. Their Mantle/Crust Setting, Diamonds and Diamond Exploration*. Geol. Soc. Aust., Spec. Publ. No. 14, Blackwell: 827-832.
- McGetchin, T. R. and Besançon, J. R. 1973. Carbonate inclusions in mantle-derived pyropes. *Earth Planet. Sci. Lett.*, **18**: 408-410.
- Melton, C. E. and Giardini, A. A. 1974. The composition and significance of gas released from natural diamonds from Africa and Brazil. *Am. Mineral.*, **59**: 775-782.
- Melton, C. E. and Giardini, A. A. 1975. Experimental results and a theoretical interpretation of gaseous inclusions found in Arkansas natural diamonds. *Am. Mineral.*, **60**: 413-417.
- Melton, C. E. and Giardini, A. A. 1981. The nature and significance of occluded fluids in three Indian diamonds. *Am. Mineral.*, **66**: 746-750.
- Melton, C. E., Salotti, C. A. and Giardini, A. A. 1972. The observation of nitrogen, water, carbon dioxide, methane and argon as impurities in natural diamonds. *Am. Mineral.*, **57**: 1518-1523.
- Mendelssohn, M. J. and Milledge, H. J. 1995. (in prep.) Recent developments in the interpretation of the mid-infrared absorption spectra of diamond. Sixth International Kimberlite Conf., Novosibirsk, *Extended Abstr.*
- Menzies, M. A. and Hawkesworth, C. J. 1987. *Mantle Metasomatism*, Academic Press, London.
- Meyer, H. O.A. 1985. Genesis of diamond: a mantle saga. *Am. Mineral.*, **70**: 344-355.
- Meyer, H. O. A. 1987. Inclusions in diamond. *In: Nixon, P. H., ed., Mantle Xenoliths*, John Wiley & Sons, Chichester: 501-522.
- Meyer, H. O. A. and Boyd, F. R. 1968. Mineral inclusions in diamond. *Carnegie Inst. Wash. Yearbook*, **67**: 130-135.
- Meyer, H. O. A. and McCallum, M. E. 1986. Mineral inclusions in diamonds from the Sloan kimberlites, Colorado. *J. Geology*, **94**: 600-612.
- Meyer, H. O. A. and Svisero, D. P. 1975. Mineral inclusions in Brazilian diamonds. *In: Ahrens, L. H., Dawson, J. B., Duncan, A. R. and Erlank, A. J., eds, Phys. Chem. Earth*, **9**, Pergamon Press, Oxford: 785-795.
- Meyer, H. O. A. and Tsai, H. M. 1976a. Mineral inclusions in natural diamond - their nature and significance: A review. *Min. Sci. Eng.*, **8**: 242-261.
- Meyer, H. O. A. and Tsai, H. M. 1976b. Mineral inclusions in diamond: Temperature and pressure of equilibration. *Science*, **191**: 849-851.
- Milledge, H. J. 1961. Coesite as an inclusion in G.E.C. synthetic diamonds. *Nature*, **190**: 1181.
- Milledge, H. J. and Mendelssohn, M. J. 1988. Infrared microspectroscopy with special reference to computer-controlled mapping of inhomogeneous specimens. *In: Creaser, C. and Davies, A., eds., Analytical Applications of Soectroscopy.*, The Royal Society of Chemistry: 217-226.
- Milledge, H. J., Mendelssohn, M. J., Boyd, S. R., Pillinger, C. T., Van Heerden, L. A. and Seal, M. 1989. I/R, C/L and MS data for Finsch diamonds and an Argyle stone exhibiting giant platelets. *Diamond Conference Abstracts*, Bristol. (unpublished)
- Milledge, H. J., Verchowsky, A. and Woods, P. A. 1994. Further studies of Yakutite from the Popigai astrobleme. *Diamond Conference Abstracts*, Reading (unpublished).
- Moore, M. and Lang, A. R. 1974. On the origin of the rounded rhombic dodecahedral habit of natural diamond. *J. Crystal Growth*, **26**: 133-139.
- Moore, R. O. 1986. A study of the kimberlites, diamonds, and associated rocks from the Monastery Mine, South Africa. Unpubl. Ph.D. Thesis, University of Cape Town, Cape Town.
- Moore, R. O. and Gurney, J. J. 1985. Pyroxene solid solution in garnets included in diamonds. *Nature*, **318**: 553-555.
- Moore, R. O. and Gurney, J. J. 1989. Mineral inclusions in diamonds from the Monastery kimberlite, South Africa. *In: Kimberlites and Related Rocks, Vol. 2. Their Mantle/Crust Setting, Diamonds and Diamond Exploration*. Geol. Soc. Aust., Spec. Publ. No. 14, Blackwell: 1029-1041.
- Moore, R. O., Otter, M. L., Rickard, R. S., Harris, J. W. and Gurney, J. J. 1986. The occurrence of moissanite and ferro-periclase as inclusions in diamond. *In: Fourth Int. Kimberlite Conf., Perth, Extended Abstr., Abstr. Geol. Soc. Aust. Ser.* **16**: 409-411.
- Mori, T. and Green, D. H. 1978. Laboratory duplication of phase equilibria observed in natural garnet lherzolites. *J. Geol.*, **86**: 83-97.
- Mvuemba Ntanda, F., Moreau, J. and Meyer, H. O. A. 1982. Particularités des inclusions cristallines primaires des diamants du Kasai, Zaire. *Can. Mineral.*, **20**: 217-230.

- Mysen, B. and Griffin, W. L. 1973. Pyroxene stoichiometry and the breakdown of omphacite. *Am. Mineral.*, **53**: 60-63.
- Naeser, C. W. and McCallum, M. E. 1977. Fission-track dating of kimberlitic zircons. Second Int. Kimberlite Conf., Santa Fe, *Extended Abstr.* (no pagination).
- Navon, O., Hutcheon, I. D., Rossman, G. R. and Wasserburg, G. J. 1988. Mantle-derived fluids in diamond micro-inclusions. *Nature*, **335**: 784-789.
- Newton, R. C. and Sharp, W. E. 1975. Stability of forsterite + CO<sub>2</sub> and its bearing on the role of CO<sub>2</sub> in the mantle. *Earth Planet. Sci. Lett.*, **26**: 239-244.
- Nickel, K. G. and Green, D. H. 1985. Empirical geothermobarometry for garnet peridotites and implications for the nature of the lithosphere, kimberlites and diamonds. *Earth Planet. Sci. Lett.*, **73**: 158-170.
- Novgorodov, P. G., Bulanova, G. P., Pavlova, L. A., Mikhaylov, V. N., Ugarov, V. V., Shebanin, A. P. and Argunov, K. P. 1990. Inclusions of potassic phases, coesite and omphacite in a coated diamond crystal from the Mir pipe. *Dokl. Akad. Nauk. S.S.S.R.*, **310**: 439-443.
- O'Hara, M. J., Saunders, M. J. and Mercy, E. L. P. 1975. Garnet-peridotite, primary ultrabasic magma and eclogite: interpretation of the upper mantle processes in kimberlites. In: Ahrens, L. H., Dawson, J. B., Duncan, A. R. and Erlank, A. J., eds, *Phys. Chem. Earth*, **9**, Pergamon Press: 571-604.
- Olafsson, M. and Eggler, D. H. 1983. Phase relations of amphibole, amphibole-carbonate, and phlogopite-carbonate peridotite: Petrologic constraints on the asthenosphere. *Earth Planet. Sci. Lett.*, **64**: 305-315.
- O'Neill, H. St C. and Wall, V. J. 1987. The olivine-orthopyroxene-spinel oxygen geobarometer, the nickel precipitation curve, and the oxygen fugacity of the Earth's upper mantle. *J. Petrol.*, **28**: 1169-1191.
- O'Neill, H. St C. and Wood, B. J. 1979. An experimental study of Fe-Mg partitioning between garnet and olivine and its calibration as a geothermometer. *Contrib. Mineral. Petrol.*, **70**: 59-70.
- Orlov, Yu. L. 1959. Mineralog. Mus. Acad. Sci. USSR, Trans, No. **10**: 103-120.
- Orlov, Yu. L. 1973. *Mineralogy of the Diamond*. Izdatel'stvo Nauka SSSR. Translated in 1977 from the Russian, John Wiley and Sons, New York: 235 pp.
- Otter, M. L. 1990. Diamonds and their mineral inclusions from the Sloan diatremes of the Colorado-Wyoming State Line Kimberlite District, North America. Unpubl. Ph.D. Thesis, University of Cape Town, Cape Town.
- Otter, M. L. and Gurney, J. J. 1989. Mineral inclusions in diamonds from the Sloan diatremes, Colorado-Wyoming State Line kimberlite district, North America. In: *Kimberlites and Related Rocks, Vol. 2. Their Mantle/Crust Setting, Diamonds and Diamond Exploration*. Geol. Soc. Aust., Spec. Publ. No. 14, Blackwell: 1042-1053.
- Otter, M. L., Gerneke, D. A., Harte, B., Gurney, J. J., Harris, J. W. and Wilding, M. C. 1991. Diamond growth histories revealed by cathodoluminescence and carbon isotope studies. Fifth Int. Kimberlite Conf., Araxa, *Extended abstr.*: 318-319.
- Pasteris, J. D. 1988. Secondary graphitization in mantle-derived rocks. *Geology*, **16**: 804-807.
- Peterman, Z. E., Hedge, C. E. and Braddock, W. A. 1968. Age of Precambrian events in the northeastern Front Range, Colorado. *J. Geophys. Res.*, **73**: 2277-2296.
- Phaal, C. 1965. Surface studies of diamond. *Ind. Diamond Rev.*, **25**: 486-489 and 591-595.
- Phillips, D., Onstott, T. C. and Harris, J. W. 1989. <sup>40</sup>Ar/<sup>39</sup>Ar laser-probe dating of diamond inclusions from the Premier kimberlite. *Nature*, **340**: 460-462.
- Pokhilenko, N. P., Sobolev, N. V. and Lavrent'ev, Yu. G. 1977. Xenoliths of diamondiferous ultramafic rocks from Yakutian kimberlites. Second Int. Kimberlite Conf., Santa Fe, *Extended Abstr.*
- Pollack, H. N. and Chapman, D.S. 1977. On the regional variation of heat flow, geotherms and lithospheric thickness. *Tectonophys.*, **38**: 279-296.
- Powell, R. 1985. Regression diagnostics and robust regression in geothermometer/geobarometer calibration: the garnet-clinopyroxene geothermometer revisited. *J. Metamorphic Geol.*, **3**: 327-432.
- Prinz, M., Manson, D. V., Hlava, P. F. and Keil, K. 1975. Inclusions in diamonds: garnet lherzolite and eclogite assemblages. In: Ahrens, L. H., Dawson, J. B., Duncan, A. R. and Erlank, A. J., eds, *Phys. Chem. Earth*, **9**, Pergamon Press: 797-815.
- Råheim, A. and Green, D. H. (1974) Experimental determination of the temperature and pressure dependence of the Fe-Mg partition coefficient for coexisting clinopyroxene and garnet. *Contrib. Mineral. Petrol.*, **48**: 179-203.
- Raman, C. V. 1944. Crystal symmetry and structure in diamond. *Proc. Ind. Acad. Sci.* **19**: 188-199.

- Reid, A. M., Brown, R. W., Dawson, J. B., Whitfield, G.G. and Siebert, J. C. 1976. Garnet and clinopyroxene compositions in some diamondiferous eclogites. *Contrib. Mineral. Petrol.*, **58**: 203-220.
- Richardson, S. H. 1986. Latter-day origin of diamonds of eclogitic paragenesis. *Nature*, **322**: 623-626.
- Richardson, S. H., Gurney, J. J., Erlank, A. J. and Harris, J. W. 1984. Origin of diamonds in old enriched mantle. *Nature*, **310**: 198-202.
- Richardson, S. H., Erlank, A. J., Harris, J. W. and Hart, S.R. 1990. Eclogitic diamonds of Proterozoic age from Cretaceous kimberlites. *Nature*, **346**: 54-56.
- Richardson, S. H., Harris, J. W. and Gurney, J. J. 1993. Three generations of diamonds from old continental mantle. *Nature*, **366**: 256-258.
- Rickard, R. S., Harris, J. W., Gurney, J. J. and Cardoso, P. 1989. Mineral inclusions in diamonds from Koffiefontein Mine. In: *Kimberlites and Related Rocks, Vol. 2. Their Mantle/Crust Setting, Diamonds and Diamond Exploration*. Geol. Soc. Aust., Spec. Publ. No. 14, Blackwell: 1054-1062.
- Rickard, R. S., Gurney, J. J. and Harris, J. W. 1991. Mineral inclusions in diamonds from Jagersfontein mine. Fifth Int. Kimberlite Conf., Araxa, *Extended Abstr*, CPRM Special Publ, 2/91: 336-338.
- Ringwood, A. E. 1982. Phase transformations and differentiation in subducted lithosphere: Implications for mantle dynamics, basalt petrogenesis and crustal evolution. *J. Geol.*, **90**: 611-643.
- Ringwood, A. E. and Major, A. 1971. Synthesis of majorite and other high pressure garnets and perovskites. *Earth Planet. Sci. Lett.*, **12**: 411-418.
- Robertson, R., Fox, J. J. and Martin, A. E. 1934. Two types of diamond. *Phil. Trans. R. Soc.*, **A232**: 463-535.
- Robie, R. A., Hemingway, B. S. and Fisher, J. R. 1978. Thermodynamic properties of minerals and related substances at 298.15 K and 1 Bar ( $10^5$  Pascals) pressure and at higher temperatures. *U. S. Geol. Surv. Bull.*, **1452**, U. S. Govt. Printing Office, Washington D.C.
- Robinson, D. N. 1979. Surface textures and other features of diamonds. Unpubl. Ph.D. Thesis, University of Cape Town, Cape Town.
- Robinson, D. N. and Swash, P. M. 1990. Witwatersrand diamonds and some interesting IR absorption data from George Creek and xenolithic diamonds. *Diamond Conference Abstracts*, Reading: 29-29.2 (unpublished).
- Robinson, D. N., Scott, J. A., Van Niekerk, A. and Anderson, V. G. 1989. The sequence of events reflected in the diamonds of some southern African kimberlites. In: *Kimberlites and Related Rocks, Vol. 2. Their Mantle/Crust Setting, Diamonds and Diamond Exploration*. Geol. Soc. Aust., Spec. Publ. No. 14, Blackwell: 990-1000.
- Roedder, E. 1984. Fluid Inclusions. In: Ribbe, P. H., ed., *Reviews in Mineralogy*, **12**, Mineral. Soc. Am., Washington D.C.: 646 pp.
- Rossmann, G. R. and Smyth, J. R. 1990. Hydroxyl contents of accessory minerals in mantle eclogites and related rocks. *Am. Mineral.*, **75**: 775-780.
- Schlossmacher, K. 1932. *Bauer's edelsteinkunde*, 3rd edn, Bernard Tauchnitz, Leipzig: 844 pp.
- Schrauder, M. and Navon, O. 1993. Solid carbon dioxide in a natural diamond. *Nature*, **365**: 42-44.
- Schrauder, M. and Navon, O. 1994. Hydrous and carbonatitic mantle fluids in fibrous diamonds from Jwaneng, Botswana. *Geochim. Cosmochim. Acta*, **58**: 761-771.
- Schulze, D. J. 1986. Calcium anomalies in the mantle and a subducted metaserpentinite origin for diamonds. *Nature*, **319**: 483-485.
- Schulze, D. J. 1992. Diamond eclogite from Sloan Ranch, Colorado, and its bearing on the diamond grade of the Sloan kimberlite. *Econ. Geol.*, **85**: 2175-2179.
- Seal, M. 1963. The growth history of natural diamonds as revealed by etching experiments. *Proc. 1st Int. Congr. Diamonds in Industry*, Paris, 1962, Industrial Diamond Information Bureau, London: 361-376.
- Shee, S. R., Gurney, J. J. and Robinson, D. N. 1982. Two diamond bearing peridotite xenoliths from the Finsch kimberlite, South Africa. *Contrib. Mineral. Petrol.*, **81**: 79-87.
- Shimizu, N. and Richardson, S. H. 1987. Trace element abundance patterns of garnet inclusions in peridotite-suite diamonds. *Geochim. Cosmochim. Acta*, **51**: 755-758.
- Smith, C. B. 1977. Kimberlite and mantle derived xenoliths at Iron Mountain, Wyoming. Unpubl. M.Sc. Thesis, Colorado State University, Fort Collins.
- Smith, C. B. 1979. Rb-Sr mica ages of various kimberlites. Kimberlite Symposium II, Cambridge, *Abstr.*: 61-66.

- Smith, C. B., Gurney, J. J., Harris, J. W., Robinson, D. N., Shee, S. R. and Jagoutz, E. (1986). Sr and Nd isotopic systematics of diamond-bearing eclogite xenoliths and eclogitic inclusions in diamonds from southern Africa. *In: Kimberlites and Related Rocks, Vol. 2. Their Mantle/Crust Setting, Diamonds and Diamond Exploration*. Geol. Soc. Aust., Spec. Publ. No. 14, Blackwell: 853-863.
- Smith, C. B., McCallum, M. E., Coopersmith, H. G. and Egger, D. H. 1979. Petrochemistry and structure of kimberlites in the Front Range and Laramie Range, Colorado- Wyoming. *In: Boyd, F. R. and Meyer, H. O. A., eds, Kimberlites, diatremes and diamonds: Their geology, petrology and chemistry*, A.G.U., Washington D.C.: 178-189.
- Snyder, G. L. 1980. Geologic map of the northernmost Park Range and southernmost Sierra Madre, Jackson and Routt Counties, Colorado. *U.S. geol. Surv. Misc. Inves. Ser. 1-1113*, 1:48 000.
- Sobolev, E. V., Lisoivan, V. I. and Lenskaya, S. V. 1968. *Sov. Phys. Dokl.*, **12**: 665-668.
- Sobolev, N. V., Galimov, E. M., Ivanovskaya, I. N. and Yefimova, E. S. 1979. Isotopic composition of carbon of the diamonds containing crystalline inclusions *Dokl. Akad. Nauk.S.S.S.R.*, **249**: 1217-1220 (in Russian).
- Sobolev, N. V., Ivanovskaya, I. N. and Galimov, E. M. 1981. Specific features of the isotopic composition of carbon of the diamonds from alluvials of south-eastern Australia. Conf. on carbon geochemistry, Moscow, *Abstr.*: 220-222 (in Russian).
- Sobolev, N. V., Yefimova, E. S., Koptil, V. I., Lavrent'yev, Yu. G. and Sobolev, V. C. 1976. Inclusions of coesite, garnet and omphacite in diamonds of Yakutia - first find of coesite paragenesis. *Trans. Dokl. U.S.S.R. Acad. Sci. Earth Sci. Sec.*, **230**: 1442-1444.
- Sobolev, N. V., Yefimova, E. S., Lavrent'yev, Yu. G. and Sobolev, V. S. 1984. Dominant calcisilicate association of crystalline inclusions in placer diamonds from southeastern Australia. *Dokl. Akad. Nauk. S.S.S.R.*, **274**: 148-153.
- Sobolev, V. S. and Sobolev, N. V. 1980. New proof on very deep subsidence of eclogitised crustal rocks. *Dokl. Akad. Nauk. S.S.S.R.*, **250**: 88-90.
- Sobolev, V. S., Sobolev, N. V. and Lavrent'yev, Yu. G. 1972. Inclusions in diamond from diamondiferous eclogite. *Dokl. Akad. Nauk. S.S.S.R.*, **207**:164-167.
- Subbarayudu, G. V. 1975. The Rb/Sr isotope composition and the origin of the Laramie anorthosite-syenite complex, Laramie Range, Wyoming. Unpubl. Ph.D. Thesis, State Univ. New York, Buffalo, New York.
- Sunagawa, I. 1984a. Morphology of natural and synthetic diamond crystals. *In: Sunagawa, I., ed., Materials Science of the Earth's Interior*, Terra Scientific, Tokyo: 303-330.
- Sunagawa, I. 1984b. Growth of crystals in nature. *In: Sunagawa, I., ed., Materials Science of the Earth's Interior*, Terra Scientific, Tokyo: 63-105.
- Sutherland, G. B. B. M., Blackwell, D. E. and Simeral, W. G. 1954. The problem of the two types of diamond. *Nature*, **174**: 901-904.
- Sutton, J. R. 1928. Kimberley diamonds: especially cleavage diamonds. *Trans. Roy. Soc. S. Afr.*, **7**: 65-96.
- Swart, P. K., Pillinger, C. T., Milledge, H. J. and Seal, M. 1983. Carbon isotopic variation within individual diamonds. *Nature*, **303**: 793-795.
- Switzer, G. and Melson, W. G. 1969. Partially melted kyanite eclogite from the Roberts Victor Mine, South Africa. *Smithson. Contrib. Earth Sci.*, **1**: 7.
- Takagi, M. and Lang, A. R. 1964. X-ray Bragg reflexion, "spike" reflexion and ultra-violet absorption topography of diamonds. *Proc. R. Soc.*, **A281**: 310-322.
- Taylor, W. R. 1988. A reappraisal of the nature of fluids included by diamond - a window to deep-seated mantle fluids and redox conditions. *Geol. Soc. Aust. Spec. Publ. No. 13*: 333-349.
- Taylor, W. R. and Green, D. H. 1989. The role of reduced C-O-H fluids in mantle partial melting. *In: Kimberlites and Related Rocks, Vol. 1. Their Composition, Occurrence, Origin and Emplacement*. Geol. Soc. Aust., Spec. Publ. No. 14, Blackwell: 592-602.
- Taylor, W. R., Jaques, A. L. and Ridd, M. 1990. Nitrogen-defect aggregation characteristics of some Australasian diamonds: time-temperature constraints on the source regions of pipe and alluvial diamonds. *Am. Mineral.*, **75**: 1290-1310.
- Thompson, A. B. 1992. Water in the Earth's upper mantle. *Nature*, **358**: 295-302.
- Tsai, H. M. 1978. Mineralogical and geochemical investigations of mineral inclusions in diamond, kimberlite and related rocks. Unpubl. Ph.D. Thesis, Purdue University, West Lafayette.

- Tsai, H. M., Meyer, H. O. A., Moreau, J. and Milledge, H.J. 1979. Mineral inclusions in diamond: Premier, Jagersfontein and Finsch kimberlites, South Africa, and Williamson Mine, Tanzania. *In: Boyd, F. R. and Meyer, H. O. A., eds, Kimberlites, diatremes and diamonds: Their geology, petrology and chemistry*, American Geophysical Union, Washington D.C.: 16-26.
- Turk, L. A. and Klemens, P. G. 1974. Phonon scattering by impurity platelet precipitation in diamond. *Phys. Rev.* **B9**: 4422-4428.
- Urusovskaya, A. A. and Orlov, Yu. L. 1964. Nature of plastic deformation of diamond crystals. *Dokl. Akad. Nauk. S.S.S.R.*, **154**: 112-115.
- Vance, E. R., Harris, J. W. and Milledge H. J. 1973. Possible origins of  $\alpha$ -particle damage in diamonds from kimberlites and alluvial sources. *Mineral. Mag.*, **39**: 349-360.
- Van Heerden, L. A., Gurney, J. J. and Deines, P. 1995. The carbon isotopic compositions of harzburgitic, lherzolitic, websteritic and eclogitic paragenesis diamonds from southern Africa: a comparison of genetic models. *S. Afr. J. Geol.*, **98**: 119-125.
- Van Schmus, W. R. and Bickford, M. E. 1981. Proterozoic chronology and evolution of the midcontinent region, North America. *In: Kroner, A., ed., Precambrian Plate Tectonics*, Elsevier, New York: 261-296.
- Van Tendeloo, G., Luyten, W. and Woods, G. S. 1990. Voidites in pure type IaB diamonds. *Phil. Mag. Letters*, **61**: 343-348.
- Veizer, J. and Hoefs, J. 1976. The nature of  $^{18}\text{O}/^{16}\text{O}$  and  $^{13}\text{C}/^{12}\text{C}$  secular trends in sedimentary carbonate rocks. *Geochim. Cosmochim. Acta*, **40**: 1387-1396.
- Vlassopoulos, D., Rossman, G. R. and Haggerty, S. E. 1993. Coupled substitution of H and minor elements in rutile and the implications of high OH contents in Nb- and Cr-rich rutile from the upper mantle. *Am. Mineral.*, **78**: 1181-1191.
- Wagner, P. A. 1914. *The Diamond Fields of Southern Africa*, Transvaal Leader, Johannesburg. Reprinted 1971 by Struik (Pty) Ltd, Cape Town, South Africa.
- Walker, J. 1979. Optical absorption and luminescence in diamond. *Prog. Phys.*, **42**: 1605-1659.
- Walmsley, J. C. and Lang, A. R. 1992a. Oriented biotite inclusions in diamond coat. *Mineral. Mag.*, **56**: 108-111.
- Walmsley, J. C. and Lang, A. R. 1992b. On sub-micrometre inclusions in diamond coat: crystallography and composition of ankerites and related rhombohedral carbonates. *Mineral. Mag.*, **56**: 533-543.
- Welt, F. and Egger, D. H. 1988. Geochemistry of mantle xenoliths in Colorado-Wyoming kimberlites: Contrasting magmatic-metasomatic overprints in upper and lower mantle lithosphere. *Geol. Soc. Am. Abstracts with Programs*, **20**: A366.
- Whitelock, T. K. 1973. Morphology of the Kao diamonds. *In: Nixon, P. H. ed., Lesotho Kimberlites*, Lesotho National Development Corporation, Maseru: 128-140.
- Wilding, M. C. 1990. A study of diamonds with syngenetic inclusions. Unpubl. Ph.D. Thesis, University of Edinburgh, Edinburgh.
- Wilding, M. C., Harte, B. and Harris, J. W. 1990. Carbon isotope variation in a zoned Bultfontein diamond, determined by S.I.M.S., *Geol. Soc. Australia, Abstracts*, **27**: 112.
- Woermann, E. and Rosenhauer, M. 1985. Fluid phases and the redox state of the Earth's mantle; Extrapolations based on experimental, phase-theoretical and petrological data. *Fortschr. Miner.*, **63**: 263-349.
- Woods, G. S. 1976. Electron microscopy of "giant" platelets on cube planes in diamond. *Phil. Mag.*, **34**: 993-1012.
- Woods, G. S. 1986. Platelets and the infrared absorption of type Ia diamonds. *Proc. R. Soc.*, **A407**: 219-238.
- Woods, G. S. and Collins, A. T. 1983. Infrared absorption spectra of hydrogen complexes in Type I diamonds. *J. Phys. Chem. Solids*, **44**: 471-475.
- Woods, G. S. and Lang, A. R. 1975. *J. Cryst. Growth*, **28**: 215-226.
- Woods, G. S., Purser, G. C., Mtimkulu, A. S. S. and Collins, A. T. 1990. The nitrogen content of Type Ia natural diamonds. *J. Phys. Chem. Solids*, **51**: 1191-1197.
- Wyllie, P. J. 1978. Mantle fluid compositions buffered in peridotite-CO<sub>2</sub>-H<sub>2</sub>O by carbonates, amphibole, and phlogopite. *J. Geol.*, **86**: 687-713.
- Wyllie, P. J. 1979. Magmas and volatile components. *Am. Mineral.*, **64**: 469-500.
- Wyllie, P. J. 1987. Metasomatism and fluid generation in mantle xenoliths. *In: Nixon, P. H., ed., Mantle Xenoliths*, John Wiley & Sons, Chichester: 609-621.

- Wyllie, P. J. and Huang, W.-L. 1975a. Influence of mantle CO<sub>2</sub> in the generation of carbonatites and kimberlites. *Nature*, **257**: 297-299.
- Wyllie, P. J. and Huang, W.-L. 1975b. Peridotite, kimberlite, and carbonatite explained in the system CaO- MgO- SiO<sub>2</sub>-CO<sub>2</sub>. *Geology*, **3**: 621-624.
- Wyllie, P. J. and Huang, W.-L. 1976. Carbonation and melting relations in the system CaO-MgO-SiO<sub>2</sub>-CO<sub>2</sub> at mantle pressures with geophysical and petrological implications. *Contrib. Mineral. Petrol.*, **54**: 79-107.
- Wyllie, P.J. and Sekine, T. 1982. The formation of mantle phlogopite in subduction zone hybridization. *Contrib. Mineral. Petrol.*, **79**: 375-380.
- Wyllie, P.J., Huang, W.-L., Otto, J. and Byrnes, A. P. 1983. Carbonation of peridotites and decarbonation of siliceous dolomites represented in the system CaO-MgO-SiO<sub>2</sub>-CO<sub>2</sub> to 30 kbar. *Tectonophys.*, **100**: 359-388.
- Yamaoka, S., Komatsu, H., Kanda, H. and Setaka, N. 1977. Growth of diamond with rhombic dodecahedral faces. *J. Crystal Growth*, **37**: 349-352.
- Yefimova, E. S., Sobolev, N. V. and Pospelova, L. N. 1983. Sulphide inclusions in diamond and specific features of their paragenesis. *Zapiski vsesoyuznogo Mineralogicheskogo Obshchestva*, **112**: 300-310 (in Russian).
- Zezin, R. B., Saporin, G. V., Smirnova, E. P., Obyden, S. K. and Chukichev, M. V. 1990. Cathodoluminescence of natural diamonds from Jakutian deposits. *Scanning*, **12**: 326-333.